Altering TDP-43 domains to understand its toxic co-pathology with tau and to better model its gain-of-function roles in neurodegenerative disease

Aaron Long

A dissertation

submitted in partial fulfillment of the

requirements for the degree of

Doctor of Philosophy

University of Washington

2026

Reading Committee:

Nicole Liachko, Chair

Caitlin Latimer

Leo Pallanck

Program Authorized to Offer Degree:

Molecular and Cellular Biology

University of Washington

Abstract

Altering TDP-43 domains to understand its toxic co-pathology with tau and to better model its gain-of-function roles in neurodegenerative disease

Aaron Long

Chair of Supervisory Committee:

Nicole Liachko

Division of Gerontology & Geriatric Medicine

While predominantly nuclear localized in healthy cells, in neurodegenerative diseases such as frontotemporal lobar degeneration (FTLD-TDP) and amyotrophic lateral sclerosis (ALS), TDP-43 accumulates in hyperphosphorylated cytoplasmic aggregates. TDP-43 aggregates can also be a co-pathology, associating with more severe clinical outcomes in Alzheimer's disease (AD). In chapter 1 we generated new *C. elegans* models with inactivating mutations in the nuclear localization sequence (NLS) of human TDP-43, uncovering distinct cellular responses to nuclear versus cytoplasmic TDP-43 localization. In chapter 2 we use point mutations to alter TDP-43 domains in a gain of function *C. elegans* model to better understand its neurotoxic synergy with tau. We generated and characterized mutant TDP-43; tau transgenic lines, finding TDP-43 post translational modifications and cellular location contribute to neurotoxic synergy with tau. In chapter 3 we characterize an 18 month old cohort of a new TDP-43; tau transgenic mouse model. We found modest neurotoxic synergy between TDP-43 and tau in behavioral tests and some sex differences. These 3 chapters improve current models for studying TDP-43 in *C. elegans* and mice with the hopes that the cytoplasmic TDP-43 models and TDP-43; tau models will lead to biological targets and translational experiments.

Introduction

TAR DNA-binding protein of 43 kDa (TDP-43), a predominately nuclear protein, performs essential RNA metabolism roles in healthy individuals (Kattuah et al., 2019). In neurodegenerative diseases such as frontotemporal lobar degeneration (FTLD) or amyotrophic lateral sclerosis (ALS), TDP-43 gets depleted from the nucleus, loses its nuclear functions, and gets mislocalized to the cytoplasm, where it gains new toxic functions (Feldman et al., 2022, Neumann et al., 2021). *C. elegans* have been used to study TDP-43 gain of function toxicity, by generating transgenic strains that overexpress human TDP-43 in neurons. These TDP-43 *C. elegans* models show motility defects, neurodegeneration, and phosphorylated TDP-43 in the nucleus but not the cytoplasm (Liachko et al., 2010). To better model human disease and to reveal differences between nuclear and cytoplasmic TDP-43 we created cytoplasmic TDP-43 *C. elegans* strains named TDP-43 ΔNLS by adding three point mutations K82A/R83A/K84A in the nuclear localization sequence (NLS) of TDP-43. Chapter 1 focuses on the differences between cytoplasmic and nuclear TDP-43, and the characterization of three TDP-43 ΔNLS strains.

In diseases that have tau pathology, TDP-43 can be a co-pathology, with evidence showing the two proteins have a neurotoxic relationship in disease states (Nelson et al., 2019, Tome et al., 2023). This co-pathology can be seen in some patients with Alzheimer's disease (AD), the main cause of dementia globally. AD pathology is normally driven by amyloid beta (Aβ) deposits and phosphorylated tau (ptau) containing neurofibrillary tangles (NFTs) (Higashi et al., 2007, Wisse et al., 2025). TDP-43 was first identified in AD patients in 2007 (Higashi et al., 2007), and this TDP-43 pathology was termed in 2019, Limbic-predominant age-related TDP-43 encephalopathy (LATE) (Nelson et al., 2019). Interestingly, looking at autopsies from 3803 participants that have tau pathology, the more severe tau pathology correlated with a higher percentage of those individuals also having TDP-43 pathology (Wisse et al., 2025). AD patients with LATE also have increased ptau in their hippocampus and frontal cortex (Tome et al., 2023). Having TDP-43 along with tau pathology worsens cognition in humans, with patients with TDP-43 and tau pathology performing worse on cognitive tests compared to patients with comparable tau pathology without TDP-43 (Josephs et al., 2014). This neurotoxic relationship has also been shown in *C. elegans,* with worms expressing human TDP-43 and human tau showing increased levels of tau and ptau compared to worms just expressing tau. These transgenic worms expressing TDP-43 and tau also have more neuronal dysfunction, shown with decreased ability to swim (Latimer et al., 2022). To better understand how TDP-43 increases tau toxicity, we created transgenic *C. elegans* strains that express human TDP-43 with different

point mutations that alter normal functions of TDP-43. These point mutations cause changes to TDP-43 that prevent TDP-43 from undergoing specific post translational modifications, reduce TDP-43 RNA binding ability, prevent TDP-43 oligomerization, and force TDP-43 to be cytoplasmic. These mutant TDP-43 strains were crossed with human tau expressing transgenic strains to detect changes in neurotoxicity. Chapter 2 describes experiments that help us better understand why tau and TDP-43 have a neurotoxic relationship in *C. elegans*. For chapter 3 we moved from *C. elegans* to study TDP-43 and tau in mice. Mice allow us to look at tau; TDP-43 synergy in a more complex organism. We crossed tau and hemizygous TDP-43 transgenic mice to create a transgenic mouse model to study TDP-43 and tau co-pathology in aging. Aging is the main risk factor for most neurodegenerative diseases, making it an important factor to consider in a mouse study (Hou et al., 2019). Chapter 3 looks at behavior and pathological changes with aging in this transgenic TDP-43; tau mouse model and determines if we can replicate tau and TDP-43 neurotoxic synergy in mice (Wheeler et al., 2015, Wils et al., 2010).

Chapter 1 reveals differences between nuclear and cytoplasmic TDP-43 functions. **Chapter 2** betters our understanding of which TDP-43 domains and functions are important to function and toxicity of tau. **Chapter 3** details age related behavioral and pathologic changes in a new mouse model co-expressing TDP-43 and tau.

TDP-43 in health

TDP-43 is a part of the heterogeneous ribonucleoprotein (hnRNP) family that functions in regulation of RNA transport, splicing, transcription, and translation (Kattuah et al., 2019). TDP-43 is 414 amino acids, has a molecular weight of 43kDa and is encoded by *TARDBP*. TDP-43 is essential for embryonic development, with knockout (KO) of the gene *TARDBP* leading to embryonic lethality in mice (Sephton et al., 2010).

In healthy cells, TDP-43 is ubiquitously expressed, predominantly nuclear, and controls many aspects of RNA metabolism. In particular, it regulates mRNA splicing of thousands of transcripts (Sephton et al., 2012). TDP-43 also participates in RNA transport, transcription, and translation (Rummens and Da Cruz, 2025). TDP-43 is composed of an N-terminal domain (NTD), nuclear localization signal (NLS), two RNA recognition motifs (RRM1 and RRM2), and a glycine rich C-terminal domain (Fig. 1).

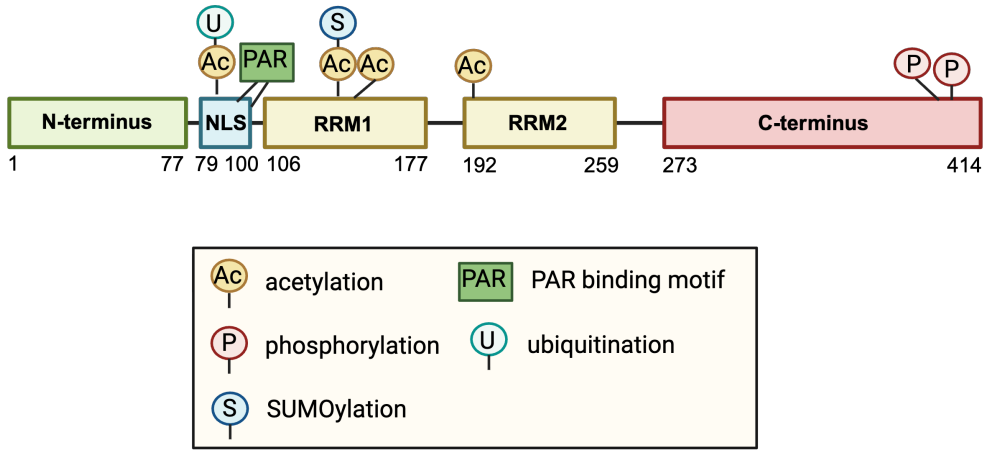

Fig. 1. TDP-43 schematic of domains with common disease state PTM. Common PTM of TDP-43 in neurodegenerative diseases.

TDP-43 has many roles, with one of its main nuclear functions being suppressing cryptic exons during pre-mRNA splicing. Cryptic exons are sequences within introns that mimic exons and can be incorrectly included in mRNA during splicing (Ling et al., 2015). Inclusion of cryptic exons destabilizes mRNA, leading to degradation, or can code for aberrant peptides. TDP-43 can bind around cryptic exon sequences, preventing them from slipping into mRNA (Koike, 2024). Stathmin 2 (STMN2) is a TDP-43 cryptic splicing target that is linked to ALS. STMN2 encodes a protein involved in neuronal microtubule stability. The depletion of TDP-43 in the nucleus leads to abnormal splicing events that lead to truncated STMN2 mRNA, reducing STMN2 protein levels, affecting motor neuron axons, which is commonly seen in sporadic and familial ALS cases with TDP-43 (Melamed et al., 2019, Klim et al., 2019). TDP-43 also plays an important role in spinogenesis, the process of generating dendritic protrusions/spines on cells. These dendritic protrusions on hippocampal neurons and are important for learning and memory (Majumder et al., 2012).

TDP-43 is passively and actively imported into the nucleus and passively exported into the cytoplasm. Nuclear RNA binding regulates TDP-43 nuclear localization and passive nuclear export. Free TDP-43 binds to GU-rich RNA in the nucleus. Disrupting the RNA binding domains of TDP-43 or disrupting RNA transcription, splicing, binding, or export results in passive diffusion of TDP-43 through nuclear pore channels to the cytoplasm (Duan et al., 2022). The nuclear localization signal (NLS) of TDP-43 promotes active import of TDP-43 into the nucleus by binding to nuclear import adaptor Importin α1, which recruits the receptor Importin β to form

an Importin α1/β/TDP-43 complex. Mutation of the TDP-43 NLS site abrogates the ability of TDP-43 to bind to Importin α1 and eliminates active transport into the nucleus (Doll et al., 2022, Winton et al., 2008). *C. elegans* express three Importin α homologs (IMA-1, IMA-2, and IMA-3) (Oka and Yoneda, 2018), which likely function similarly to promote TDP-43 nuclear localization.

Understanding why TDP-43 is depleted from the nucleus and how cytoplasmic TDP-43 is toxic to cells is crucial to future therapeutics. Nuclear TDP-43 cryptic-splicing events and TDP-43 loss-of-function pathology could be an early event preceding cytoplasmic mislocalization (Spence et al., 2024). Acetylation of lysine 82 in the NLS region of TDP-43 causes TDP-43 to have trouble binding Importin α1, resulting in cytoplasmic mislocalization (Ko et al., 2024).

TDP-43 in disease

In neurodegenerative diseases, such as ALS and FTLD-TDP, TDP-43 is frequently depleted from the nucleus and accumulates in the cytoplasm. In the cytoplasm, TDP-43 aggregates, undergoes post-translational modifications including hyperphosphorylation, and increases in toxicity (Liao et al., 2022). Other than phosphorylation, TDP-43 can also undergo post-translational modifications including oxidation, acetylation, zinc binding, SUMOylation, ubiquitination, cleavage, and PARylation. Most of these post translational modifications are only seen in neurodegenerative disorders with cytoplasmic TDP-43 (Francois-Moutal et al., 2019). TDP-43 propagation has been proposed to travel in a prion-like mechanism, by being transferred between cells by tunneling nanotubes (TNTs) or exosomes. In this proposed mechanism, TDP-43 aggregates would be released by exomes or TNTs, then bind to normal TDP-43, inducing more misfolding (Jo et al., 2020, Nonaka et al., 2013). TNTs are F-actin based, transient tubular connections between cells, with cargo being transported by molecular motors (Dagar et al., 2021).

TDP-43 in FTLD

Frontotemporal lobar degeneration (FTLD) is a term that groups neurogenerative disease associated with degeneration in the frontal and anterior temporal lobes, with symptoms causing social, emotional, and behavioral changes (Grossman et al., 2023). In 2006, TAR DNA-binding protein of 43 kDa (TDP-43) cytoplasmic inclusions were first discovered in FTLD and amyotrophic lateral sclerosis (ALS). Prior to this, ubiquitin-positive inclusions were the hallmark of frontotemporal lobar degeneration with ubiquitin positive inclusions (FTLD-U) and ALS but the protein composition of the aggregates was unknown (Neumann et al., 2006). These cytoplasmic TDP-43 inclusions were also found to be hyperphosphorylated and are the major pathologic

protein inclusion of FTLD and ALS (Arai et al., 2006). TDP-43 aggregates are present in around 97% of ALS patients and around 50% of FTLD patients (Feldman et al., 2022).

FTLD is an umbrella term that refers to non-Alzheimer disease (AD) dementias that show gliosis and focal neuronal loss in autopsies of patients with frontotemporal dementia (FTD) clinical syndrome. FTD clinical syndromes include behavioral variant frontotemporal dementia (bvFTD), progressive nonfluent aphasia (PNFA), corticobasal syndrome (CBS), and semantic dementia (SD). These syndromes have varying symptoms, for example, bvFTD involves social behavior and personality changes, while in PNFA consists of speech and language impairments (Dickson et al., 2011).

Abnormal tau is the second most common aggregate causing FTLD, with FTLD-tau individuals having abnormal tau pathology in glia and neurons (Dickson et al., 2011). The third most common type of protein in FTLD inclusions, involving 5-10% of individuals, are from the FUS-Ewing sarcoma-TAF15 family (FTLD-FET). Around 20-25% of FTLD cases are familial, with the three most common genetic mutations involving MAPT, causing FTLD-tau, or GRN and C9orf72 causing FTLD-TDP (Grossman et al., 2023).

FTLD patients can have co-pathologies of multiple proteins, including having both TDP-43 and tau present in autopsies. In a screening of 201 FTLD-TDP patients with confirmed TDP pathology, 42% of the patients also had ageing related tau astrogliopathy (ARTAG), and 36% with primary age-related tauopathy (PART) (Koga et al., 2022). ARTAG involves ptau staining in astrocytes and is commonly seen in individuals over 60 years old (Kovacs et al., 2016). ARTAG is detectible in one-third of brains autopsied over 80. ARTAG is likely to be found as a co-pathology to LATE and brains with cerebrovascular pathology but is not associated with AD PART (Katsumata et al., 2024). PART encompasses neuronal changes as well as neurofibrillary tangles (NFT) but unlike AD has very little to no Aβ plaques (Kovacs et al., 2016).

Neocortical features are used to sub-classify FTLD-TDP-43 into four main types: A, B, C, and D (Fig. 2). Most cases of FTLD type A commonly have bvFTD, with abundant neuronal cytoplasmic inclusions (NCI), neuronal intranuclear inclusions (NII), dystrophic neurites (DN), and abundant hippocampal sclerosis. FTLD type B often has bvFTD in combination with ALS, with moderate NCI, especially in lower motor neurons, and few DN, and no NII (Neumann et al., 2021) FTLD type C is common in semantic variant primary progressive aphasia (svPPA), with loss of empathy, prosopagnosia, obsessive/compulsive disorder, and have a slower disease progression than other sub-types. FTLD type C have few to no NCI, no NII, and is predominately DN. FTLD type D is found in familial cases with *VCP* mutations, that can cause FTD or ALS, with DN and NII but no NCI. FTLD type A has cytoplasmic and nuclear TDP-43

aggregates, FTLD types B and C have cytoplasmic TDP-43 aggregates, and FTLD type D has nuclear TDP-43 aggregates (Neumann et al., 2021).

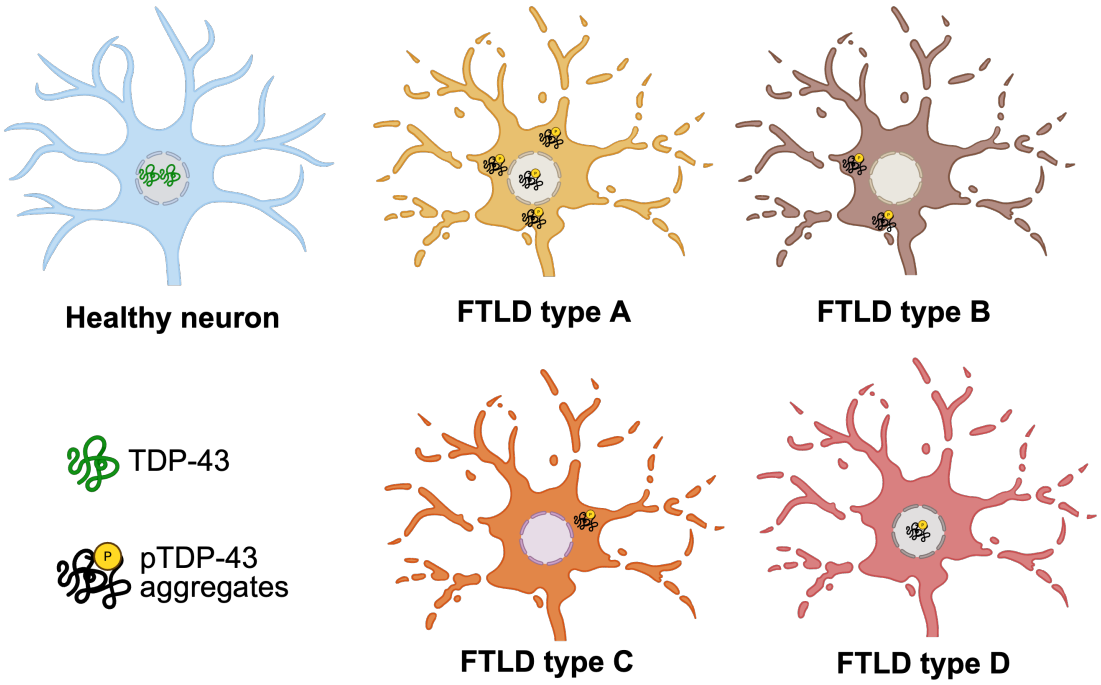

Fig. 2. FTLD subtypes A-D. pTDP-43 is cytoplasmic in type B and C, nuclear in type D, and cytoplasmic and nuclear in type A.

With such variety in FTLD-TDP pathology, it is important to understand nuclear and cytoplasmic TDP-43. TDP-43 aggregates found in the nucleus or cytoplasm might be having different gain of function affects. Non-aggregating TDP-43 could be losing its normal cellular roles, leading to cellular dysfunction (Jo et al., 2020). This complexity of TDP-43 pathology makes it important to make better model organisms that closely mimic different aspects of TDP-43 in human disease.

TDP-43 in ALS

Amyotrophic lateral sclerosis (ALS) is a fatal neurodegenerative disease that affects upper and lower motor neurons and leads to progressive weakness of skeletal muscles, as well as autonomic dysfunction, trouble swallowing, speaking, and decreased respiratory function. Around 15% of ALS cases are familial and there are over 40 known ALS associated genes (Feldman et al., 2022). Mutations in *TARDBP*, the gene encoding TDP-43, can cause ALS in an

autosomal dominate pattern, but accounts for less than 4% of ALS patients (Jo et al., 2020) and very rare cases of FTD (Borroni et al., 2009). There have been more than 40 ALS-linked dominant mutations in *TARDBP*, with most of them being in the C-terminus of TDP-43 protein (Sreedharan et al., 2008, Conicella et al., 2016). TDP-43 pathology in ALS resembles TDP-43 pathology in FTLD-TDP but in motor neurons, where TDP-43 is depleted in the nucleus, accumulates in the cytoplasmic and becomes phosphorylated (Balendra et al., 2025**).** Patients can get diagnosed with multiple diseases that can greatly alter disease prognoses. For example, bvFTD patients have a median survival of 9.6 years but bvFTD patients with ALS co-pathology have a median survival of just 2.8 years (Grossman et al., 2023).

Tau and Alzheimer's disease

Tau was first discovered in 1975 as a protein essential for microtubule (MT) stability (Weingarten et al., 1975). In the brain, tau regulates axon outgrowth, axonal MT stability, and axonal transport (Wegmann et al., 2021). Tau gene transcripts undergo alternative splicing to form 6 tau protein isoforms, ranging from 352 to 441 amino acids long. Tau can have 0 to 2 N-terminal repeats (0N, 1N, or 2N) and 3 or 4 microtubule binding repeats (3R or 4R). In healthy adult brains, 1N is the most common isoform and there is an even ratio of 3R and 4R. In AD there is an uneven ratio of 3R and 4R, with the 4R isoform aggregating 2.5 to 3 times more rapidly than the 3R. Hyperphosphorylation of tau leads to a decreased affinity for microtubules and there is a disruption of microtubule assembly and stability (Boyarko and Hook, 2021). There are 2084 proteins that interact with tau in human tissue, with tau having an enrichment of interactions with proteins involved in RNA binding, proteosome, and ribosome function (Kavanagh et al., 2022). Tau aggregates contain RNA, can localize to splicing speckles in the nucleus, speckle components can mislocalize to tau aggregates in the cytoplasm, and tau can alter nuclear speckle composition. Nuclear speckles are non-membranous assemblies of RNA, splicing machinery, and protein containing nascent RNA transcripts (Lester et al., 2021).

Alzheimer's disease (AD) is the main cause of dementia, with 60-80% of the cumulative risk to get AD comes from heritable factors, with there being over 40 known AD associated genetic risk loci identified (Scheltens et al., 2021). The two protein aggregate hallmarks of AD pathology are amyloid β (Aβ) plaques and neurofibrillary tangles. Aβ is a peptide that can aggregate into insoluble fibrils that clump together to form extracellular plaques in the brain (Hampel et al., 2023), while neurofibrillary tangles are intracellular and are primarily made up of the phosphorylated tau (Tome et al., 2021) While both protein aggregates are present, hyperphosphorylated tau is likely the primary driver of neurodegeneration (Long and Holtzman,

2019). In 1991 Heiko Braak developed a staging protocol of AD pathology based on the predictable gradual deposition of hyperphosphorylated tau, with the higher ptau burden corelating to a more severe stage of disease (Braak et al., 2006).

TDP-43 in aging and Alzheimer's disease

In 2007, TDP-43-positive inclusions were found in Alzheimer's disease (AD), the main cause of dementia globally (Higashi et al., 2007). When looking at older individuals, TDP-43 is related to age related cognitive decline. Brains with TDP-43 pathology had declines in episodic and working memory (Wilson et al., 2013). When looking at 188 pathologically confirmed AD brains, TDP-43 was found in 59% of brains with typical AD pathology and 67% of the brains with Limbic AD pathology. Having TDP-43 present in the brain leads to greater memory loss, and smaller hippocampal volumes (Josephs et al., 2015). The accumulation of TDP-43 aggregates is often seen in older adults, termed limbic-predominant age related TDP-43 encephalopathy (LATE) (Nelson et al., 2019). Unlike FTLD and ALS where TDP-43 is the major disease-causing pathologic protein, TDP-43 is a co-pathology in AD LATE and DLB. In AD LATE, cytoplasmic TDP-43 inclusions are associated with more severe clinical outcomes than AD without TDP-43 pathology. In samples from the CA1 in the hippocampus and the frontal cortex, the presence of TDP-43 in AD LATE brains increased the amount of p-tau compared to AD brains (Tome et al., 2023).

LATE is often comorbid with AD and is the second most common neurodegenerative disease behind AD in individuals over 90 years old. LATE pathologic changes involve the accumulation of pTDP-43 in the limbic system with or without hippocampal sclerosis (Butler Pagnotti et al., 2023, Nelson et al., 2019). LATE is associated with cognitive impairment and amnestic dementia (Nelson et al., 2019). Individuals with LATE present with less cognitive and functional complaints compared to those with AD or AD LATE. Individuals with AD LATE show comorbidity, with higher levels of dementia and greater amount of caregiver reported memory decline compared to LATE and AD individuals (Butler Pagnotti et al., 2023). The reported percentage of AD patients that have TDP-43 inclusions varies greatly, with reports ranging from 20-50% of most AD patients, and up to 75% in AD patients with severe symptoms (Jo et al., 2020).

TDP-43 in LBD

First seen in Lewy body disorders in 2007 (Nakashima-Yasuda et al., 2007), TDP-43 can be a frequent co-pathology in Lewy body dementia (LBD) (Uemura et al., 2022). LBD is the second most common dementia behind AD and encompasses dementia with Lewy bodies (DLB) and Parkinsons disease dementia (PDD). If you have dementia within one year of motor symptoms for Parkinsons it is classified as DLB but if dementia comes later it is diagnosed as PDD (Chiu et al., 2022). LBD has intraneuronal cytoplasmic α-synuclein positive Lewy bodies and neurites in the brainstem, limbic, and cortical regions. Lewy bodies are highly variable in shape and cause neuronal dysfunction and degeneration by disrupting normal cellular functions (Nouraei et al., 2018, Scholz et al., 2025). A contrary belief is that Lewy bodies play a protective role by sequestering α-synuclein, the real toxic driver of disease pathology (Kramer and Schulz-Schaeffer, 2007). Interestingly, TDP-43 is detected in 30 to 63% of LBD autopsy cases. Having TDP-43 present in LBD pathology can lead to a misdiagnosis based on clinical presentation since TDP-43 might be causing hippocampal atrophy, resulting in memory loss, while LBD tend to have a more variable cognitive profile. Some LBD patients have memory impairment, but others may have attention, executive, and visuospatial dysfunction (Buciuc et al., 2020). Understanding the co-pathologies in neurodegenerative diseases is important to accurately diagnosing patients and finding the most appropriate treatments (Fig. 3).

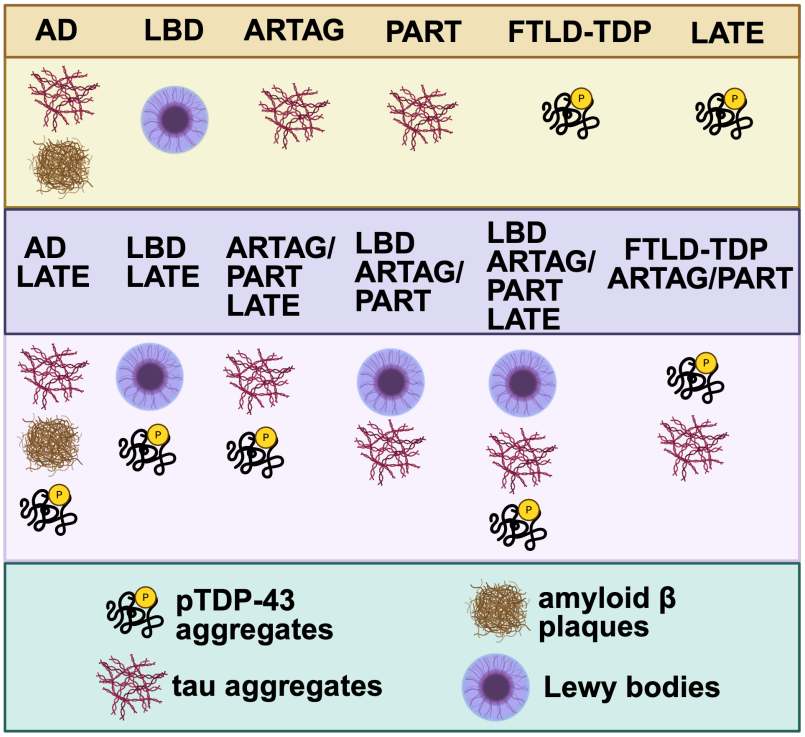

Fig. 3. Protein co-pathologies in neurodegenerative diseases.

ER and mitochondrial Unfolded protein response (UPR)

The accumulation of misfolded or unfolded proteins such as tau and TDP-43 in the cytoplasm and the endoplasmic reticulum (ER) lumen, can cause disrupted protein folding homeostasis and ER stress. ER stress triggers the unfolded protein response (UPR^{ER}), resulting in the activation of protein degradation pathways (He et al., 2024). Part of this stress response involves mRNA of the transcription factor XBP-1 getting alternatively spliced to its active form, XBP-1s. XBP-1s translocates to the nucleus where it increases transcription of genes involving ER chaperones and ER-associated degradation (ERAD) machinery, related to degrading misfolded proteins (Duran-Aniotz et al., 2023, Calfon et al., 2002). ERAD leads to the ubiquitination of these misfolded proteins, and their degradation in the proteosome (Fig. 4). XBP-1 activation has been shown to triggers the UPR^{ER} protecting against tau neurotoxicity (Waldherr et al., 2024, Duran-Aniotz et al., 2023).

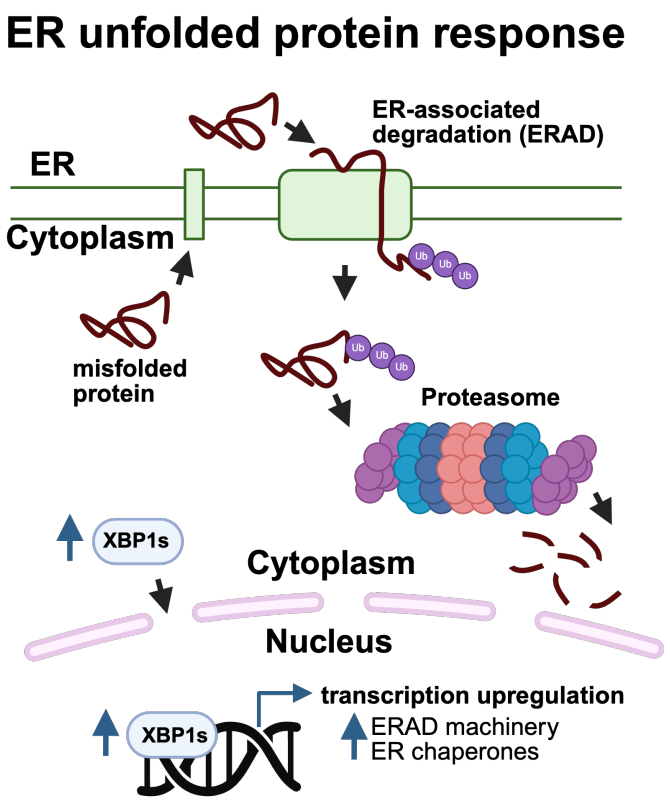

Fig. 4. Activation of XBP1s upregulates machinery for the ER unfolded protein response

TDP-43 can co-localize with mitochondria, with TDP-43 being able to go into mitochondrial matrix (Wang et al., 2016), causing mitochondrial dysfunction, increased reactive oxygen species (ROS), decreased mitochondrial membrane potential, and the triggering of the mitochondrial unfolded protein response (UPR^{mt}). The UPR^{mt} is activated by misfolded proteins in the mitochondrial matrix, causing signaling to the nucleus to increase expression of chaperones and protases to reduce the abnormal mitochondrial protein load (Torres et al., 2024).

The mitochondrial protease LonP1 can regulate TDP-43, with down-regulation of LonP1 resulting in increased mitochondrial TDP-43 levels (Wang et al., 2019). Deletion of the *lonp-1* gene in *C. elegans* increases ROS, decreases mitochondrial function, impacts behavior and lifespan (Taouktsi et al., 2022). In LONP-1 deficient *C. elegans*, the transcription factor ZIP-2 is activated in a PMK-3-dependent manner. ZIP-2 can be important in ageing by maintaining

mitochondrial homeostasis. Deletion of *zip-2* shortens lifespan of *lonp-1* mutants. (Taouktsi et al., 2023).

TDP-43 PTM

Post-translational modifications (PTMs) are reversible covalent bonded adducts to the primary structure of proteins that add to chemical diversity and can modify protein structure and function (Keenan et al., 2021). Understanding post-translational modifications of TDP-43 may uncover mechanisms of TDP-43 in disease (Fig. 5). Hyperphosphorylated TDP-43 is a pathological hallmark in familial and sporadic TDP-43 proteinopathies, including most forms of FTLD, and ALS. Phosphorylation of serine residues 409/410 of TDP-43 is consistently seen in

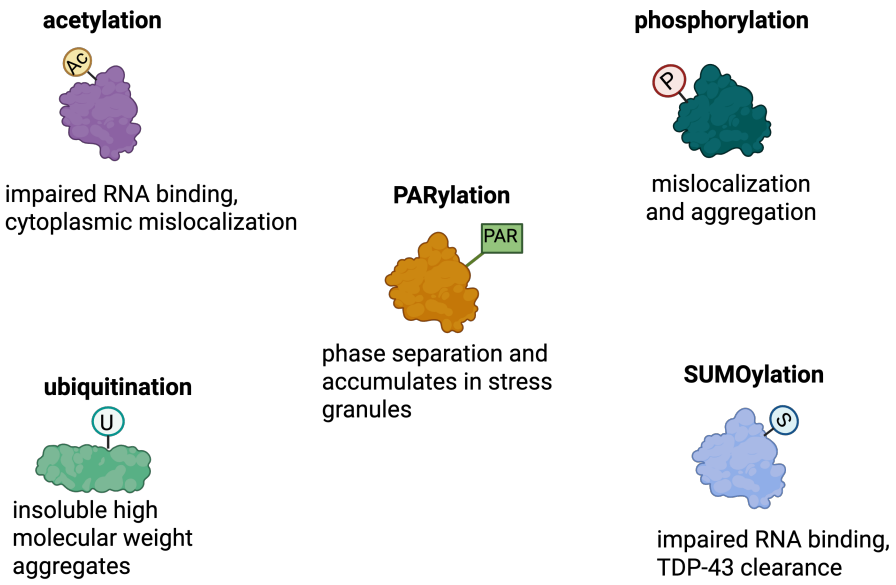

Fig. 5. Common TDP-43 PTM in a diseased state and their effects on TDP-43

abnormal inclusions in TDP-43 proteinopathies (Neumann et al., 2009). Phosphorylation of S409/410 also increases toxicity of TDP-43 in *C. elegans*. *C. elegans* that express ALS TDP-43 mutations such as A315T or M337V are sicker than *C. elegans* expressing WT human TDP-43. This toxicity is driven by the higher levels of phosphorylated TDP-43 in the ALS mutant strains (Liachko et al., 2010). TDP-43 is dephosphorylated by the phosphatase calcineurin, which directly binds to TDP-43 and reduces the accumulation of phosphorylated TDP-43. *C. elegans* has a single homolog of calcineurin, TAX-6. Loss of function of *tax-6* results in increased

phosphorylation of TDP-43 and worsened motility defects in TDP-43-Tg and TDP-43 M337V (Liachko et al., 2016b).

Acetylation of TDP-43 K82 disrupts nuclear import of TDP-43 by disrupting importin $\alpha 1/\beta$ (Ko et al., 2024). Acetylation of TDP-43 K145 increases nuclear and cytoplasmic TDP-43 aggregation, increases TDP-43 phosphorylation, and alters TDP-43 RNA binding (Cohen et al., 2015). PARylation of TDP-43 occurs in the NLS region, causing TDP-43 to localize in cytoplasmic stress granules (McGurk et al., 2018a). In humans, SUMOylation of TDP-43 increases with aging and in ALS/FTLD patients. SUMOylation involves the addition of a covalent conjugation of a small ubiquitin-like modifier (SUMO) to proteins like TDP-43 to target them for cellular processes or degradation. Nuclear location is essential for TDP-43 K408 SUMOylation, with a TDP-43 NLS mutation resulting in almost complete loss of TDP-43 SUMOylation in HEK293T cells (Suk et al., 2025). Following SUMOylation, TDP-43 clearance happens through the ubiquitin proteasome system. SUMOylation and phosphorylation of TDP-43 have an inverse relationship, with the loss of phosphorylation causing an increase in SUMOylation (Suk et al., 2025).

Modeling neurodegenerative diseases

Between 1880 and 1920, parasitic nematodes such as *Ascaris*, were among the first model organisms. Around 1966, Sydney Brenner started working with a different nematode, *C. elegans*, with hopes to be a tool to better research biology and neurobiology. Sydney's work helped popularize *C. elegans* as a commonly used model organism (Nigon and Felix, 2017). *C. elegans* primarily exist as self-fertilizing hermaphrodites that are small in size, have a rapid life cycle, transparent, have a well-annotated genome, and go from an egg to an adult in just 3 days (Corsi et al., 2015).

C. elegans have a simple nervous system consisting of 302 neurons allowing for a simplistic way to study complex mechanisms (White et al., 1986). There have been many useful *C. elegans* models generated to study neurodegenerative diseases, with transgenic strains often expressing neurodegenerative-linked aggregating proteins such as tau, amyloid-β, α-synuclein, and TDP-43 (Torres et al., 2025). Expression of TDP-43 and mutant forms of TDP-43 such as TDP-43 M337 linked to ALS, results in motor dysfunction, phosphorylated TDP-43, and neurodegeneration (Liachko et al., 2010). Similarly, expression of human tau in *C. elegans* can cause motor dysfunction, phosphorylated tau, and neurodegeneration (Brandt et al., 2009). Interestingly, if TDP-43 and tau are co-expressed in *C. elegans* there is a neurotoxic synergy

observed, with motor dysfunction, increased tau and pTau, and selective neurodegeneration (Latimer et al., 2022).

TDP-1 is the *C. elegans* highly conserved ortholog to mammalian TDP-43. TDP-1 shares similar sequence homology with TDP-43 in the N-terminus, RNA recognition motifs, and nuclear localization sequence. The main difference between is in the C-terminus, where TDP-1 has much fewer amino acids in the C-terminus, lacks a Q/N and Gly-rich region that is important for TDP-43 phase separation and aggregation. Unlike TDP-43, TDP-1 does not aggregate (Pir et al., 2026). *tdp-1* null worms have reduced egg laying, slight defect in locomotion, and an elongated lifespan (Zhang et al., 2012).

Similar to *C. elegans*, mice have been used to study TDP-43. TDP-43 mouse models have struggled to closely follow human disease pathology, having trouble showing cytoplasmic TDP-43 inclusions that target specific neuronal and non-neuronal populations (Armas et al., 2025). Human TDP-43 can also be hard to study due to its toxicity in model organisms. The homozygous Kumar-Singh mouse model overexpresses wild-type human TDP-43 in postnatal neurons causing severe motor impairment and death by one month of age (Wils et al., 2010). Due to this toxicity researchers typically use heterozygotes of the Kumar-Singh mice that still have TDP-43 pathology but a less severe phenotype.

To improve cytoplasmic localization to more closely mimic human disease, mice (rNLS) have been made that express human TDP-43 with a defective nuclear localization signal (NLS) with doxycycline (Dox)-suppressible expression. These rNLS mice have accumulation of cytoplasmic pTDP-43 in the brain and spinal cord, brain atrophy, motor neuron loss, and decreased lifespan (Spiller et al., 2016, Walker et al., 2015). TDP-43 mouse models allow for studying disease mechanisms in a complex organism closer to humans, but the complexities of each model can lead to interpretation difficulties as well as the long lifespans of mice can make experiments costly and time consuming. For these reasons I have predominantly focused on using *C. elegans*, a more tractable model, to study TDP-43. In chapter 1 I create a C. elegans TDP-43 model with a defective NLS to study the differences between cytoplasmic and nuclear TD-43.

Chapter 1: Shared and distinct gain-of-function consequences from pathologic cytoplasmic versus nuclear TDP-43

Abstract:

While predominantly nuclear localized in healthy cells, TDP-43 can transit between the nucleus and cytoplasm. In frontotemporal lobar degeneration (FTLD-TDP) and amyotrophic lateral sclerosis (ALS), TDP-43 accumulates in hyperphosphorylated cytoplasmic aggregates. However, a subset of patients develop nuclear aggregates. Expression of wild-type TDP-43 in *C. elegans* neurons results in nuclear protein accumulation and toxic gain of function. To enable comparative study of nuclear and cytoplasmic TDP-43 phenotypes, we generated new models with inactivating mutations in the nuclear localization sequence (NLS) of TDP-43. When compared to nuclear TDP-43 strains, similar protein levels of cytoplasmic TDP-43 cause less neuronal dysfunction in *C. elegans*. Using RNA sequencing, we determine transcriptomes are largely unchanged in these models. However, we identify innate immune pathway increases in response to cytoplasmic but not nuclear TDP-43. We find phosphorylation-mediated neurotoxicity of both cytoplasmic and nuclear localized TDP-43 is controlled by the phosphatase calcineurin. We also find that overexpression of the unfolded protein response (UPR) transcription factor XBP-1s worsens outcomes for wild-type TDP-43 animals but improves TDP-43 ΔNLS, suggesting different pathways controlling toxicity and clearance of nuclear versus cytoplasmic TDP-43. Taken together, these data support shared and distinct cellular responses to nuclear versus cytoplasmic TDP-43 localization in an intact animal nervous system. This comparative approach supports a better understanding of human disease and informs therapeutic development for pathological subtypes of TDP-43 proteinopathies.

Introduction

In 2006, TAR DNA-binding protein of 43 kDa (TDP-43) was identified as the major pathologic protein inclusion in the fatal neurodegenerative diseases amyotrophic lateral sclerosis (ALS) and frontotemporal lobar degeneration (FTLD-TDP) (Neumann et al., 2006, Arai et al., 2006). ALS is characterized by loss of upper and lower motor neurons which leads to progressive weakness of skeletal muscles, autonomic dysfunction, difficulty swallowing, speaking, and decreased respiratory function (Feldman et al., 2022), while FTLD presents with degeneration in the frontal and anterior temporal lobes of the brain, resulting in social, emotional, and behavioral changes (Grossman et al., 2023). Following the discovery of TDP-43 inclusions in ALS and FTLD-TDP, TDP-43-positive inclusions were also found as a secondary pathology in Alzheimer's disease (AD), the main cause of dementia globally (Higashi et al., 2007). The accumulation of TDP-43 aggregates in older adults, now termed limbic-predominant age related TDP-43 encephalopathy (LATE), can be a frequent co-pathology in other neurodegenerative diseases including Lewy body disease (LBD) and Huntington's disease

(Jiang et al., 2024). AD patients that have TDP-43 co-pathology have greater functional impairment, memory loss, poorer naming ability, and decreased hippocampal volume (Josephs et al., 2015). In many of these neurodegenerative diseases, TDP-43 is depleted from the nucleus and accumulates in the cytoplasm, where it undergoes post-translational modifications including hyperphosphorylation (Liao et al., 2022). Some exceptions exist, with FTLD type A exhibiting both cytoplasmic and nuclear TDP-43 aggregates and FTLD type D having nuclear but not cytoplasmic TDP-43 aggregates (Neumann et al., 2021). Cytoplasmic mislocalization of TDP-43 results in a loss of its normal nuclear functions, while gaining new functions by interacting with or disrupting cytoplasmic pathways. Similarly, a recent study implicates nuclear TDP-43 pathology as an early event preceding cytoplasmic mislocalization (Spence et al., 2024). How or why nuclear versus cytoplasmic TDP-43 aggregates occur, and whether they engage in similar pathways for disease pathogenesis and progression remains to be determined.

In healthy cells, TDP-43 is ubiquitously expressed, predominantly nuclear, and controls many aspects of RNA metabolism. In particular, it regulates mRNA splicing of thousands of transcripts (Sephton et al., 2012). TDP-43 also participates in RNA transport, transcription, and translation (Rummens and Da Cruz, 2025). In support of these roles, TDP-43 has protein domains including an N-terminal domain (NTD), nuclear localization signal (NLS), two RNA recognition motifs (RRM1 and RRM2), and a glycine rich C-terminal domain thought to regulate protein-protein interactions. TDP-43 can undergo post-translational modifications, including oxidation, acetylation, phosphorylation, zinc binding, SUMOylation, ubiquitination, cleavage, and PARylation. Most of these post translational modifications are only detected on aggregated TDP-43 in neurodegenerative disorders (Francois-Moutal et al., 2019).

TDP-43 is actively imported into the nucleus and passively exported into the cytoplasm through the nuclear pore complex. In the nucleus, TDP-43 binds RNA with a preference for GU rich sequences. Disrupting TDP-43 interactions with RNA by mutating the RNA binding domains of TDP-43 or preventing RNA transcription, splicing, binding to other RNA binding proteins, or export results in increased passive diffusion of TDP-43 through nuclear pore channels and the accumulation of TDP-43 in the cytoplasm (Duan et al., 2022). The nuclear localization signal (NLS) of TDP-43 promotes active import of TDP-43 into the nucleus by binding to nuclear import adaptor Importin α1, which recruits the receptor Importin β to form an Importin α1/β/TDP-43 complex. Mutation of the TDP-43 NLS site abrogates the ability of TDP-43 to bind to Importin α1 and eliminates active transport into the nucleus (Doll et al., 2022, Winton et al., 2008). *C.*

elegans express three Importin α homologs (IMA-1, IMA-2, and IMA-3) (Oka and Yoneda, 2018), which likely function similarly to promote TDP-43 nuclear localization.
TDP-43 is evolutionarily conserved, with a homolog in *C. elegans* designated TDP-1. TDP-1 is structurally similar to human TDP-43 but lacks a glycine-rich C-terminus. While in vertebrates TDP-43 is an essential gene (Kraemer et al., 2010, Wu et al., 2010, Sephton et al., 2010, Chiang et al., 2010), deletion of *C. elegans tdp-1* is tolerated, and does not result in apparent neuronal dysfunction. However, overexpression of TDP-1 results in an uncoordinated motor phenotype in *C. elegans* (Ash et al., 2010). To better understand the role of TDP-43 in disease, transgenic models expressing human TDP-43 throughout the *C. elegans* nervous system have been generated and characterized (Ash et al., 2010, Pir et al., 2025, Liachko et al., 2010, Eck et al., 2023). Human TDP-43 has been shown to function appropriately in *C. elegans*, with genetic mutations causing similar dysfunction in *C. elegans* as in humans (Saldi et al., 2014). Expression of human TDP-43 in *C. elegans* causes progressive motor dysfunction, neuronal loss, a shortened lifespan, and the accumulation of insoluble, post-translationally modified TDP-43 in nuclear puncta without apparent cytoplasmic accumulation (Liachko et al., 2010, Ash et al., 2010, Park et al., 2025). These models represent TDP-43 gain-of-function neurotoxicity, as their phenotypes do not recapitulate loss of *tdp-1* (Liachko et al., 2010).

To examine differences in outcomes between pathological accumulation of TDP-43 in the nucleus versus the cytoplasm, we have generated and characterized new transgenic *C. elegans* strains that express human TDP-43 with point mutations inactivating the nuclear localization sequence (TDP-43 ΔNLS). We generated three TDP-43 ΔNLS strains with varying levels of TDP-43 protein in the cytoplasm. We then compared these strains to well characterized *C. elegans* strains that express TDP-43 in the nucleus. Using neurofunctional, genetic and transcriptomic characterizations, we find shared and distinct pathogenic outcomes between nuclear versus cytoplasmic localized TDP-43. These models allow exploration of TDP-43 gain-of-function effects in the absence of loss-of-function, enabling clear dissection of pathogenic consequences with relevance to human ALS and FTLD-TDP.

Materials and Methods

Strains and transgenics

Wild-type (non-Tg) *C. elegans* (Bristol strain N2) was maintained as previously described (Brenner, 2003). A plasmid carrying human TDP-43 coding sequence downstream of

Strain abbreviations	Strain name	Strain genotype
non-Tg	N2	Wildtype
TDP-43 ΔNLS (low)	NLS152	*liaIs152[Psnb-1::TDP-43 (K82A/R83A/K84A) + Pmyo-3::dsRED]*
TDP-43 ΔNLS (med)	NLS151	*liaIs151[Psnb-1::TDP-43 (K82A/R83A/K84A) + Pmyo-3::dsRED]*
TDP-43 ΔNLS (high)	NLS142	*liaIs142[Psnb-1::TDP-43 (K82A/R83A/K84A) + Pmyo-3::dsRED]*
TDP-43-Tg	CK410	*bkIs410[Psnb-1::TDP-43; Pmyo-2::dsRED + Pmyo-2::dsRED]*
TDP-43 M337V	CK423	*bkIs423[Psnb-1::TDP-43 (M337V) + Pmyo-2::dsRED]*
CZ1200/control	CZ1200	*juIs76[unc-25p::GFP + lin-15(+) II.]*
CZ1200; TDP-43 ΔNLS (med)	CZ1200; NLS151	*juIs76[unc-25p::GFP + lin-15(+)] II] ;liaIs151[Psnb-1::TDP-43 (K82A/R83A/K84A) + Pmyo-3::dsRED]*
CZ1200; TDP-43 ΔNLS (high)	CZ1200; NLS142	*juIs76[unc-25p::GFP + lin-15(+)] II]; liaIs142[Psnb-1::TDP-43 (K82A/R83A/K84A) + Pmyo-3::dsRED]*
TDP-43-Tg 2	CK403	*bkIs403[Psnb-1::TDP-43 + Pmyo-3::GFP]*
TDP-43-Tg (low)	CK1943	*bkIs1943[Psnb-1::hTDP-43 (WT)::K4aptazyme:unc-54 3'UTR + Pmyo-3::mCherry]*
tax-6 KO	RB1667	*tax-6(ok2065)*
TDP-43 ΔNLS (med); tax-6 KO	NLS220	*tax-6(ok2065); liaIs151[Psnb-1::TDP-43 (K82A/R83A/K84A) + Pmyo-3::dsRED]*
TDP-43-Tg; tax-6 KO	NLS221	*tax-6(ok2065); bkIs410[Psnb-1::TDP-43 + Pmyo-3::dsRED]*
tax-6 GOF	KJ306	*tax-6(jh107)*
TDP-43 ΔNLS (med); tax-6 GOF	NLS268	*tax-6(jh107); liaIs151[Psnb-1::TDP-43 (K82A/R83A/K84A) + Pmyo-3::dsRED]*
TDP-43-Tg; tax-6 GOF	NLS269	*tax-6(jh107); bkIs410[Psnb-1::TDP-43 + Pmyo-3::dsRED]*
xbp-1s o/ex	AGD927	*uthIs270[Prab-3::xbp-1s+ Pmyo-2::tdTomato]*
TDP-43 ΔNLS (med); xbp-1s o/ex	NLS234	*uthIs270[Prab-3::xbp-1s+ Pmyo-2::tdTomato]; liaIs151[Psnb-1::TDP-43 (K82A/R83A/K84A) + Pmyo-3::dsRED]*
TDP-43 ΔNLS (high); xbp-1s	CK2961	*uthIs270[Prab-3::xbp-1s+ Pmyo-2::tdTomato]; liaIs142[Psnb-1::TDP-43(K82A/R83A/K84A) + Pmyo-3::dsRED]*
TDP-43-Tg-2 ; xbp-1s o/ex	CK2994	*uthIs270[Prab-3::xbp-1s+ Pmyo-2::tdTomato]; bkIs403[Psnb-1::TDP-43 + Pmyo-3::GFP]*
TDP-43-Tg (low); xbp-1s o/ex	CK1943;AGD927	*uthIs270[Prab-3::xbp-1s+ Pmyo-2::tdTomato]; bkIs1943[Psnb-1::hTDP-43 (WT)::K4aptazyme:unc-54 3'UTR + Pmyo-3::mCherry]*
tau-Tg; xbp-1s o/ex	CK933	*uthIs270[Prab-3::xbp-1s+ Pmyo-2::tdTomato]; bkIs144[Paex-3::Tau WT (4R1N) + Pmyo-2::GFP]*
tau-Tg	CK144	*bkIs144[Paex-3::Tau WT (4R1N) + Pmyo-2::GFP]*
zip-2(ok3730)	VC3056	*zip-2(ok3730)*
TDP-43 ΔNLS (high); zip-2(ok3730)	NLS271	*zip-2(ok3730); liaIs142[Psnb-1::TDP-43 (K82A/R83A/K84A) + Pmyo-3::dsRED]*
TDP-43-Tg; zip-2(ok3730)	NLS272	*zip-2(ok3730); bkIs410[Psnb-1::TDP-43 + Pmyo-3::dsRED]*
TDP-43-Tg 3	CK402	*bkIs402[Psnb-1::TDP-43 + Pmyo-2::GFP]*
tdp-1 KO	CK3053	*tdp-1(bk3053)*
TDP-43 ΔNLS (med); tdp-1 KO	NLS273	*tdp-1(bk3053); liaIs151[Psnb-1::TDP-43 (K82A/R83A/K84A) + Pmyo-3::dsRED]*
TDP-43-Tg 3; tdp-1 KO	NLS274	*tdp-1(bk3053); bkIs402[Psnb-1::TDP-43 + Pmyo-2::GFP]*
srrt-1	CK3138	*srrt-1(bk3138)*
TDP-43 ΔNLS (med); srrt-1 KO	NLS151; CK3138	*srrt-1(bk3138); liaIs151[Psnb-1::TDP-43 (K82A/R83A/K84A) + Pmyo-3::dsRED]*
TDP-43 ΔNLS M337V	NLS217	*liaIs151[Psnb-1::TDP-43 (K82A/R83A/K84A/M337V) + Pmyo-3::dsRED]*

Table 1. complete list of all strains used in this chapter 1

the pan-neuronal *C. elegans snb-1* promoter underwent site-directed mutagenesis (Agilent Quikchange) to incorporate three point mutations K82A/R83A/K84A (Keating et al., 2023), generating TDP-43 ΔNLS. As previously described (Han et al., 2024), multicopy integrated transgenes were produced by microinjection of transgene marker and the transgene into the germline of N2adults, followed by integration and outcrossing. Three strains, NLS152, NLS151, and NLS142, were categorized by TDP-43 protein level into TDP-43 ΔNLS (low), TDP-43 ΔNLS (med), and TDP-43 ΔNLS (high).

Additional strains used include CK410 (TDP-43-Tg), CK403 (TDP-43-Tg 2), CK402 (TDP-43-Tg 3), CK1943 (TDP-43-Tg (low), CK423 (TDP-43 M337V), AGD927 (xbp-1s o/ex), RB1667 (tax-6-KO), KJ306 (tax-6 GOF), CK3053 (tdp-1 KO), VC3056 (zip-2(ok3730)), and CZ1200 (Control [Unc-25p::GFP]). CK410, CK403, CK402, CK1943, and CK423 use a P_{snb-1} pan-neuronal promoter to drive human wild-type TDP-43 or TDP-43 M337V expression. The

strain CZ1200 (a gift from Dr. Y. Jin, University of California, San Francisco, CA) has an integrated p_{unc-25}::GFP transgene expressed in GABAergic neurons that marks cell bodies and axons (Cinar et al., 2005). NLS152, NLS151, and NLS142 were crossed with CZ1200 to generate TDP-43 ΔNLS low, medium, and high strains that have GFP labeled GABAergic neurons. CK144 uses the P_{aex-3} pan-neuronal promoter to drive expression of human WT Tau (4R1N). AGD927 expresses constitutively active XPB-1s under a P_{rab-3} pan-neuronal promoter. AGD927 was crossed with nuclear and cytoplasmic TDP-43 strains as well as a tau strain. See Table 1 for a complete list of all strains used in this chapter

Immunoblotting

Stage matched day 1 adult *C. elegans* were harvested into 50μl pellets and flash frozen in liquid nitrogen. Pellets were resuspended in 1x sample buffer, sonicated 3 X 60% amplitude for 10 sec, and boiled for 10 min. 4-10μl of samples were loaded into 4–15% Criterion™ Tris-HCl Protein Gels (BioRad), and transferred onto PVDF membrane. TDP-43 was detected by monoclonal Anti-TDP43 antibody (ab190963[EPR18554], Abcam, 1:1000), pTDP-43 was detected by monoclonal Anti-phospho TDP-43 (pS409/410, CAC-TIP-PTD-M01A, CosmoBio, 1:1000), tubulin was detected by monoclonal antibody E7 (Developmental Studies Hybridoma Bank, 1:5000). Secondary antibodies used were Sheep anti-Mouse IgG peroxidase-linked whole antibody Secondary Antibody (Cytiva, 45-000-692, 1:5000) and Donkey anti-Rabbit IgG, peroxidase-linked species-specific whole antibody Secondary Antibody (Cytiva, 45-000-682, 1:10000). Signal was visualized on film using ECL (Clarity Western ECL Substrate 1705061) in a 1:1 ratio for up to 15 minutes. Quantification was completed in Image J using densitometry of scanned film.

C. elegans immunohistochemistry

Slides were coated with poly-L-lysine and baked at 60°C for 40 min. Day 1 adult animals were washed with M9 and then transferred into 5μl droplet of 1% PFA. After 5 min, animals were compressed under a cover slip. Slides were left on a dry-ice chilled metal block for 30 min. The cover slip was quickly removed to tear away upper levels of *C. elegans* cuticle, and slides were dipped in ice cold methanol for 5 min, followed by acetone for 5 min. Slides entered a humidified chamber for block, antibody incubation steps, and counterstain. Fixed whole animals were stained with anti-TAR DNA-binding protein 43 (TDP-43) (AbCam, ab57105) at a titer of 1:500. ALEXA 647-conjugated anti-mouse antibody was used as the secondary antibody at a titer of 1:1000. Slides were counterstained with 300 nM 4,6-diamidino-2-phenylindole (DAPI)

nuclear stain in PBS. Images were acquired on Andor Dragonfly 200 100 × oil immersion lens (Andor UK, Bellfast). Images were processed in FIJI:imageJ from 30.72x30.72 micron (512x512) ROI OEM TIFF files.

Motility assays

Radial locomotion (crawling) and thrashing (swimming) assays were conducted on unstimulated staged-matched day 1 adult *C. elegans* at room temperature as previously described (Currey and Liachko, 2021). In brief, for an individual radial locomotion assays, 10-15 worms were placed in the center of a 10 cm NGM plate with OP-50 bacteria (food source) and allowed to crawl freely on the plate for an hour, and linear distance measured from the starting point. Radial locomotion assays are conducted in duplicate on an individual testing day (n = 20-30), and with three independent testing days (N=3), for a total n = 60-90 animals. For thrashing assays, roughly 50 *C. elegans* were transferred in 1 ml M9 buffer onto 35mm NGM assay plates. Worms were recorded for 1 min at 14 frames per second by WormLab system (MBF Bioscience). Swimming tracks were verified post recording and repaired as needed. Thrashing assays are conducted on three independent testing days (N=3), for an estimated total n = 150 animals. Figures from radial locomotion and thrashing are from at least three independent biological replicates per genotype.

Neurodegeneration

Live day 1 adult worms were placed on a 3% agarose pad and immobilized with 0.01% sodium azide. GABAergic neurons were counted using fluorescence microscopy using a 60x objective on an upright microscope (Leica DM4 B). Scoring was conducted blinded to the genotype. Neuronal death, axonal defasciculation, gaps in the continuity of the nerve cord, and non-neuronal puncta were scored as signs of neurodegeneration. Figures are from at least three independent replicates. Representative images of axonal defasciculation, gaps in the continuity of the nerve cord were taken using the Andor Dragonfly at 100x and processed in FIJI.

RNA extraction

RNA was extracted from snap-frozen *C. elegans* pellets using the Thermo Fisher Scientific TRIzol RNA extraction protocol. RNA was resuspended in nuclease free water, run on an agarose gel to assess integrity, and concentration was assessed using a NanoPhotometer NP80 spectrophotometer (Implen GMbH).

qRT-PCR

Day 1 adult *C. elegans* cDNA was synthesized from RNA using iScript Reverse Transcription Supermix for RT-qPCR (Bio-Rad) and a T100 Thermal Cycler (Bio-Rad). Controls include no-RT supermix without the reverse transcriptase enzyme, and no template reaction mix. cDNA samples and no-RT controls were mixed with SYBR supermix and primers for TDP-43, *act-1*, or *rpl-32* and run on a CFX Connect RT-PCR Detection System (Bio-Rad). The strain CK423 was used to make a standard curve, using concentrations of 100ng, 10ng, 1ng, and 0.1ng of cDNA. All experimental samples and controls were run at 10ng of cDNA per well.

RNA sequencing

RNA extracted from L4 stage *C. elegans* was assembled into poly-A enriched libraries and sequenced at a read-depth of 25 million pair-end reads per sample as a fee-for-service (Novogene). FASTQ files were pre-processed with FASTP (version 0.23.4) (Chen et al., 2018), aligned with STAR two-pass-mapping (version 2.7.10b) (Dobin et al., 2013), and quantified with featureCounts (version 2.20.0) in R (version 4.4.2) without multi-mapping reads (Liao et al., 2014) against the *C. elegans* genome WBcel235 (version 113) (Harrison et al., 2024). Differential gene expression was calculated with DESeq2 (version 1.46.0) (Love et al., 2014) in R (version 4.4.2) (Team, 2021). Transcription factor activity was estimated with CelEsT (version 1.0) (Perez, 2024) in R (version 4.4.2) (Team, 2021) using decoupleR (version 2.12.0) (Badia-I-Mompel et al., 2022) and the recommended database of TF-target pairs from previously generated differential gene expression data. Differential mRNA splicing was calculated for both annotated and novel splicing sites with SpliceWiz (version 1.8.0) (PMC10753292) and DESeq2 (version 1.46.0) (Love et al., 2014) in R (version 4.4.2) (Team, 2021) with default SpliceWiz filters. All visualizations were created with ggplot2 (version 3.5.1) (Wickham, 2016) in R (version 4.4.2) (Team, 2021).

Statistical analysis

All data was analyzed using GraphPad Prism software, unless otherwise described. Statistical significance was determined using one-way ANOVA with Tukey's multiple comparison test. Error bars on graphs represent standard error of the mean. P-values were expressed as: * ($p<0.05$), **($p<0.01$), ***($p<0.001$), ****($p<0.0001$) and ns is not statistically significant ($p>0.05$).

Results

It has been previously shown that wild-type human TDP-43 expressed in *C. elegans* (TDP-43-Tg) is strongly localized to the nucleus (Liachko et al., 2010). To characterize differences between the gain-of-function consequences of nuclear versus cytoplasmic TDP-43, we developed new *C. elegans* models with cytoplasmic-localized TDP-43, referred to as TDP-43 ΔNLS. TDP-43 ΔNLS was created by adding three point mutations (K82A/R83A/K84A) in the nuclear localization sequence of TDP-43, consistent with mammalian TDP-43 ΔNLS models generated previously (Walker et al., 2015, Winton et al., 2008) (Fig. 6A). Using this strategy, we established three TDP-43 ΔNLS strains with differing levels of transgene expression referred to as TDP-43 ΔNLS (low), TDP-43 ΔNLS (med), and TDP-43 ΔNLS (high).

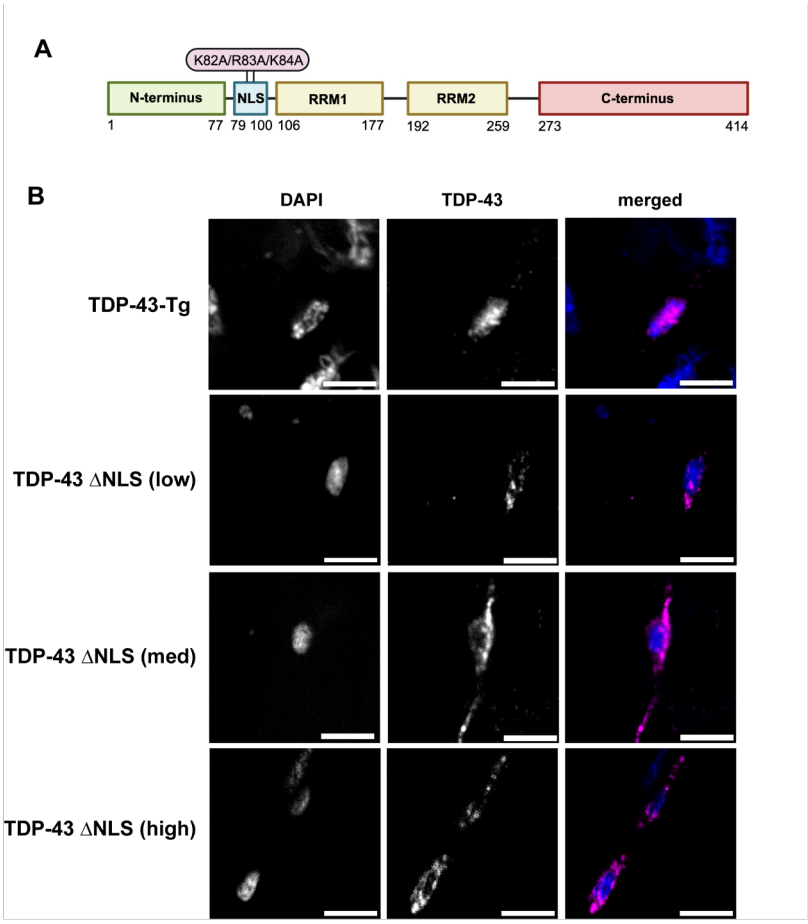

Fig. 6. TDP-43 is localized in the cytoplasm and not the nucleus in TDP-43 ΔNLS worms. (A) TDP-43 protein domains including the N-terminus, nuclear localization signal (NLS), RNA recognition motifs (RRM1 and RRM2), and C-terminus. The location of inactivating point mutations within the NLS are shown. **(B)** Immunostaining for nuclei (DAPI) and total TDP-43 in day 1 adult nerve cord of TDP-43-Tg, and TDP-43 ΔNLS (low), TDP-43 ΔNLS (medium), and TDP-

TDP-43 ΔNLS is localized to the cytoplasm

To confirm localization of TDP-43 in the TDP-43 ΔNLS strains, we performed TDP-43 immunohistochemistry with nuclear counterstaining in four strains: TDP-43-Tg (expresses wild-type human TDP-43), TDP-43 ΔNLS (low), TDP-43 ΔNLS (med), and TDP-43 ΔNLS (high) (Fig. 6B). In these strains, TDP-43 ΔNLS (low), TDP-43 ΔNLS (med), and TDP-43 ΔNLS (high) appeared predominantly cytoplasmic, more closely resembling the cytoplasmic distribution of TDP-43 in human disease, while TDP-43-Tg was strongly nuclear, consistent with previously published results (Fig. 6B, Fig. 7).

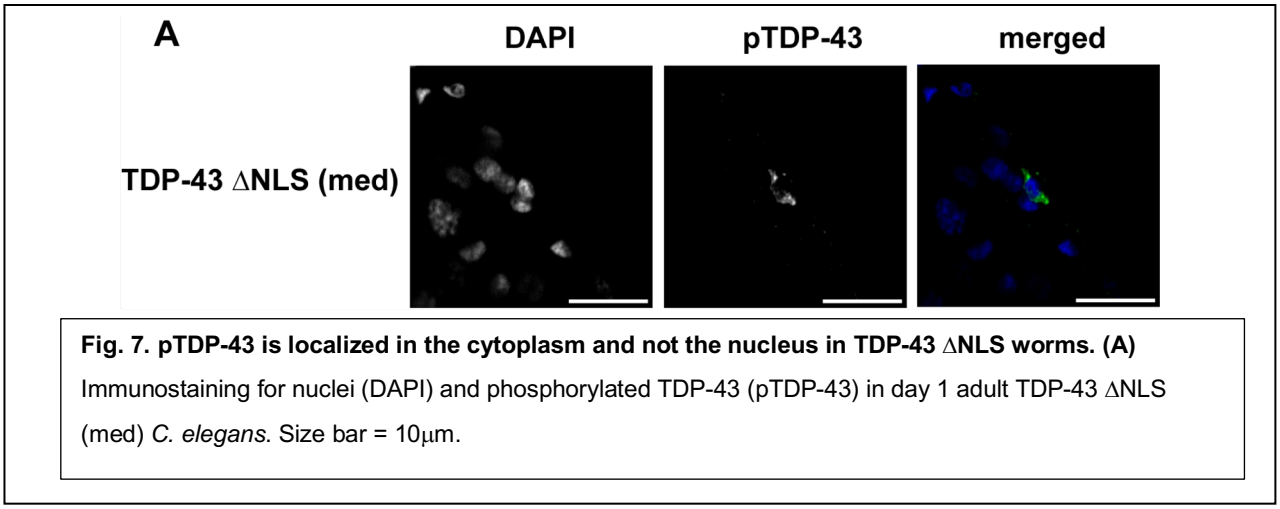

Fig. 7. pTDP-43 is localized in the cytoplasm and not the nucleus in TDP-43 ΔNLS worms. (A) Immunostaining for nuclei (DAPI) and phosphorylated TDP-43 (pTDP-43) in day 1 adult TDP-43 ΔNLS (med) *C. elegans*. Size bar = 10μm.

TDP-43 ΔNLS strains exhibit dose-responsive neurotoxicity

We performed several measures to characterize TDP-43 ΔNLS strains. To determine expression levels of TDP-43, we performed immunoblot analyses on stage matched day 1 adult populations of animals. We determined the three TDP-43 ΔNLS strains had varying levels of TDP-43 expression and were designated TDP-43 ΔNLS (low), TDP-43 ΔNLS (med), and TDP-43 ΔNLS (high) based on detected protein (Fig. 8A-C, Fig. 9). As comparators we included well-characterized *C. elegans* strains expressing wild-type TDP-43 (TDP-43-Tg) or familial ALS (fALS) mutant TDP-43 (TDP-43 M337V) (Liachko et al., 2010).

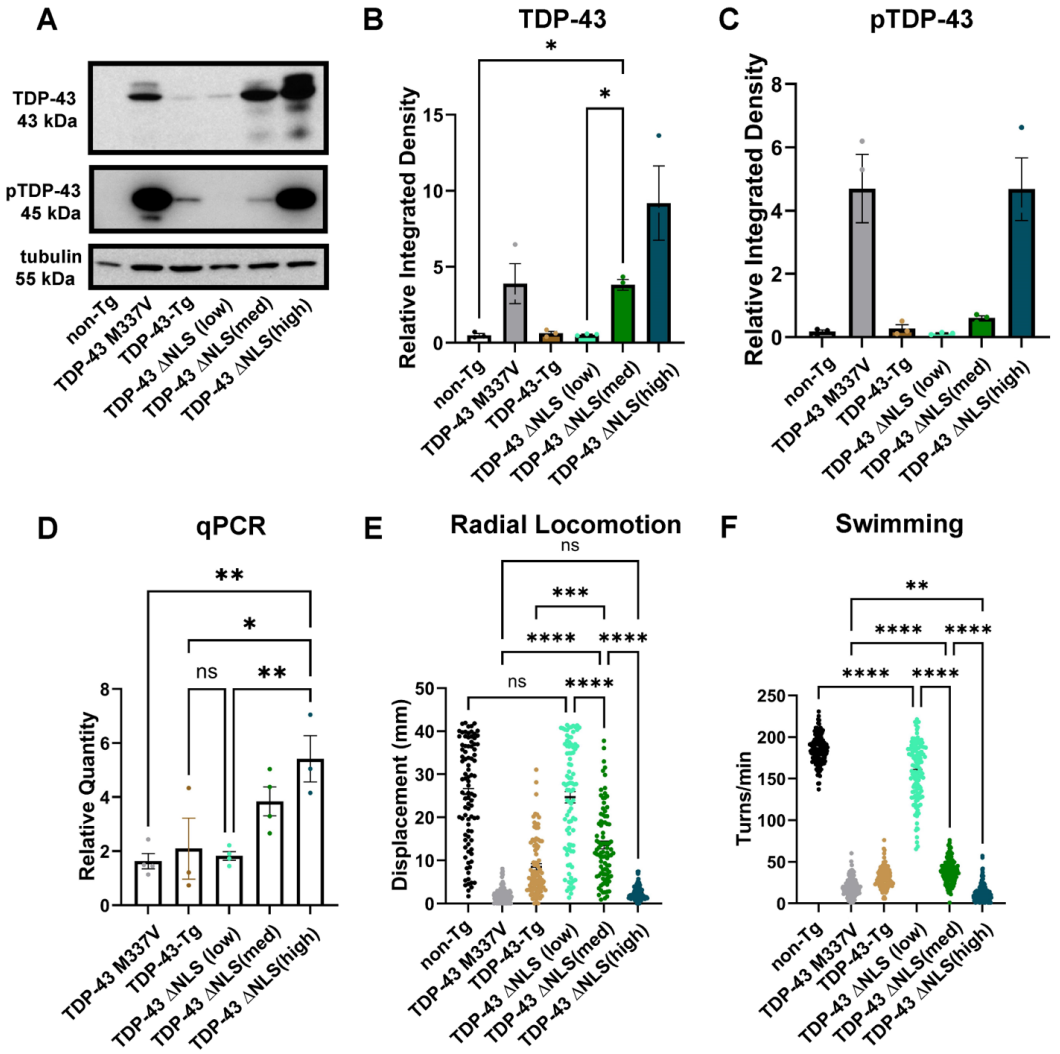

Fig. 8. TDP-43 ΔNLS causes dose-dependent motility impairment. (A) Synchronized day 1 adult *C. elegans* were tested by immunoblot for total TDP-43, phosphorylated TDP-43, and tubulin (load control). Immunoblot is representative of three independent biological replicates. **(B-C)** Quantification of protein levels from scanned film images. *p<0.05 **(D)** qRT-PCR of TDP-43 expression in day 1 adult *C. elegans*. *act-1* mRNA was used as an internal expression control. TDP-43 mRNA was highest in the TDP-43 ΔNLS (high) strain. *p<0.05, **p<0.01. **(E-F)** Motility impairment of TDP-43 ΔNLS as measured by **(E)** radial locomotion (linear distance crawling in one hour on an agar plate) or **(F)** swimming (rates of thrashing in liquid for a minute). Higher levels of cytoplasmic TDP-43 resulted in decreased crawling and fewer turns/minute. One-way ANOVA with Tukey's multiple comparison test. **p<0.01, ***p<0.001, ****p<0.0001. ns, not significant. Data are mean ± s.e.m.

We found that TDP-43 ΔNLS (low) had low levels of TDP-43 that were clearly detected upon overexposure (Fig. 9). There was no detectable pTDP-43 in TDP-43 ΔNLS (low) upon

overexposure (data not shown). TDP-43 ΔNLS (med) had similar levels of TDP-43 as TDP-43 M337V but much less pTDP-43. TDP-43 ΔNLS (high) had roughly twice as much TDP-43 as TDP-43 M337V and comparable levels of pTDP-43 as TDP M337V (Fig. 8A-C).

We also determined mRNA expression levels of TDP-43 ΔNLS (low), TDP-43 ΔNLS (med), and TDP-43 ΔNLS (high) using quantitative reverse transcription PCR (qRT-PCR) (Fig. 8D). mRNA levels of the TDP-43 ΔNLS strains followed similar trends as protein quantity, with increasing levels of TDP-43 mRNA corresponding to higher amounts of protein detected (Fig. 8A-D).

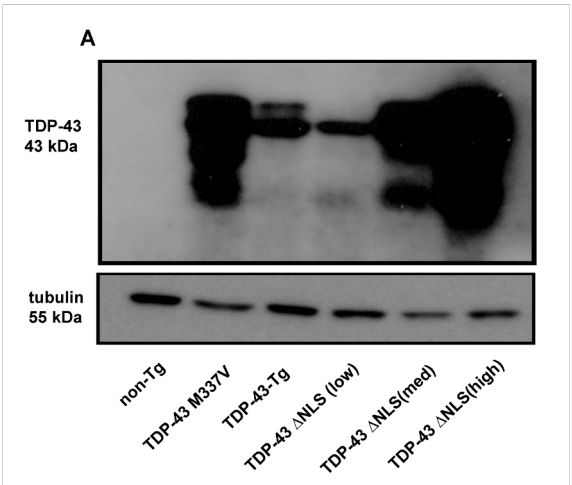

Fig. 9. TDP-43 is visible in TDP-43 ΔNLS (low) but not non-Tg control in long exposure. (A) Synchronized day 1 adult *C. elegans* were tested by immunoblot for total TDP-43, and left overnight to maximize signal on film. TDP-43 is visible in all the lanes other than the non-Tg lane.

Neuronal dysfunction corresponds to expression level of TDP-43 ΔNLS

Motility of *C. elegans* can serve as a sensitive readout of neuronal function (Zhen and Samuel, 2015) and has been used to quantify neuronal dysfunction and neurodegeneration in models of neurodegenerative diseases (Kraemer et al., 2003, Koopman et al., 2024). To quantify motility defects in TDP-43 ΔNLS strains, we performed two assays: radial locomotion for assessment of the ability to crawl on a solid agar surface, and swimming testing the ability to thrash in liquid (Currey and Liachko, 2021, Pierce-Shimomura et al., 2008). Radial locomotion and swimming both give a readout of GABAergic and cholinergic neurons, as well as associated circuits responsible for movement initiation, propagation, and cessation (Koopman et al., 2024, Currey and Liachko, 2021).

For both radial locomotion and swimming, our TDP-43 ΔNLS strains had an inverse relationship with TDP-43 protein levels; with TDP-43 ΔNLS (low) having near normal motility,

TDP-43 ΔNLS (med) having moderate impairment, and TDP-43 ΔNLS (high) having severe impairment (Fig. 8E-F). Surprisingly, TDP-43 ΔNLS (med) had similar crawling and swimming as TDP-43-Tg (Fig. 8E-F) even though the strain has significantly more total TDP-43 protein (Fig. 8A-B). Likewise, TDP-43 ΔNLS (high) had similar crawling and swimming as TDP-43 M337V (Fig. 8E-F) despite accumulating more TDP-43 protein (Fig. 8B-C). However, levels of pTDP-43 are comparable between TDP-43 ΔNLS (med) and TDP-43-Tg, and between TDP-43 ΔNLS (high) and TDP-43 M337V, which may support previous findings that abundance of pTDP-43 correlates with neurotoxicity in *C. elegans* (Liachko et al., 2010).

To examine whether the endogenous *C. elegans* homolog of TDP-43, *tdp-1*, contributes to motility defects in TDP-43 ΔNLS, we crossed *tdp-1(bk3053)*, a CRISPR-generated whole-gene deletion of *tdp-1,* with a TDP-43 ΔNLS (med) and TDP-43-Tg 3. However, we did not see any significant differences in motility in the absence of *tdp-1* (Fig. 10).

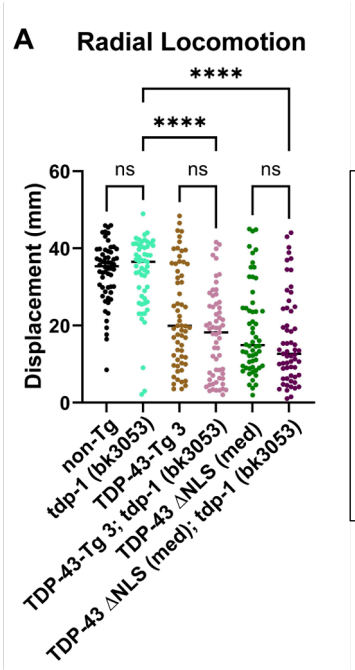

Fig. 10. *tdp-1 KO* does not alter motility in nuclear or cytoplasmic TDP-43 strains. (A) Motility of *tdp-1 KO* day 1 adults was measured by radial locomotion (linear distance crawling in one hour on an agar plate). Neither TDP-43-Tg 3 nor TDP-43 ΔNLS (med) strains exhibited altered motility in the presence of *tdp-1(bk3053)*. One-way ANOVA with Tukey's multiple comparison test. ****p<0.0001. ns, not significant. Data are mean ± s.e.m.

High levels of cytoplasmic phosphorylated TDP-43 cause neurodegeneration

TDP-43 ΔNLS (med) and TDP-43 ΔNLS (high) have clear motility defects, indicating possible neurodegeneration. GABAergic neurons control *C. elegans* motility (Schuske et al., 2004) and are vulnerable to TDP-43-Tg and TDP-43 M337V (Liachko et al., 2010). To examine the integrity of GABAergic neurons in TDP-43 ΔNLS, we used a transgenic reporter that expresses GFP in the 19 GABAergic neurons (*unc-25p::GFP*) to visualize and quantify changes

in GABAergic neurons (Liachko et al., 2010). *C. elegans* have 19 D-type GABAergic motor neurons. Control animals (*unc-25p::GFP*) had intact GABAergic neurons and axons with a continuous nerve cord, no non-neuronal puncta, and no visual signs of neurodegeneration (Fig. 11A,B). TDP-43 ΔNLS (med) worms appeared similar to controls, but about half of the worms had one fewer GABAergic neuron (Fig. 11A,C). However, TDP-43 ΔNLS (high) animals

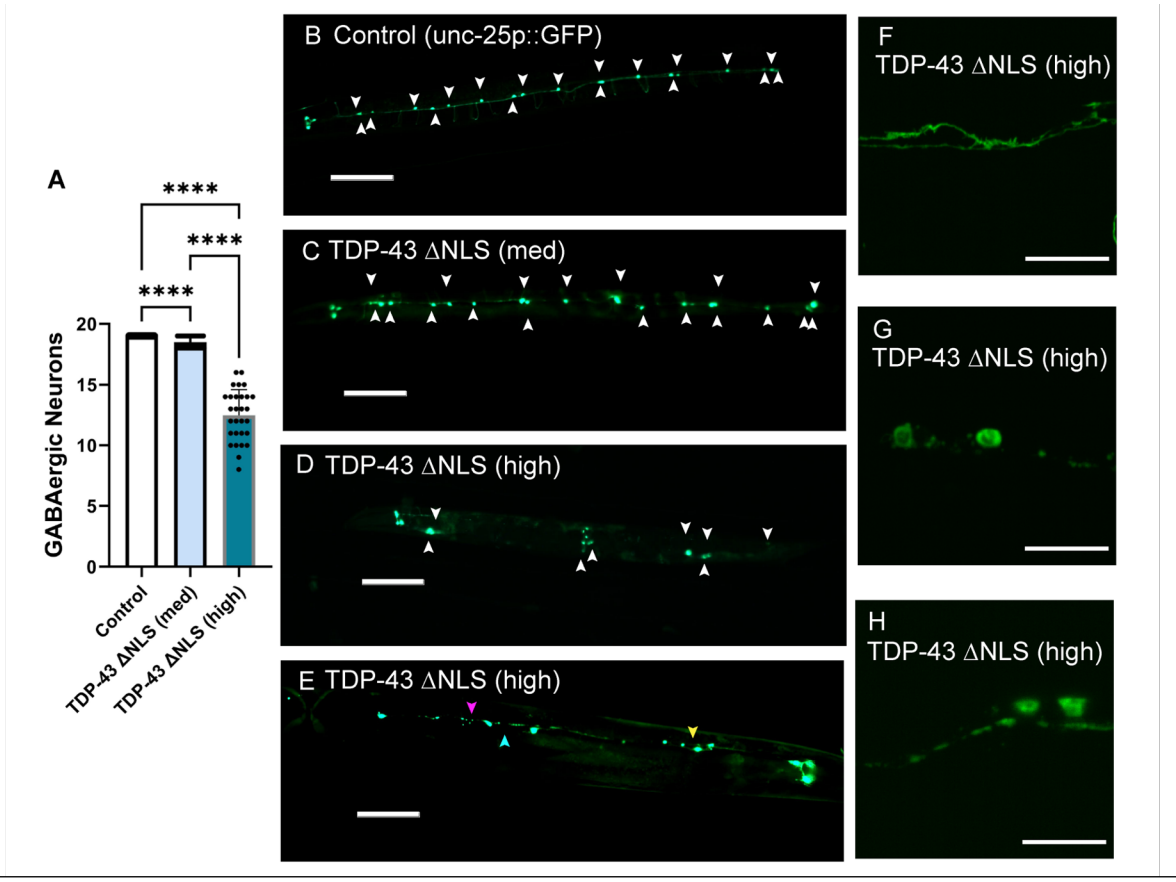

Fig. 11. TDP-43 ΔNLS causes loss of GABAergic neurons in a dose dependent manor. GABAergic neurons were counted *in vivo* in TDP-43 ΔNLS (high) and TDP-43 ΔNLS (med) strains using an *unc-25p::GFP* reporter. Neuronal death, axonal defasciculation, gaps in the continuity of the nerve cord, and non-neuronal puncta along the nerve cord were scored signs of neurodegeneration. **(A)** Number of GABAergic neurons present, with TDP-43 ΔNLS (med) (n=20) and TDP-43 ΔNLS (high) (n=19) having respectively 0.5 and 6.5 neurons less than the control (n=30). **(B-E)** A representative nerve cord in control **(B)**, TDP-43 ΔNLS (med) **(C)**, and TDP-43 ΔNLS (high) **(D)**. White arrows point to each GABAergic neuron. Scale bar = 80μM. **(E)** Examples of the neurodegenerative changes in a TDP-43 ΔNLS (high) worm. The yellow arrows point at axonal defasciculation, magenta arrow points at non-neuronal puncta, and the turquoise arrow points at gaps in the nerve cord. Scale bar = 40μM. **(F-H)** Representative images of axonal defasciculation **(F)**, non-neuronal puncta **(G)**, and gaps in the nerve cord **(H)** in TDP-43 ΔNLS (high). Scale bar = 10μM.

exhibited much more neurodegeneration, with an average of 6.5 fewer GABAergic neurons than the control (Fig. 11A,D). In addition to loss of GABAergic neurons, we also saw axonal defasciculation, gaps in the continuity of the nerve cord, and non-neuronal puncta along the nerve cord in all TDP-43 ΔNLS (high) worms analyzed (Fig. 11E-H).

Transcriptome differences between models of cytoplasmic versus nuclear TDP-43

To determine the molecular consequences of nuclear and cytoplasmic TDP-43 in *C. elegans*, we performed RNA sequencing on polyA-enriched RNAs from TDP-43-Tg and TDP-43 ΔNLS (med) at the L4 stage. Overall, there were relatively few transcriptomic differences among TDP-43 ΔNLS, TDP-43-Tg, or N2 controls. These results are consistent with principal component analysis (PCA) where the groups are largely overlapping (Fig. 12A).

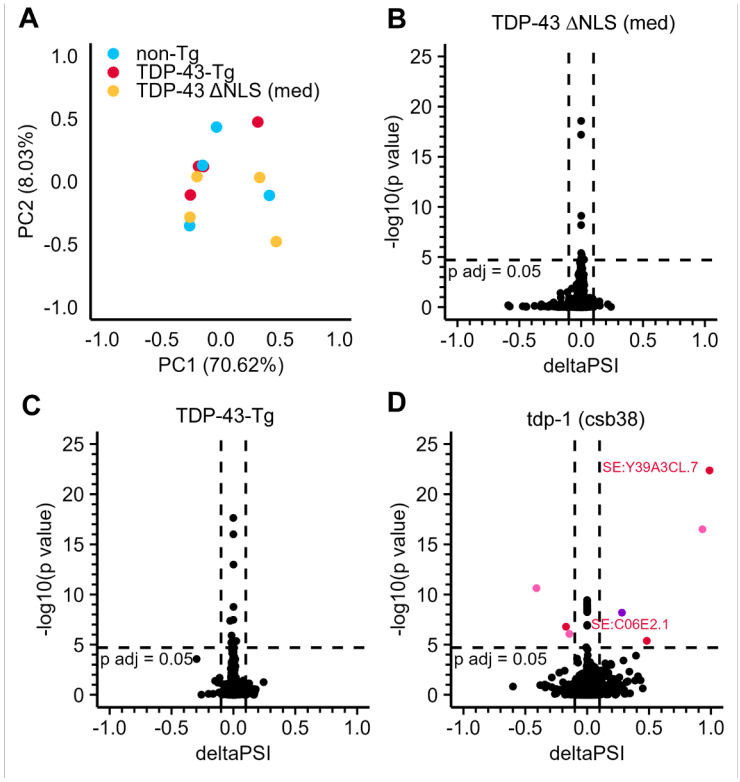

Fig. 12. (A) Principal component analysis of gene expression in TDP-43 ΔNLS (med) Tg, TDP-43-Tg, and non-Tg controls (n = 12). **(B)** A volcano plot of differential RNA splicing in TDP-43 ΔNLS (med) Tg animals compared to non-Tg controls (n =8). **(C)** A volcano plot of differential RNA splicing in TDP-43-Tg animals compared to non-Tg controls (n =8). **(D)** A volcano plot of differential RNA splicing in tdp-1(csb38) null animals compared to non-Tg controls re-analyzed from (Taylor et al., 2023)(n =6)

However, compared to stage-matched non-Tg controls, TDP-43 ΔNLS (med) animals significantly differentially expressed 11 genes (p adj < 0.05 & |log2 fold change| > 1.0) (Fig. 13A, Table 2A) including the downregulation of immunoglobulin *zig-2*, which can be secreted from

neurons to influence axon maintenance and interact with insulin (Benard et al., 2009, Nawrocka

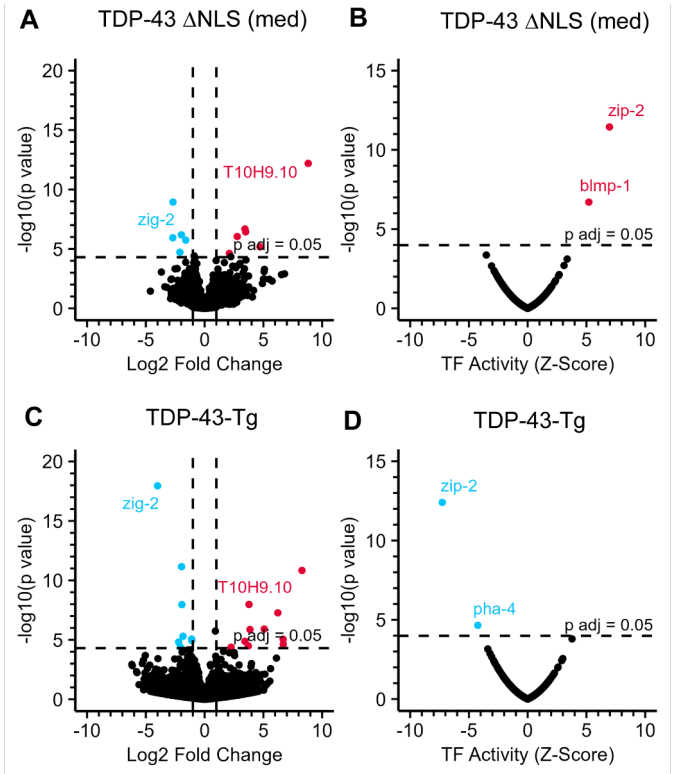

Fig. 13. Differential gene expression in nuclear and cytoplasmic TDP-43 strains. **(A)** A volcano plot of differential gene expression in TDP-43 ΔNLS (med) Tg animals compared to wildtype controls (n = 8). **(B)** A volcano plot of estimated differential transcription factor activity in TDP-43 ΔNLS (med) Tg animals compared to non-Tg controls (n = 8). **(C)** A volcano plot of differential gene expression in TDP-43-Tg animals compared to non-Tg controls (n = 8). **(D)** A volcano plot of estimated differential transcription factor activity in TDP-43-Tg animals compared to non-Tg controls (n = 8). **(A-D)** Dotted line represents threshold for p adj = 0.05.

et al., 2024). To gain insight into the compensatory or effector cellular signals initiated by cytoplasmic TDP-43 aggregation and responsible for driving gene expression changes, we performed transcription factor (TF) network analysis to estimate significantly differentially active TFs using the computational tool CelEst (p adj < 0.05) (Perez, 2024). We found that the stress and infection-sensing TF ZIP-2 (Kniazeva and Ruvkun, 2025) and cell-death regulator BLMP-1

A

Name	log2FoldChange	pvalue	padj
T10H9.10	8.818152963	6.42E-13	1.10E-08
zig-2	-2.691845251	1.15E-09	9.84E-06
Y102A5C.35	3.432829389	2.10E-07	0.00119868
C38D9.2	3.496354024	3.67E-07	0.00156801
exh-1	-1.976278665	6.49E-07	0.00221905
Y68A4A.12	2.776086143	9.09E-07	0.00259077
C46G7.5	-2.709382741	1.15E-06	0.00281585
Y75B8A.44	-1.60323168	1.82E-06	0.00390017
clec-237	4.711855256	6.68E-06	0.01268468
C36C5.12	-2.104036218	1.92E-05	0.03283578
Y48G1BM.6	2.101896255	2.39E-05	0.03709238

B

Name	Score	pvalue	padj
zip-2	6.95909	3.58E-12	1.74E-09
blmp-1	5.204153	1.98E-07	9.63E-05
vab-3	-3.520785	0.00043165	2.10E-01
elt-7	3.363436	0.00077187	3.76E-01
elt-1	3.094456	0.00197567	9.62E-01
syd-9	-3.075387	0.00210639	1.00E+00
nhr-76	-2.864203	0.00418687	1.00E+00
xbp-1	-2.783288	0.00538839	1.00E+00
cebp-1	2.680008	0.00737075	1.00E+00
nhr-234	-2.644483	0.00819079	1.00E+00

Table 2. (A) Differential gene expression and (B) estimated transcription factor activity in TDP-43 ΔNLS (med) animals.

(Jiang et al., 2021) displayed an upregulation of their predicted target genes in TDP-43 ΔNLS (med) animals (Fig. 13B, Table 2B).

We also performed RNA sequencing on TDP-43-Tg animals which accumulate nuclear soluble and insoluble TDP-43. We found TDP-43-Tg animals significantly differentially express 19 genes relative to non-Tg controls (Fig. 13C, Table 3A), sharing five with TDP-43 ΔNLS (med) animals including *zig-2*. We estimated 2 TFs had significantly decreased activity in TDP-43 animals (Fig. 13D, Table 3B), including ZIP-2 and the forkhead box PHA-4. Notably, ZIP-2's activity is reversed compared to that in TDP-43 ΔNLS (med) animals.

A

Name	log2FoldChange	pvalue	padj
zig-2	-4.002190591	1.12E-18	2.22E-14
ttr-39	-1.96481429	7.09E-12	7.06E-08
T10H9.10	8.28571584	1.47E-11	9.77E-08
Y102A5C.35	3.777120596	1.06E-08	4.33E-05
Y75B8A.44	-1.937628265	1.09E-08	4.33E-05
Y71G12B.28	6.231190555	5.35E-08	0.00017765
clec-237	5.070868312	1.24E-06	0.003374835
Y102A5C.5	3.859399791	1.36E-06	0.003374835
mtch-1	0.915608928	1.84E-06	0.0040604
R02C2.7	-1.836457328	5.00E-06	0.009945071
cyp-34A9	-1.106196747	8.62E-06	0.015069163
col-51	6.685190244	9.08E-06	0.015069163
C53B7.3	-1.091880762	1.14E-05	0.017435524
Y102A5C.6	3.430034126	1.34E-05	0.019038426
adh-1	-2.210613109	1.53E-05	0.020317347
col-183	6.695198838	2.44E-05	0.030370891
Y102A5C.43	3.718065345	3.23E-05	0.037855116
W09G12.7	-2.062567896	4.03E-05	0.043864416
C30G12.1	2.251569271	4.19E-05	0.043864416

B

Sequence	Name	Score	pvalue	padj
K02F3.4	zip-2	-7.265695	3.91E-13	1.90E-10
F38A6.1	pha-4	-4.241581	2.23E-05	1.09E-02
F25D7.3	blmp-1	3.775763	0.000160185	7.80E-02
C11G6.4	nhr-28	-3.39442	0.000689667	3.36E-01
C34H3.2	odd-2	-3.382289	0.000720831	3.51E-01
K02D7.2	snai-1	-3.204189	0.0013575	6.61E-01
H10E21.3	nhr-80	-3.059791	0.002219149	1.00E+00
Y102A5C.18	efl-1	2.991259	0.002783184	1.00E+00
W09C2.1	elt-1	2.93586	0.003331705	1.00E+00
M6.3	pha-2	2.902188	0.003711499	1.00E+00
Y38E10A.18	nhr-234	-2.902075	0.003712836	1.00E+00
T07C12.11	madf-4	2.895335	0.003793456	1.00E+00
F31E3.1	ceh-20	-2.829062	0.004675164	1.00E+00
F56F11.3	klf-1	-2.755942	0.005859979	1.00E+00
C25A1.11	aha-1	-2.604023	0.009223484	1.00E+00
F22D3.1	ceh-38	2.588447	0.009651055	1.00E+00

Table 3. (A) Differential gene expression and (B) estimated transcription factor activity in TDP-43-Tg animals.

To examine the inverse relationship between estimated ZIP-2 transcription factor activity in TDP-43 ΔNLS versus TDP-43-Tg, we crossed a partial deletion of the *zip-2* coding sequence, *zip-2(ok3730)* into these strains. We tested whether ZIP-2 transcription factor activity modifies TDP-43 phenotypes by evaluating motility of TDP-43 ΔNLS; zip-2(ok3730) and TDP-43-Tg; zip-2(ok3730). However, we found that there were no significant differences between these strains and controls (Fig. 14), suggesting that ZIP-2 transcription factor activity is not promoting either neuroprotective or neurodegenerative outcomes.

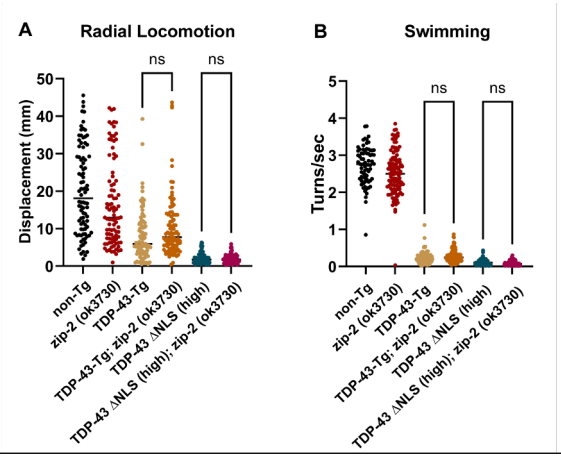

Fig. 14. *zip-2(ok3730)* does not alter motility in nuclear or cytoplasmic TDP-43 strains. Motility of *zip-2(ok3730)* day 1 adults was measured by **(A)** radial locomotion (linear distance crawling in one hour on an agar plate) and **(B)** swimming in liquid. Neither TDP-43-Tg nor TDP-43 ΔNLS (high) strains exhibited altered motility in the presence of *zip-2(ok3730)*. One-way ANOVA with Tukey's multiple comparison test. ns, not significant. Data are mean ± s.e.m.

To identify the relative contribution of gain-of-function and loss-of-function mechanisms to TDP-43 toxicity in *C. elegans,* we also performed RNA splicing analysis on our RNA sequencing from TDP-43 ΔNLS (med) and TDP-43-Tg animals and previously published RNA sequencing from *tdp-1(csb38)* null animals (Taylor et al., 2023). We found that TDP-43 ΔNLS (med) and TDP-43-Tg animals did not significantly alter the splicing of any events (p adj < 0.05 & |deltaPSI| > 0.1) (Fig. 12B,C). Consistent with known effects of TDP-43 loss of function, the loss of *tdp-1* did alter splicing, including exon retention events (12. D). The excessive activity of nuclear TDP-43 is associated with an increase in exon-skipping (Carmen-Orozco et al., 2024), which we did not observe in TDP-43-Tg animals. Taken together, these transcriptomic analyses suggest both shared and distinct cellular responses to the presence of cytoplasmic versus nuclear TDP-43 aggregation. Our transcriptomic data does not support a major role for altered RNA splicing to be driving the molecular mechanisms for TDP-43-driven.

Calcineurin phosphatase activity protects against both nuclear and cytoplasmic TDP-43

Phosphorylation of TDP-43 S409/S410 is consistently present in familial and sporadic TDP-43 proteinopathies (Neumann et al., 2009), and in *C. elegans* potentiates worsened motility (Liachko et al., 2010). The phosphatase calcineurin directly binds and dephosphorylates TDP-43, reducing accumulation of phosphorylated TDP-43 (Liachko et al., 2016a). *C. elegans* has a single homolog of calcineurin, TAX-6. Loss of function mutations in *tax-6* result in severely

worsened motility defects in TDP-43-Tg and TDP-43 M337V (Liachko et al., 2016a). To test whether calcineurin/*tax-6* similarly influences cytoplasmic TDP-43, we crossed *tax-6(ok2065)* to TDP-43-Tg and TDP-43 ΔNLS (med). In the absence of functional *tax-6*, both TDP-43-Tg and TDP-43 ΔNLS (med) strains had significantly increased total and phosphorylated TDP-43, worsened radial locomotion and swimming (Fig. 15A-D). These data support TAX-6 mediated protection against phosphorylation-driven neurotoxicity of both cytoplasmic and nuclear TDP-43.

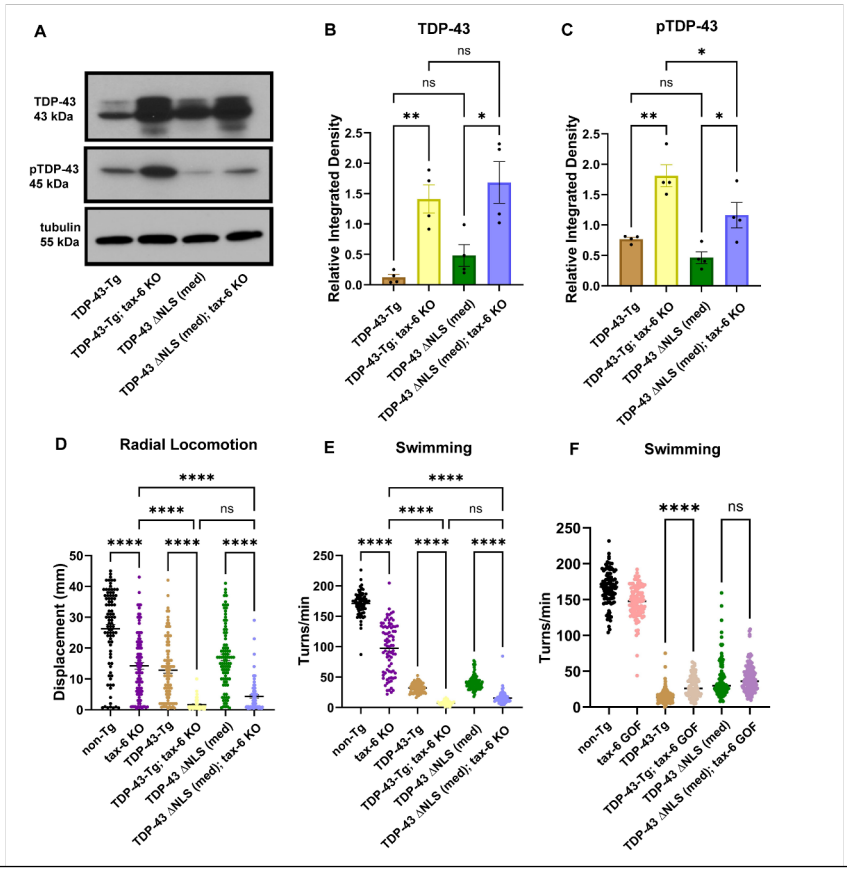

Fig. 15. *tax-6* controls TDP-43 phosphorylation levels in both *nuclear* and cytoplasmic TDP-43 strains. **(A)** Synchronized populations of day 1 adult *C. elegans* were tested by immunoblot for total TDP-43, phosphorylated TDP-43**,** and tubulin (load control). Immunoblots shown are representative of four independent biological replicates. **(B-C)** Quantification of protein levels from four independent biological replicates. *p<0.05, **p<0.01. ns, not significant. **(D-E)** *tax-6 KO* day 1 adult motility as measured by **(D)** radial locomotion (linear distance crawling in one hour on an agar plate) or **(E)** swimming (rates of thrashing in liquid for a minute). TDP-43-Tg and TDP-43 ΔNLS (med) strains were both equally affected by *tax-6 KO*. **(F)** *tax-6 GOF* motility measured by swimming. Motility impairment of TDP-43-Tg but not TDP-43 ΔNLS (med) strains were partly rescued by tax-6 GOF. One-way ANOVA with Tukey's multiple comparison test. ****p<0.0001. ns, not significant. Data are mean ± s.e.m.

We also tested whether a constitutively active *tax-6* gain-of-function mutant, tax-6 GOF, could protect against TDP-43-Tg and TDP-43 ΔNLS (med) motility defects. We found this was able to partly rescue TDP-43-Tg but not TDP-43 ΔNLS (med) (Fig. 15E), which may reflect differences in constitutive TAX-6 activity in the nucleus versus cytoplasm, differing contributions of phosphorylated TDP-43 to toxicity in TDP-43-Tg versus TDP-43 ΔNLS, or variability due to the relatively low levels of phosphorylated TDP-43 at baseline in these strains.

XBP-1s differentially modifies cytoplasmic versus nuclear TDP-43 in *C. elegans* neurotoxicity.

Proteostatic endoplasmic reticulum (ER) stress initiates the unfolded protein response (UPR^{ER}), resulting in expression of the active form of the transcription factor X-box binding protein, XBP-1s (Calfon et al., 2002). In aging *C. elegans,* expression of XBP-1s activates the UPR^{ER}, enables resistance to ER stress, and extends lifespan (Taylor and Dillin, 2013). In some neurodegenerative disease models, XBP-1 activation triggers the UPR^{ER} protecting against tau neurotoxicity (Loewen and Feany, 2010, Kraemer et al., 2006, Waldherr et al., 2019, Duran-Aniotz et al., 2023). To determine whether XBP-1s modifies nuclear or cytoplasmic TDP-43

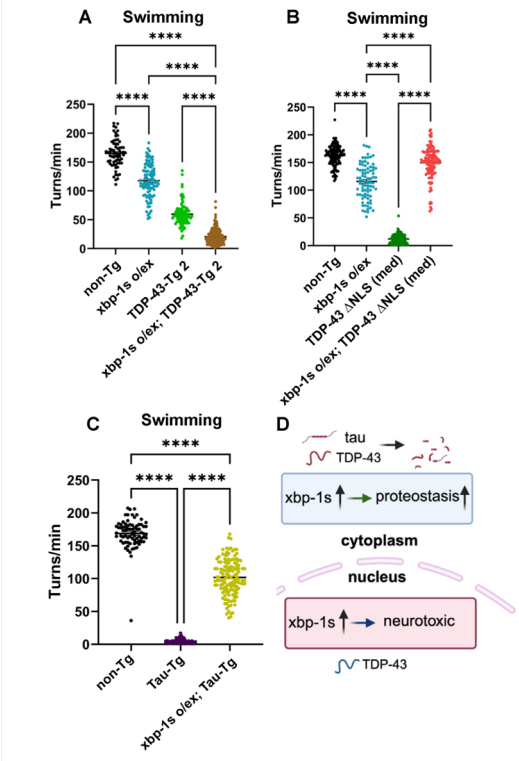

Fig. 16. *xbp-1s* overexpression protects against cytoplasmic TDP-43 but worsens outcomes for nuclear TDP-43 strains. (A-C) *xbp-1s o/e* driven motility changes of day 1 adults as measured by swimming (rates of thrashing in liquid for a minute). *xbp-1s o/ex* **(A)** worsened swimming in TDP-43-Tg-2 but rescued swimming in **(B)** TDP-43 ΔNLS (med) and **(C)** tau-Tg. **(D)** Schematic of XBP-1s activation outcomes targeting nuclear versus cytoplasmic TDP-43. Increasing XBP-1s increases proteostasis to protect against TDP-43 and tau in the cytoplasm, but leads to increased neurotoxicity when TDP-43 is nuclear. Higher levels of XBP-1s is only beneficial when dealing with cytoplasmic proteinopathies. One-way ANOVA with Tukey's multiple comparison test. ****p<0.0001. Data are mean ± s.e.m.

phenotypes, we crossed an established transgenic *xbp-1s* overexpression strain (*xbp-1s o/ex)* with TDP-43-Tg and TDP-43 ΔNLS to generate double transgenic strains TDP-43-Tg; *xbp-1s*

o/ex and TDP-43 ΔNLS; *xbp-1s o/ex.* Using swimming as readout of neuronal dysfunction, we found that increased XBP-1s worsened motility in two independent TDP-43-Tg strains (Fig. 16, Fig. 17), but improved two independent TDP-43 ΔNLS strains (TDP-43 ΔNLS (med) Fig. 16B, and TDP-43 ΔNLS (high) Fig. 17B,C).

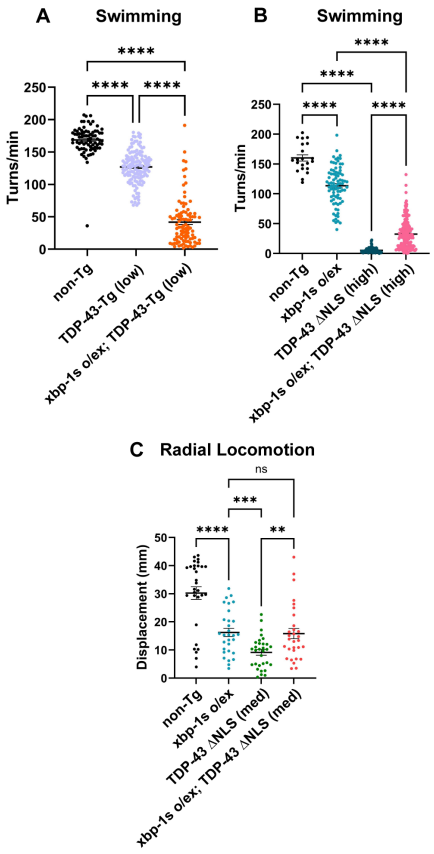

Fig. 17. *xbp-1s* overexpression protects against cytoplasmic TDP-43 but worsens outcomes for nuclear TDP-43 strains. (A-C) *xbp-1s o/ex* driven motility changes of day 1 adults as measured by swimming (rates of thrashing in liquid for a minute) and radial locomotion (linear distance crawling in one hour on an agar plate). *xbp-1s o/ex* **(A)** worsened swimming in TDP-43-Tg (low) but improves swimming in **(B)** TDP-43 ΔNLS (high). *xbp-1s o/ex* **(C)** improves radial locomotion in TDP-43 ΔNLS (med). One-way ANOVA with Tukey's multiple comparison test. **p<0.01, ***p<0.001, ****p<0.0001. ns, not significant. Data are mean ± s.e.m.

To confirm *xbp-1s o/ex* was behaving consistently with prior published work (Waldherr et al., 2024, Waldherr et al., 2019), we crossed it with a *C. elegans* model expressing wild-type human tau pan-neuronally (tau-Tg). In tau-Tg; *xbp-1s o/ex* animals, we saw a robust improvement in swimming (Fig. 16C), consistent with prior publications. Taken together, our data suggests that the location of toxic pTDP-43, whether it is in the nucleus or the cytoplasm, influences cellular responses and mechanisms of clearance (Fig. 16D).

We were curious if a TDP-43 with an ALS causing mutation, such as M337V, would behave the same way in the cytoplasm as in the nucleus. We created a TDP-43 ΔNLS M337V strain (Table 1) that has a similar amount of total TDP-43 to TDP-43 M337V but much less pTDP-43 (Fig. 18A,B). We ran behavior on these strains and found TDP-43 ΔNLS M337V to have much better motility than TDP-43 M337V (Fig. 18C). This motility difference could be

partially due to TDP-43 ΔNLS M337V being cytoplasmic but it's likely that the low levels of pTDP-43 make TDP-43 ΔNLS M337V less toxic. It is possible cytoplasmic TDP-43 aggregates do not get phosphorylated as much as nuclear TDP-43 aggregates.

The lab has performed RNAseq on TDP-43 M337V and found that L4 developmental stage, TDP-43 M337V animals significantly differentially express 398 genes compared to N2 controls (Fig. 18D). This is much more than the 19 differentially expressed genes seen in TDP-43-Tg animals (Table 3A). We plan to perform RNAseq on TDP-43 ΔNLS M337V to determine if cytoplasmic TDP-43 M337V has a similar differential gene expression to nuclear TDP-43 M337 or cytoplasmic TDP-43.

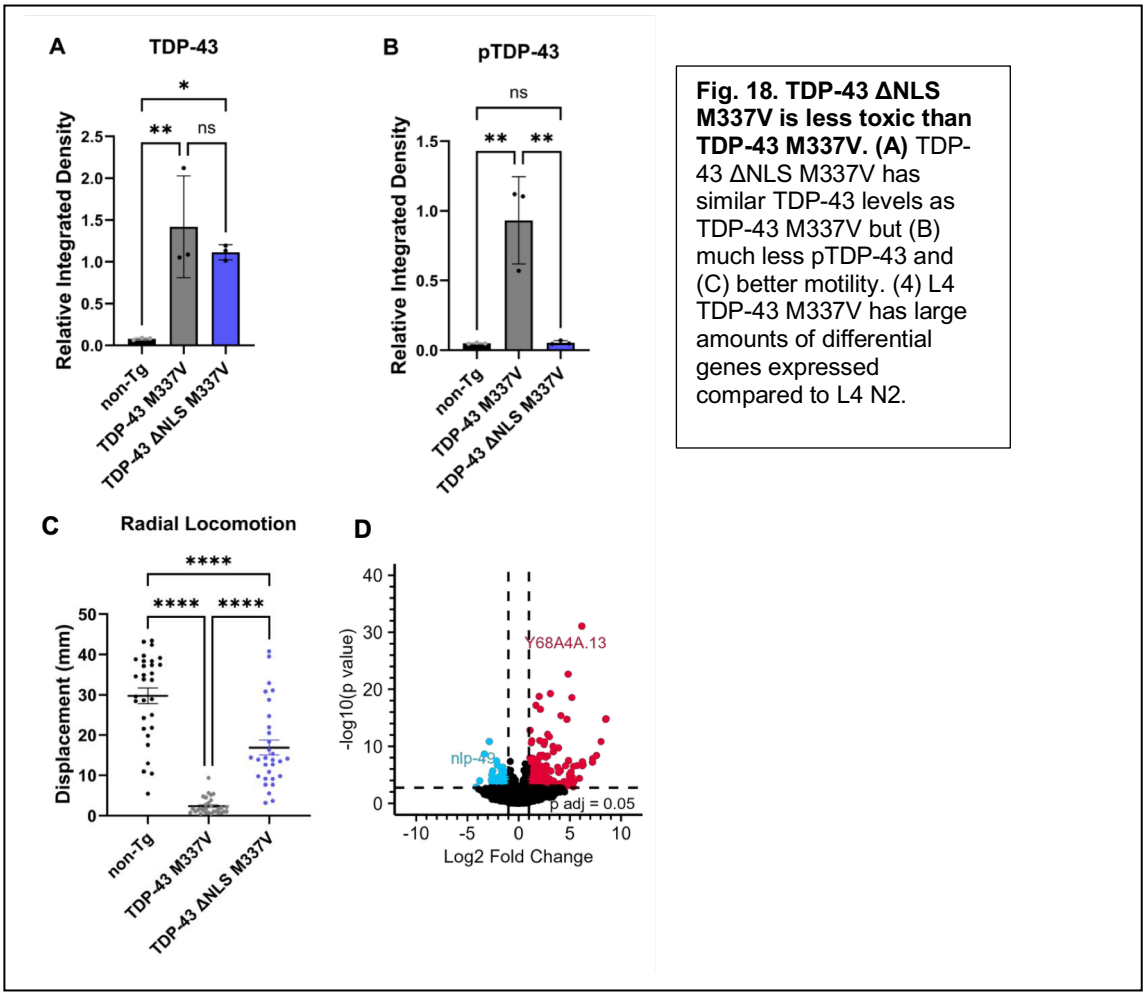

Fig. 18. TDP-43 ΔNLS M337V is less toxic than TDP-43 M337V. (A) TDP-43 ΔNLS M337V has similar TDP-43 levels as TDP-43 M337V but (B) much less pTDP-43 and (C) better motility. (4) L4 TDP-43 M337V has large amounts of differential genes expressed compared to L4 N2.

When studying disease causing proteins in neurodegenerative diseases it can be very helpful to find suppressors of those proteins (Kraemer and Schellenberg, 2007, Currey et al., 2023, Kow et al., 2022). Our lab often studies suppressors of TDP-43 and tau but we do not know if these suppressors would also suppress cytoplasmic TDP-43. KO of Srrt-1 has been

shown to suppress tau and TDP-43 in C. elegans (data not shown). Srrt-1 is a RNA binding partner of nuclear cap-binding complex and helps determine mRNA fate (Lykke-Andersen et al., 2021) When crossing TDP-43 ΔNLS worms with Srrt-1 KO worms we also saw suppression of the TDP-43 ΔNLS phenotype (Fig. 19). Trying to find more TDP-43 ΔNLS suppressors will be useful to studying cytoplasmic TDP-43. We will also look for suppressors of nuclear TDP-43 in C. elegans that will not work on TDP-43 ΔNLS, allowing for us to uncover more differences between cytoplasmic and nuclear TDP-43.

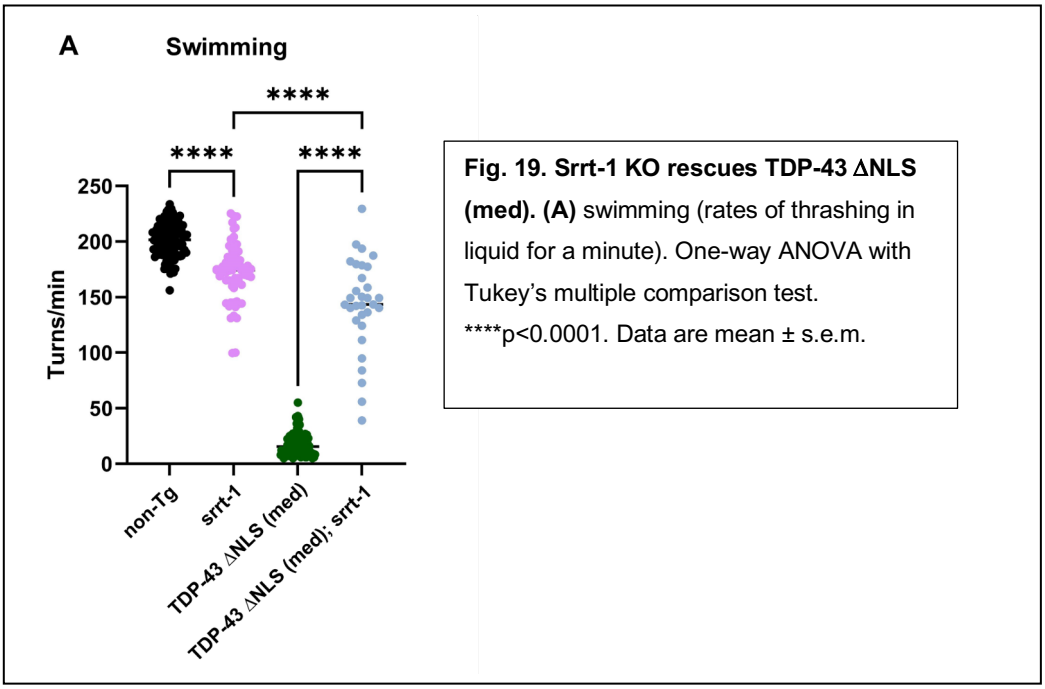

Fig. 19. Srrt-1 KO rescues TDP-43 ΔNLS (med). (A) swimming (rates of thrashing in liquid for a minute). One-way ANOVA with Tukey's multiple comparison test. ****p<0.0001. Data are mean ± s.e.m.

Discussion

Although TDP-43 can form cytoplasmic or nuclear pathologic protein inclusions in FTLD-TDP (Neumann et al., 2006), little is known about whether disease processes differ based on localization of pathology. Expression of human TDP-43 in *C. elegans* neurons provides a tractable, gain-of-function system to dissect disease mechanisms (Wolozin et al., 2011, Liachko et al., 2010, Pir et al., 2025). However, previously generated strains accumulate TDP-43 predominantly in the nucleus. To address this question, we have developed new transgenic *C. elegans* models that accumulate cytoplasmic TDP-43, enabling comparative evaluations of nuclear versus cytoplasmic localized TDP-43.

In this study, we mutated the TDP-43 NLS to generate three *C. elegans* strains that accumulate predominantly cytoplasmic localized TDP-43. We compared these cytoplasmic

TDP-43 strains to previously existing, well characterized nuclear TDP-43 strains to identify similarities and differences in neurotoxic phenotypes, cellular responses, and protein homeostasis mechanisms. These data provide important insights into FTLD-TDP biology, and represent a new system to better understand TDP-43 in disease.

From our characterization of TDP-43 ΔNLS strains, we found dose-dependent toxicity of cytoplasmic TDP-43 (Fig. 8). Interestingly, cytoplasmic TDP-43 appears to cause less severe motility deficits at equivalent protein levels than nuclear TDP-43. When there were similar amounts of cytoplasmic and nuclear TDP-43, the strains with nuclear TDP-43 had more severe motility defects indicating greater neuronal dysfunction. However, burden of phosphorylated TDP-43 correlated with motility deficits similarly whether nuclear or cytoplasmic (Fig. 8). Likewise, loss-of-function mutation in *tax-6*, the *C. elegans* homolog of the TDP-43 phosphatase calcineurin, worsened both TDP-43-Tg and TDP-43 ΔNLS (med) strains and led to increased accumulation of phosphorylated TDP-43 (Fig. 15). In mouse models of TDP-43 proteinopathy, robust calcineurin depletion occurs during disease course (Waldherr et al., 2026, Davis et al., 2017). In patients with ALS, calcineurin activity is decreased (Ferri et al., 2004, Wagey et al., 1997), supporting loss of this neuron resilience factor as a contributor to worsened disease outcomes. Our *C. elegans* data suggest that TDP-43 phosphorylation is toxic regardless of subcellular localization, and that calcineurin/ *tax-6* mechanisms controlling toxicity of phosphorylated TDP-43 are shared between the nucleus and the cytoplasm.

At high expression levels of cytoplasmic TDP-43, we observed severe neurodegeneration with prominent GABAergic neuronal loss, axonal defasciculation, gaps in the continuity of the nerve cord, and GFP-positive puncta along the nerve cord (Fig. 11). We found mild neurodegeneration in the medium expressing TDP-43 ΔNLS strain, with only about half of the worms developing detectable neuronal loss (Fig. 11A).

When comparing RNA transcriptome data from nuclear versus cytoplasmic TDP-43 strains, we found few differentially expressed genes and no alterations to RNA splicing. Transcription factor network analysis did suggest an opposite regulation of the transcription factor ZIP-2 between these strains, supporting distinct cellular responses to cytoplasmic versus nuclear TDP-43. In nuclear-localized TDP-43-Tg, ZIP-2 targets were decreased, but in cytoplasmic-localized TDP-43 ΔNLS, ZIP-2 targets were increased (Fig. 13). ZIP-2 is an immune response effector in *C. elegans* (Estes et al., 2010) that has also been shown to be activated due to age-related mitochondrial dysfunction in *C. elegans* and stalled translation elongation (Hahm et al., 2020, Kniazeva and Ruvkun, 2025). TDP-43 has been previously implicated in mitochondrial health and function (Wang et al., 2016, Huang et al., 2020, Xu et al., 2010). Looking more into

the effect of TDP-43 on mitochondrial function between nuclear and cytoplasmic TDP-43 would be telling if there are mitochondrial differences. Blocking on of the mitochondrial targeting sequences, such as M5 (294-300), would cause TDP-43 to not localize to mitochondria (Wang et al., 2016). We can make TDP-43-Tg M5 and TDP-43 ΔNLS M5 mutants to look at mitochondrial changes in nuclear vs cytoplasmic TDP-43. We can also see if the M5 mutation changes ZIP-2 targets.

To follow up the RNAseq, we determined a partial deletion of *zip-2* failed to impact motility phenotypes of TDP-43-Tg or TDP-43 ΔNLS, which may indicate that transcriptomic changes are not the major driver of phenotypes observed in this model. While the transcriptomic changes are minimal in nuclear and cytoplasmic strains expressing TDP-43, there are much more transcriptomic changes in the nuclear TDP-43 M337V model (Fig. 18D). We will need to run RNAseq on TDP-43 ΔNLS M337V to see if TDP-43 M337V also has large transcriptomic changes in the cytoplasm.

ER stress can be triggered by accumulation of misfolded or unfolded proteins in the cytoplasm and in the ER lumen, resulting in activation of the unfolded protein response (UPR^{ER}). During activation of the UPR^{ER}, XBP1 mRNA becomes alternatively spliced into the activated form XBP1s, which then increases transcription of genes related to degrading misfolded proteins (He et al., 2024). Reduced XBP-1 exacerbates neurotoxicity in tau models of *D. melanogaster* (Loewen and Feany, 2010) and *C. elegans* (Kraemer et al., 2006), while overexpressing XBP-1s is neuroprotective in tau models of *C. elegans* (Waldherr et al., 2019, Waldherr et al., 2024). Interestingly, we found divergent effects of *xbp-1s* overexpression on nuclear versus cytoplasmic expressing TDP-43 strains. *xbp-1s* suppressed neurotoxic motility phenotypes of cytoplasmic TDP-43 ΔNLS strains, but worsened motility of nuclear TDP-43-Tg strains (Fig. 16, Fig 17). The neuroprotection against cytoplasmic TDP-43 aligns with its ability to protect against tau, another cytoplasmic accumulating aggregating protein. However, it is not clear why increased *xbp-1s* results in worsened outcomes for strains with nuclear-localized TDP-43. It is possible an *xbp-1s* mediated increase in cytoplasmic protein clearance decreases cellular ability to respond and clear nuclear proteins. This contrast between *xbp-1s* overexpression driving either a protective or worsened reaction based on the location of TDP-43 in the cell highlights potential differences in disease mechanisms or cellular responses to pathological variation in human disease. Nuclear versus cytoplasmic TDP-43 inclusions may be physical manifestations of differences in disease etiology, progression, or cellular responses among individuals critical for effective treatments. The *C. elegans* models described here provide a comparative study of outcomes from TDP-43 pathologic localization, enabling a

greater understanding of TDP-43 in normal and disease states essential for development of effective therapies.

Chapter 2: Using point mutations to alter TDP-43 domains in a gain of function *C. elegans* model to better understand its neurotoxic synergy with tau

Introduction

Limbic-predominant age related TDP-43 encephalopathy (LATE) is often comorbid with Alzheimer's disease (AD), especially with older patients (Nelson et al., 2019). Roughly half of Alzheimer's disease (AD) patients have TDP-43 aggregates along with amyloid β plaques and neurofibrillary tangles that contain phosphorylated tau (p-tau) (Jo et al., 2020). The presence of TDP-43 aggregates in AD brains correlate with increased cognitive impairment and brain atrophy (Butler Pagnotti et al., 2023, Nelson et al., 2019). It has also been shown that TDP-43 and p-tau interact and are associated with each other using biological approaches (Tome et al., 2021) and AD cases with TDP-43 have an increased burden of pre-tangles and phosphorylated tau (Tome et al., 2023).

In *C. elegans*, our lab has shown the co-expression of human tau and human TDP-43 caused selective neuronal loss and increased neuronal dysfunction compared to either protein alone (Latimer et al., 2022). While there is an observed neurotoxic synergy between TDP-43 and tau, there is little understanding of the mechanism behind the synergy. Chapter 2 seeks to identify the mechanism responsible for the neurotoxic synergy between tau and TDP-43 in AD. To accomplish this, we looked at the domains and functions of TDP-43, and if putative loss-of-function mutations would alter the neurotoxicity with tau. We generated and characterized TDP-43; tau transgenic lines that have mutations in TDP-43 domains. The TDP-43 mutants that we looked at included mutations that altered post translational modifications (PTM), RNA binding, oligomerization, and nuclear location. We found post-translational modifications, as well as the cellular location of TDP-43 to be important in the neurotoxic synergy with tau. We have started trying to replicate our findings by crossing our TDP-43 mutant strains into a second tau-Tg *C. elegans* strain. We have also started investigating singular TDP-43 post translational modification sites, to confirm the potential mechanism of synergy.

TDP-43 is composed of a N-terminal domain (NTD), nuclear localization signal (NLS), two RNA recognition motifs (RRM1 and RRM2), and a C-terminal domain, and can undergo many PTMs (Fig. 1) (Francois-Moutal et al., 2019). PTM such as acetylation, phosphorylation, SUMOylation, ubiquitination, and Poly ADP-ribosylation (PARylation) can change the function of

TDP-43 and play a role in pathogenic TDP-43 (Fig. 5) (Neumann et al., 2009, Verde et al., 2025, Cohen et al., 2015, Duan et al., 2019).

The N-terminal domain (NTD), amino acids 1-77, can form dimers and oligomers, with the reversible formation of polymers being required for splicing activity as well as phase separation and liquid droplet formation (Francois-Moutal et al., 2019). The nuclear localization signal (NLS), amino acids 78-100, links the NTD to the RRM1. The NLS is important for TDP-43 localizing in the nucleus and can undergo post translational modifications, such as PARylation, acetylation, and ubiquitination (Winton et al., 2008, Francois-Moutal et al., 2019, Hans et al., 2018). Acetylation of Lysine 82 alters the ability of TDP-43 to bind to importin-α1, resulting in cytoplasmic mislocalization of TDP-43 ((Ko et al., 2024). Acetylation of Lysine 84 can also reduce nuclear import and cytoplasmic mislocalization of TDP-43 (Khosravi et al., 2020). Many of these amino acids of TDP-43 can undergo multiple PTM, making the study of their effects complex. For example, Lysine 84 is also a novel ubiquitination site for TDP-43 (Hans et al., 2018).

The N-terminal domain is also involved in TDP-43 self-oligomerization (Chang et al., 2012). There is not much known about the role of TDP-43 oligomerization. TDP-43 oligomerization is required for some alternative splicing (Jiang et al., 2017), could be an intermediate species providing scaffolding for formation of aggregates (French et al., 2019), or helps keep TDP-43 in the nucleus preventing cytoplasmic aggregation (Perez-Berlanga et al., 2023).

Poly(ADP-ribose) polymerase (PARP) can link ADP ribosyl units, forming large negatively charged branched Poly-ADP-ribose (PAR) polymers (Francois-Moutal et al., 2019). PARylation is linked to DNA damage repair, RNA biology, metabolism, cellular stress, and the unfolded protein response (Gupte et al., 2017). In *Drosophila*, reduction of Tankyrase, a PARP, reduced cytoplasmic accumulation of TDP-43. TDP-43 has PAR binding motifs located in its NLS, that allow it to bind PAR. This non-covalent binding leads to liquid-liquid phase separation of TDP-43, which is a requirement for TDP-43 accumulation in stress granules (McGurk et al., 2018b). Stress granules accumulate RNA-binding proteins that regulate stability and translation of mRNA when under stress (Leung et al., 2011). PAR-binding motifs are important for promoting granulo-filamentous aggregation of TDP-43, with PAR binding causing TDP-43 to make thread like fibrils (McGurk et al., 2018b, McGurk et al., 2018a).

RNA recognition motifs (RRM1 and RRM2), amino acids 106-177 and 192-259, are required for nucleic acid binding (Francois-Moutal et al., 2019). TDP-43 binds both mRNA and DNA, making it important for gene transcription and regulating mRNA, stability, and translation

(Cohen et al., 2011). TDP-43 can undergo SUMOylation of lysine 136 in RRM1, altering TDP-43 splicing activity, localization, and exon skipping (Maurel et al., 2020, Maraschi et al., 2021). Lysine 136 can also be acetylated, resulting in impaired RNA binding and splicing of TDP-43 leading to phase separation (Garcia Morato et al., 2022). Acetylation of lysine 145, in the RRM1 domain, can drive neuronal dysfunction, aberrant splicing, and transcription of genes (Necarsulmer et al., 2023). In the RRM2 domain TDP-43 can undergo acetylation of K192, hindering nuclear acid binding (Cohen et al., 2015).

The TDP-43 C-terminal domain (CTD), amino acids 260-414, is important for hnRNP binding, self regulation, is the location of most of the phosphorylation sites, and is involved with many disease-linked mutations (Francois-Moutal et al., 2019, Mackenzie and Rademakers, 2008). TDP-43 is able to downregulate it's own mRNA transcript levels through the C-terminal region 321-366. (Ayala et al., 2011). TDP-43 has 64 potential phosphorylation sites (Eck et al., 2021), with Serine 409/410 in the C-terminus being the most commonly phosphorylated sites in disease (Neumann et al., 2009). Most phosphorylation is thought to occur as a later event in pathology; when TDP-43 is mislocalized in the cytoplasm, phosphorylation could be an attempt to trigger degradation (Francois-Moutal et al., 2019). SUMOylation of TDP-43 increases with aging and in ALS/FTLD patients. TDP-43 K408 SUMOylation could be protective, with TDP-43 clearance happening post SUMOylation through the ubiquitin proteasome system. SUMOylation and phosphorylation of TDP-43 have an inverse relationship in HEK293T cells, with a decrease of phosphorylation increasing TDP-43 SUMOylation (Suk et al., 2025).

Previous work also suggests that TDP-43 toxicity may derive from mitochondrial dysfunction (Gao et al., 2019, Wang et al., 2019). TDP-43 has been shown to co-localize with mitochondria in ALS spinal cord motor neurons and FTD cortical neurons. TDP-43 mitochondrial import is dependent on the TOM and TIM22 complex. TDP-43 has six predicted mitochondrial localization sequences, named M1-M6, with deletion of M1 (35-41), M3 (146-150), or M5 (294-300) significantly reducing mitochondrial localization. TDP-43 overexpression in cultured rat primary neurons resulted in mitochondrial fragmentation and dysfunction which was followed by neuronal death. TDP-43 binds mRNA that encodes for mitochondrial electron transport chain (ETC) complex I subunits ND3 and ND6, causing inhibition of translation. The suppression of TDP-43 localization in mitochondria reversed the toxicity of WT and mutant TDP-43 in mitochondria and neurons. Deletion of M1 in the TDP-43 plasmid, rescued mitochondrial membrane potential, oxygen consumption rate (OCR), ATP levels, and mitochondrial fragmentation (Wang et al., 2016). It has been recently found that the mitophagy receptor gene FUNDC1 is co-expressed with TDP-43 and can promote TDP-43 mitochondrial transport.

Interestingly, overexpression of FUNDC1 enhances TDP-43 damage of mitochondria, while downregulation reverses the mitochondrial damage (Ma et al., 2023).

Materials and Methods

Strains and transgenics

Wild-type (non-Tg) *C. elegans* (Bristol strain N2) was maintained as previously described (Brenner, 2003). TDP-43 mutant strains were created by injecting plasmids carrying human TDP-43 coding sequence downstream of the pan-neuronal *C. elegans snb-1* promoter that had specific point mutations altering domains. As previously described (Han et al., 2024), multicopy integrated transgenes were produced by microinjection of transgene marker and the transgene into the germline of N2 adults, followed by integration and outcrossing. To study how TDP-43 alters tau toxicity we created transgenic *C. elegans* strains that expressed mutant forms of human TDP-43 and crossed these worms with *C. elegans* expressing human tau. TDP-43 strains were crossed into two different tau strains, CK1441 (tau-TG), and CK1044 (tau-Tg (low)).

These TDP-43 mutations altered normal TDP-43 functions, such as RNA binding, oligomerization, nuclear localization, or common post translational modification sites in disease states. A few of the post translational modifications that we blocked at specific sites were acetylation, SUMOylation, Ubiquitination, and Phosphorylation. Acetylation involves attaching an acetyl group to a lysine residue, while phosphorylation involves a kinase attaching a phosphate group to a serine, threonine, or tyrosine. Ubiquitination is the attachment of a ubiquitin to a protein lysine group, often playing a role in protein degradation. SUMOylation is

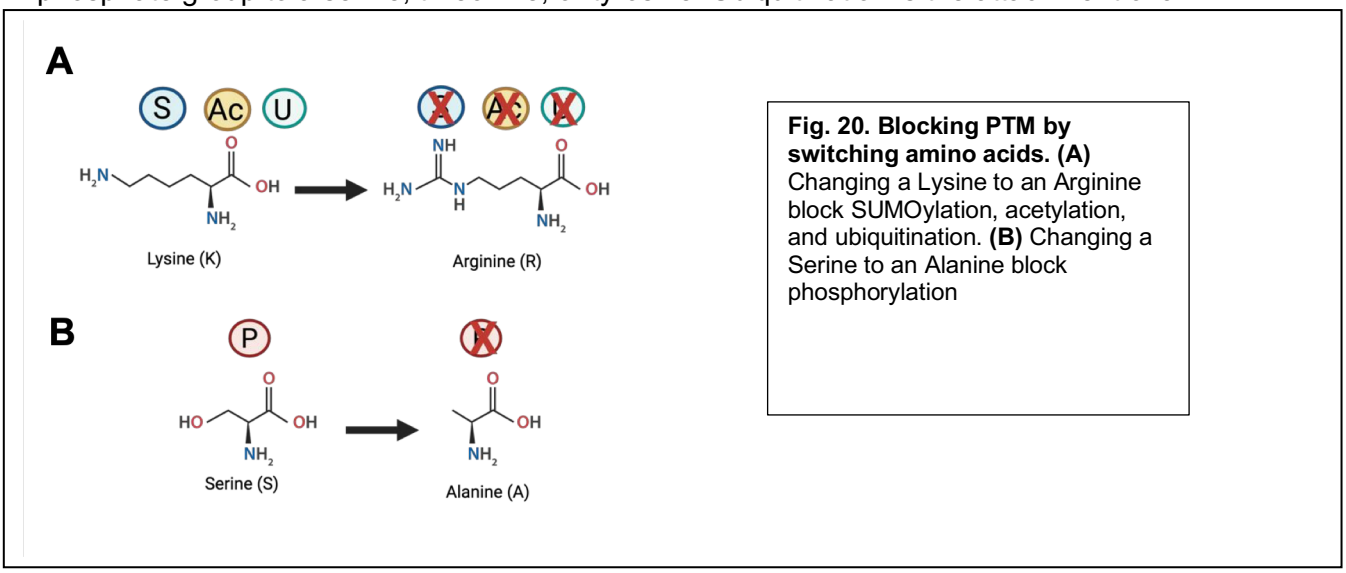

Fig. 20. Blocking PTM by switching amino acids. (A) Changing a Lysine to an Arginine block SUMOylation, acetylation, and ubiquitination. **(B)** Changing a Serine to an Alanine block phosphorylation

the addition of a small ubiquitin-like modifier (SUMO) to a lysine residue. Poly ADP-ribosylation (PARylation) is the attachment of a ADP-ribose to an acidic amino acid, such as aspartate of glutamate (Ramazi and Zahiri, 2021). TDP-43 has 41 serine, 15 threonine, and 8 tyrosine residues that can act as potential sites of phosphorylation, as well as 20 lysine residues that can act as potential ubiquitination, acetylation, or SUMOylation sites (Prasad et al., 2019). To block SUMOylation, acetylation, and ubiquitination we added point mutations on TDP-43 to change Lysine into Arginine (Fig. 20A). To block phosphorylation, we added point mutations on TDP-43 to change Serine to Alanine (Fig. 20B). See Table 4 for a complete list of all strains used in this chapter.

Strain abbreviations	Strain name	*Strain genotype*
non-Tg	N2	Wildtype
TDP-43 ΔNLS (low)	NLS152	*lials152[Psnb-1::TDP-43 (K82A/R83A/K84A) + Pmyo-3::dsRED]*
TDP-43 ΔNLS (med)	NLS151	*lials151[Psnb-1::TDP-43 (K82A/R83A/K84A) + Pmyo-3::dsRED]*
TDP-43 ΔNLS (high)	NLS142	*lials142[Psnb-1::TDP-43 (K82A/R83A/K84A) + Pmyo-3::dsRED]*
TDP-43-Tg	CK410	*bkls410[Psnb-1::TDP-43; Pmyo-2::dsRED + Pmyo-2::dsRED]*
TDP-43 M337V	CK423	*bkls423[Psnb-1::TDP-43 (M337V) + Pmyo-2::dsRED]*
tau-Tg	CK1441	*bkls1441[Paex-3::tau + Pmyo-2::dsRED]*
TDP-43 ΔNLS (low); tau-Tg	NLS162	*lials152[Psnb-1::TDP-43 (K82A/R83A/K84A) + Pmyo-3::dsRED]; bkls1441[Paex-3::tau + Pmyo-2::dsRED]*
TDP-43 ΔNLS (med); tau-Tg	NLS161	*lials151[Psnb-1::TDP-43 (K82A/R83A/K84A) + Pmyo-3::dsRED]; bkls1441[Paex-3::tau + Pmyo-2::dsRED]*
TDP-43 ΔNLS (high); tau-Tg	NLS144	*lials142[Psnb-1::TDP-43 (K82A/R83A/K84A) + Pmyo-3::dsRED]; bkls1441[Paex-3::tau + Pmyo-2::dsRED]*
TDP-43 Δoligo	NLS209	*lials[Psnb-1::TDP-43(E14A/E17A/E21A/Q34A/R52A/R55A) + Pmyo-3::dsRED]*
TDP-43 Δoligo; tau-Tg	NLS215	*lials[Psnb-1::TDP-43(E14A/E17A/E21A/Q34A/R52A/R55A) + Pmyo-3::dsRED]; bkls1441[Paex-3::tau + Pmyo-2::dsRED]*
TDP-43 ΔRRM (low)	NLS206	*lials206[Psnb-1::TDP-43(F147A/F149A/F194A/F229A/F231A) + Pmyo-3::dsRED]*
TDP-43 ΔRRM	NLS207	*lials207[Psnb-1::TDP-43(F147A/F149A/F194A/F229A/F231A) + Pmyo-3::dsRED]*
TDP-43 ΔRRM (low); tau-Tg	NLS210	*lials206[Psnb-1::TDP-43(F147A/F149A/F194A/F229A/F231A) + Pmyo-3::dsRED]; bkls1441[Paex-3::tau + Pmyo-2::dsRED]*
TDP-43 ΔRRM; tau-Tg	NLS211	*lials207[Psnb-1::TDP-43(F147A/F149A/F194A/F229A/F231A) + Pmyo-3::dsRED]; bkls1441[Paex-3::tau + Pmyo-2::dsRED]*
TDP-43 4xPTM	NLS168	*lials168[Psnb-1::TDP-43(K84R/K136R/K145R/K192R) + Pmyo-3::dsRED]*
TDP-43 4xPTM; tau-Tg	NLS176	*lials168[Psnb-1::TDP-43(K84R/K136R/K145R/K192R) + Pmyo-3::dsRED]; bkls1441[Paex-3::tau + Pmyo-2::dsRED]*
TDP-43 M337V Δphos	CK507	*bkls507[Psnb-1::TDP-43 (M337V/S409/410A) + Pmyo-3::dsRED]*
TDP-43 M337V Δphos; tau-Tg (low)	CK507;CK1044	*bkls507[Psnb-1::TDP-43 (M337V/S409/410A) + Pmyo-3::dsRED]; bkls1044[Paex-3::Tau WT (4R1N) + Pmyo-2::GFP]*
tau-Tg (low)	CK1044	*bkls1044[Paex-3::Tau WT (4R1N) + Pmyo-2::GFP]*
TDP-43 ΔRRM (low); tau-Tg (low)	NLS259	*lials206[Psnb-1::TDP-43(F147A/F149A/F194A/F229A/F231A) + Pmyo-3::dsRED]; bkls1044[Paex-3::Tau WT (4R1N) + Pmyo-2::GFP]*
TDP-43 ΔRRM; tau-Tg (low)	NLS260	*lials207[Psnb-1::TDP-43(F147A/F149A/F194A/F229A/F231A) + Pmyo-3::dsRED]; bkls1044[Paex-3::Tau WT (4R1N) + Pmyo-2::GFP]*
TDP-43 Δoligo; tau-Tg (low)	NLS257	*lials[Psnb-1::TDP-43(E14A/E17A/E21A/Q34A/R52A/R55A) + Pmyo-3::dsRED]; bkls1044[Paex-3::Tau WT (4R1N) + Pmyo-2::GFP]*
TDP-43 4xPTM; tau-Tg (low)	NLS242	*lials168[Psnb-1::TDP-43(K84R/K136R/K145R/K192R) + Pmyo-3::dsRED]; bkls1044[Paex-3::Tau WT (4R1N) + Pmyo-2::GFP]*
TDP-43 ΔNLS (med); tau-Tg (low)	NLS266	*lials151[Psnb-1::TDP-43 (K82A/R83A/K84A) + Pmyo-3::dsRED]; bkls1044[Paex-3::Tau WT (4R1N) + Pmyo-2::GFP]*
TDP-43 K192R	NLS170	*lials151[Psnb-1::TDP-43 (K192R) + Pmyo-3::dsRED]*
TDP-43 K192R; tau-Tg (low)	NLS264	*lials151[Psnb-1::TDP-43 (K192R) + Pmyo-3::dsRED]; bkls1044[Paex-3::Tau WT (4R1N) + Pmyo-2::GFP]*
TDP-43 K136/145R	NLS237	*lials151[Psnb-1::TDP-43 (K136R/K145R) + Pmyo-3::dsRED]*
TDP-43 K136/145R; tau-Tg (low)	NLS244	*lials151[Psnb-1::TDP-43 (K136R/K145R) + Pmyo-3::dsRED]; bkls1044[Paex-3::Tau WT (4R1N) + Pmyo-2::GFP]*
TDP-43 K84R	NLS239	*lials151[Psnb-1::TDP-43 (K84R) + Pmyo-3::dsRED]*
TDP-43 K84R; tau-Tg (low)	NLS246	*lials151[Psnb-1::TDP-43 (K84R) + Pmyo-3::dsRED]; bkls1044[Paex-3::Tau WT (4R1N) + Pmyo-2::GFP]*
TDP-43 K408R	CK627	*bkls627[Psnb-1::TDP-43 (K408R) + Pmyo-2::dsRED]*

Table 4. complete list of all strains used in this chapter 2

Immunoblotting

See chapter one.

C. elegans immunohistochemistry

See chapter one.

Motility assays

See chapter one.

Statistical analysis

See chapter one.

Results

TDP-43 Δoligo does not prevent neurotoxic synergy with tau

To determine if oligomerization of TDP-43 is important for its neurotoxic synergy with tau, we developed a new *C. elegans* model of TDP-43, referred to as TDP-43 Δoligo. TDP-43 oligomerization of the N terminus is essential for TDP-43 splicing activity (Lye and Chen, 2022) and liquid-liquid phase separation (LLPS) (Wang et al., 2018). TDP-43 Δoligo was created by

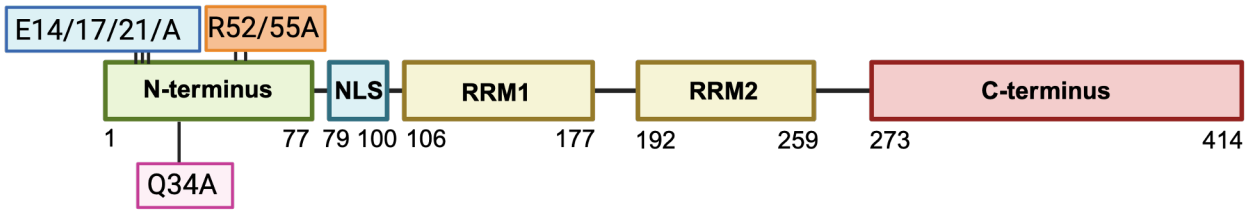

Fig. 21. TDP-43 oligomerization mutant schematic. The 5 point mutations in the N-terminus domain will block the ability of TDP-43 to self-oligomerization.

adding 5 point mutations (E14/17/21/A, R52/55A) in the nuclear N-terminus of TDP-43 (Fig. 21), consistent with mammalian TDP-43 Δoligo cell models generated previously (Perez-Berlanga et al., 2023). TDP-43 Δoligo was then crossed with *C. elegans* strain CK1441 (tau-Tg) expressing human tau. TDP-43 Δoligo had better motility than tau-Tg and worse than non-Tg. Interestingly, TDP-43 Δoligo; tau-Tg had significant worse motility than tau-Tg worms, indicating oligomerization is not essential for the neurotoxic synergy between tau and TDP-43 (Fig. 22A,B).

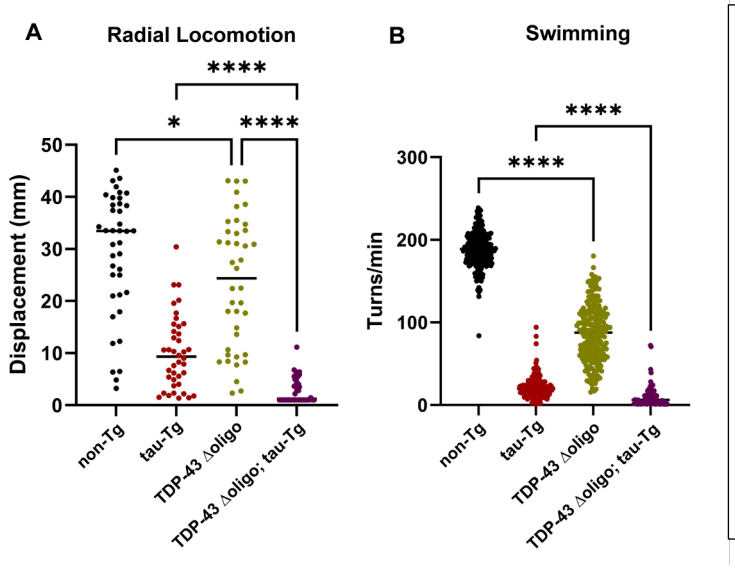

Fig. 22. TDP-43 Δoligo does not prevent TDP-43 neurotoxic synergy with tau. (A,B) Motility impairment of TDP-43 Δoligo as measured by **(A)** radial locomotion (linear distance crawling in one hour on an agar plate) or **(B)** swimming (rates of thrashing in liquid for a minute). TDP-43 Δoligo; tau-Tg had worse motility than tau-Tg alone. One-way ANOVA with Tukey's multiple comparison test. *p<0.05, ****p<0.0001. ns, not significant. Data are mean ±

Cytoplasmic TDP-43 has reduced neurotoxic synergy with tau

In chapter 1 we characterized cytoplasmic TDP-43 in *C. elegans* by creating three TDP-43 ΔNLS strains. These strains have three point mutations (K82A/R83A/K84A) in the nuclear localization sequence of TDP-43 and range from low to high levels of TDP-43 (Fig. 6A,B). To determine if nuclear location is required for TDP-43-tau synergy we crossed TDP-43 ΔNLS (low), TDP-43 ΔNLS (med), and TDP-43 ΔNLS (high) with tau-Tg. We found that TDP-43 ΔNLS (low); tau-Tg, TDP-43 ΔNLS (med); tau-Tg, and TDP-43 ΔNLS (high); tau-Tg had the same radial locomotion as tau-Tg *C. elegans* (Fig. 23A). For swimming, TDP-43 ΔNLS (med); tau-Tg, and TDP-43 ΔNLS (high); tau-Tg had slightly worse swimming than tau-Tg (Fig. 23B). These motility results indicate cytoplasmic TDP-43 does not have as severe neurotoxic synergy with tau as nuclear TDP-43. Cytoplasmic TDP-43 could be altering different pathways than nuclear TDP-43, resulting in less enhancement of tau toxicity.

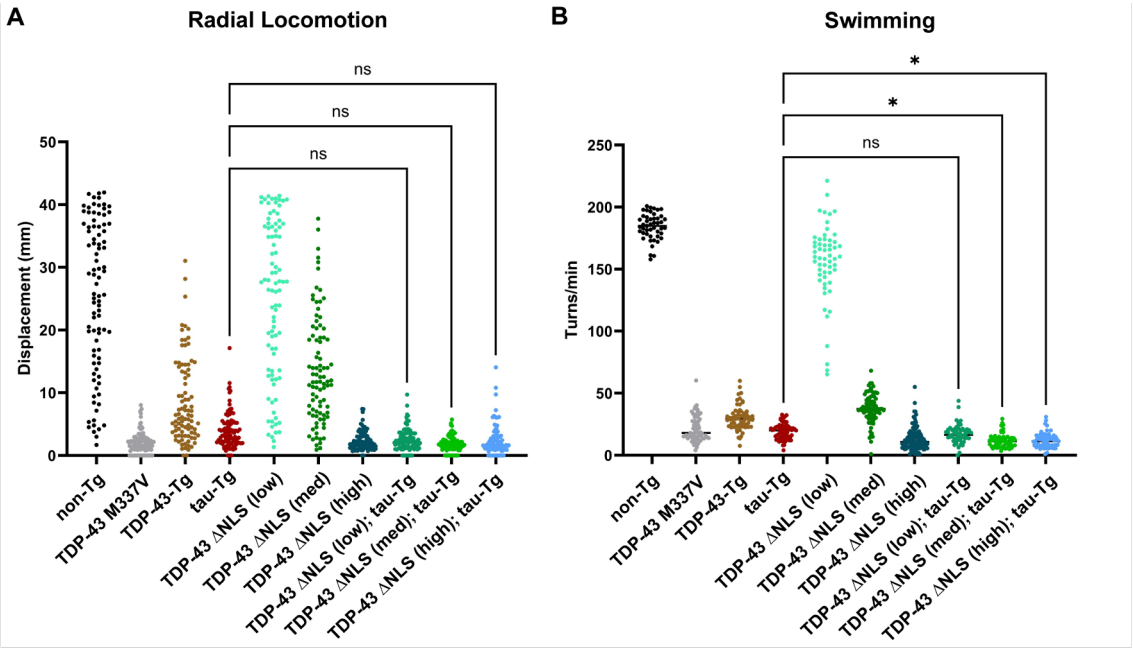

Fig. 23. TDP-43 ΔNLS has reduced neurotoxic synergy with tau-Tg. (A,B) Motility impairment of TDP-43 ΔNLS as measured by **(A)** radial locomotion (linear distance crawling in one hour on an agar plate) or **(B)** swimming (rates of thrashing in liquid for a minute). **(A)** All 3 TDP-43 ΔNLS; tau-Tg strains had the same crawling deficit as tau-Tg alone **(B)** TDP-43 ΔNLS (med); tau-Tg and TDP-43 ΔNLS (high); tau-Tg had worse swimming than tau-Tg alone. TDP-43 ΔNLS (low) ; tau-Tg had the same swimming deficit as tau-Tg alone. One-way ANOVA with Tukey's multiple comparison test. *p<0.05, ns, not significant. Data are mean ± s.e.m.

TDP-43 RNA binding does not prevent neurotoxic synergy with tau

To determine if the RNA binding ability of TDP-43 is important for its neurotoxic synergy with tau, we developed a new *C. elegans* model of TDP-43, referred to as TDP-43 ΔRRM. RNA binding is essential for TDP-43 to perform is normal functions in RNA metabolism and is

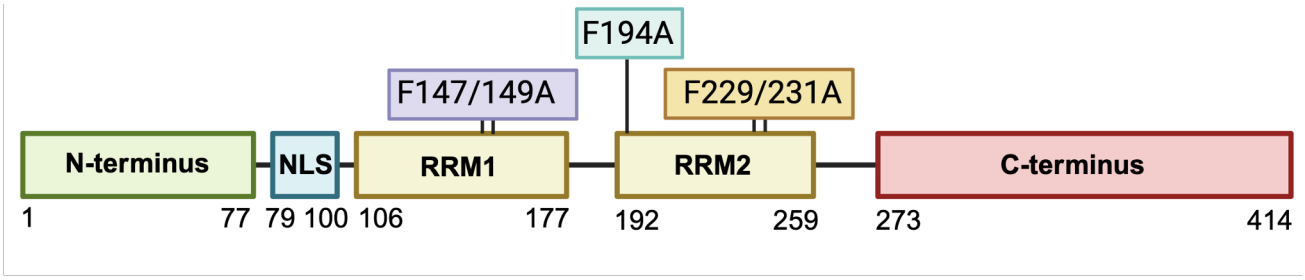

Fig. 24. TDP-43 RNA binding mutant schematic. 2 point mutations in the RRM1 and 3 in the RRM2 will decrease the ability of TDP-43 to bind RNA.

important for LLPS (Perez-Berlanga et al., 2023). TDP-43 RRM1 and RRM2 are important for binding GU rich RNA sequences and organizing TDP-43 cooperative binding (Feng et al., 2026).

TDP-43 ΔRRM was created by adding 2 point mutations (F147/149A) in the RNA recognition motif 1 (RRM1) and 3 point mutations (F194A/229/231A) in the RNA recognition motif 2 (RRM1) of TDP-43 (Fig. 24). These point mutations are consistent with mammalian TDP-43 ΔRRM cell models generated previously (Perez-Berlanga et al., 2023). We created two TDP-43 ΔRRM strains, with variable TDP-43 levels named TDP-43 ΔRRM and TDP-43 ΔRRM (low) and crossed those two strains with tau-Tg. TDP-43 ΔRRM; tau-Tg and TDP-43 ΔRRM (low); tau-Tg had worse radial locomotion and swimming than tau-Tg (Fig. 25A,B). The TDP-43 ΔRRM (low) strain didn't have a motility difference from non-Tg but when crossed with tau-Tg it was sicker than tau-Tg. This indicates that the ability of TDP-43 to bind RNA is not required for its neurotoxic synergy with tau.

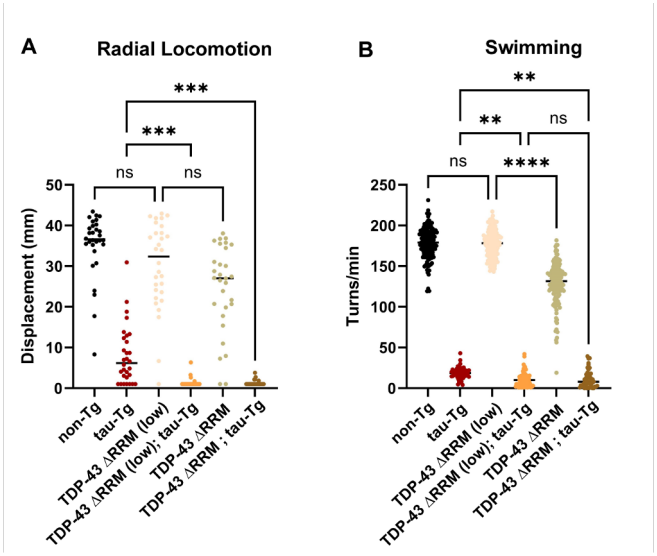

Fig. 25. TDP-43 ΔRRM does not prevent TDP-43 neurotoxic synergy with tau. (A,B) Motility impairment of TDP-43 ΔRRM as measured by **(A)** radial locomotion (linear distance crawling in one hour on an agar plate) or **(B)** swimming (rates of thrashing in liquid for a minute). TDP-43 ΔRRM; tau-Tg and TDP-43 ΔRRM (low); tau-Tg had worse motility than tau-Tg alone. One-way ANOVA with Tukey's multiple comparison test. **p<0.01, ***p<0.001, ****p<0.0001. ns, not significant. Data are mean ± s.e.m.

TDP-43 post translational modifications can be important for its neurotoxic synergy with tau

TDP-43 can undergo many PTM, with some of them more characterized, such as phosphorylation of S409/410 (Neumann et al., 2009, Liachko et al., 2010), while others like acetylation of K145 are less well studied (Necarsulmer et al., 2023). None of these post translational modifications of TDP-43 have been investigated if they are important for TDP-43-tau neurotoxic synergy. We decided to investigate four acetylation sites on TDP-43: K84, K136,

K145, and K192. All four of these sites can be acetylated and some of them have also been shown to undergo SUMOylated and/or ubiquitinated modifications (Khosravi et al., 2020, Maraschi et al., 2021, Necarsulmer et al., 2023, Cohen et al., 2015). Post translational modifications on these sites are linked to potential disease progression, with links to neuronal dysfunction (Necarsulmer et al., 2023), nuclear binding (Cohen et al., 2015), RNA binding/splicing (Garcia Morato et al., 2022), and nuclear import (Khosravi et al., 2020). We hypothesis that blocking these 4 PTM would make TDP-43 less toxic and potentially reduce the neurotoxic synergy with tau.

To determine the effect these 4 TDP-43 PTM sites have on its neurotoxic synergy with tau, we developed a new *C. elegans* model of TDP-43, referred to as TDP-43 4xPTM. TDP-43 4xPTM was created by adding 4 point mutations K84/136/145/192R to TDP-43 (Fig. 26).

We then crossed TDP-43 4xPTM with CK1441, tau-Tg, and performed radials and

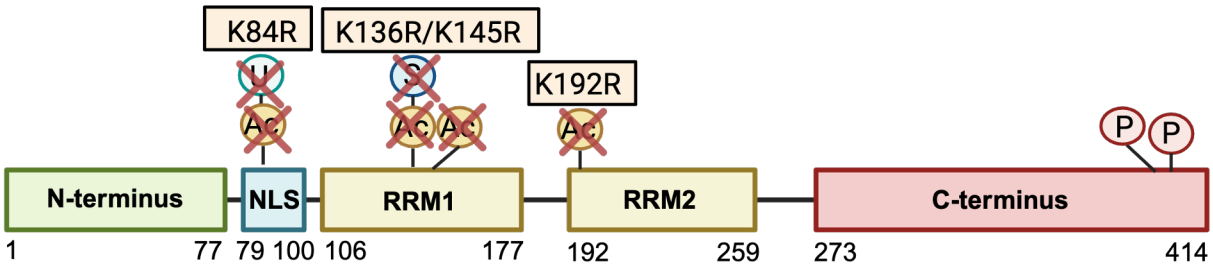

Fig. 26. TDP-43 4xPTM. 4 point mutations K84/136/145/192R to block acetylation, SUMOylation, and ubiquitination at those sites.

swimming (Fig. 27A,B). TDP-43 4xPTM; tau-Tg did not have a significant crawling or swimming deficit worse than tau-Tg alone, indicating a less severe neurotoxic synergy. TDP-43 4xPTM; tau-Tg was still very sick, making there be some concern for slight floor effect. The motility data in (Fig. 27) indicates that acetylation, SUMOylation, and ubiquitination of the NLS, RRM1, and RRM2 alters TDP-43 toxicity and potentially its synergy with tau.

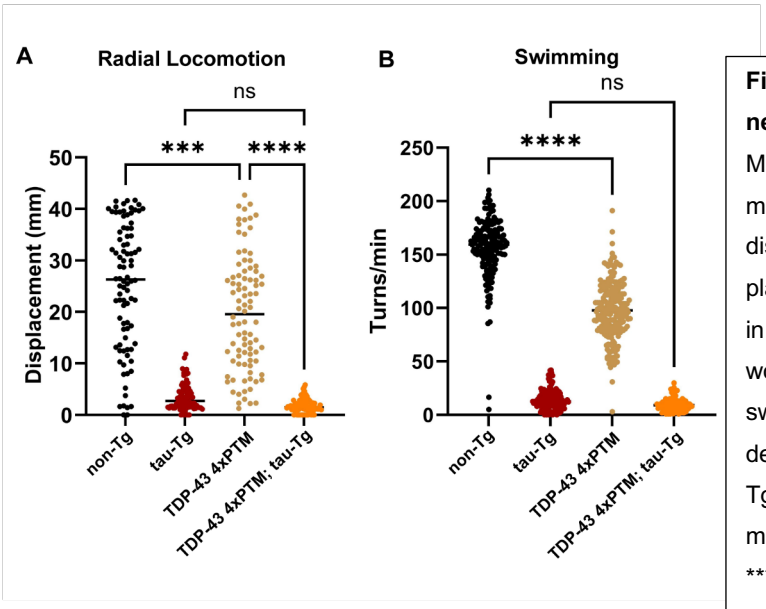

Fig. 27. TDP-43 4xPTM has reduced neurotoxic synergy with tau-Tg. (A,B) Motility impairment of TDP-43 4xPTM as measured by **(A)** radial locomotion (linear distance crawling in one hour on an agar plate) or **(B)** swimming (rates of thrashing in liquid for a minute). TDP-43 4xPTM worms had decreased crawling and swimming when crossed to tau-Tg. This deficit was not significantly less than tau-Tg alone. One-way ANOVA with Tukey's multiple comparison test. ***p<0.001,****p<0.0001, ns, not significant. Data are mean ± s.e.m.

In Limbic-predominant age related TDP-43 encephalopathy (LATE), pathologic changes involve the accumulation of pTDP-43 in the limbic system (Butler Pagnotti et al., 2023, Nelson et al., 2019). Phosphorylated TDP-43 is also used as disease marker for TDP-43 pathology, indicating a more toxic form of TDP-43 (Neumann et al., 2021). We wanted to see if phosphorylation of the main phosphorylation sites of TDP-43, serine 409/410 (Neumann et al., 2009) are important for synergy with tau. To determine if phosphorylation of TDP-43 is essential

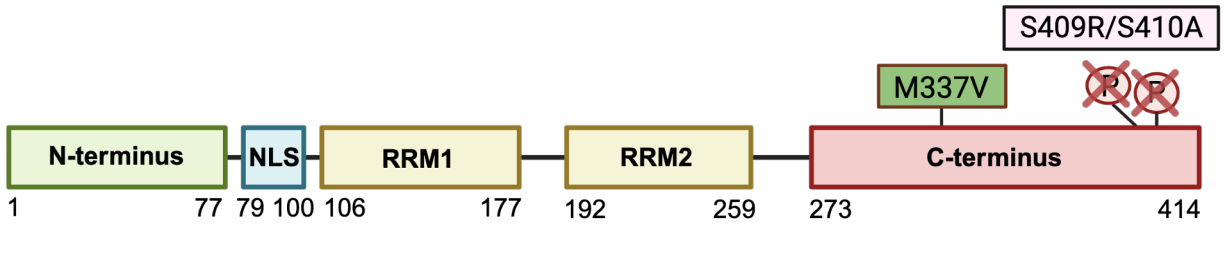

Fig. 28. TDP-43 M337V Δphos. 2 point mutations in the C-terminus domain will block phosphorylation of S409/410.

for its neurotoxic synergy with tau we developed new *C. elegans* model of TDP-43, referred to as TDP-43 Δphos, which had 2 point mutations, S409/410A. TDP-43 Δphos crossed with CK1441 was not viable, making us try a weaker tau strain, CK1044 (tau-Tg (low)). TDP-43 Δphos crossed with tau-Tg (low) was also not viable but we were able to get viable offspring from a slightly different TDP-43 mutant, TDP-43 M337V Δphos. TDP-43 M337V Δphos has the

same 2 point mutation, S409/410A, as well as the familial ALS disease causing mutation M337V (Fig. 28).

To our surprise, TDP-43 M337V Δphos but not TDP-43 Δphos was viable when crossed with CK1044 (tau-Tg (low)). Typically TDP-43 M337V strains have higher pTDP-43 levels than WT TDP-43 strains, driving toxicity (Liachko et al., 2010). TDP-43 M337V Δphos; tau-Tg (low) had swimming deficits that were significantly worse than tau-Tg (low) (Fig. 29). Using tau-Tg (low) instead of tau-Tg allows for a clearer visual of TDP-43; tau neurotoxic synergy and provides a larger range for detecting enhancement, reducing the worry that there could be a floor effect.

We then crossed all our existing TDP-43 strains from this chapter to tau-Tg (low) to confirm our data in an independent tau strain that enables a larger range to detect enhancement. We generated: TDP-43 NLS (med); tau-Tg (low), TDP-43 ΔRRM; tau-Tg (low), TDP-43 ΔRRM (low); tau-Tg (low), TDP-43 Δoligo; tau-Tg (low), TDP-43 4xPTM; tau-Tg (low).

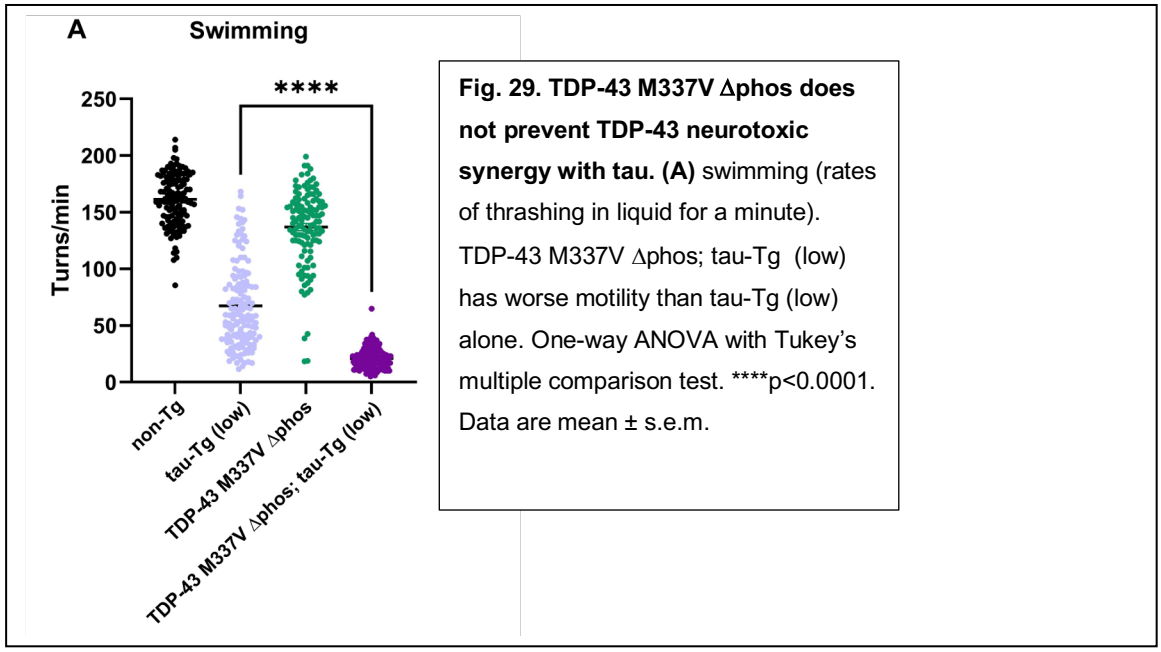

Fig. 29. TDP-43 M337V Δphos does not prevent TDP-43 neurotoxic synergy with tau. (A) swimming (rates of thrashing in liquid for a minute). TDP-43 M337V Δphos; tau-Tg (low) has worse motility than tau-Tg (low) alone. One-way ANOVA with Tukey's multiple comparison test. ****p<0.0001. Data are mean ± s.e.m.

In (Fig. 22) and (Fig. 25) we show TDP-43 oligomerization and TDP-43 RNA binding are not crucial for synergy with tau. When crossing TDP-43 ΔRRM and TDP-43 Δoligo with a weaker expressing tau strain, CK1044 (tau-Tg (low), we saw the same result (Fig. 30). Tau-Tg (low) has a less severe motility deficit than Tau-Tg, allowing there to be a clearer difference between the single transgenic strains and the double transgenic strains.

In (Fig. 27) we show the potential importance of acetylation, SUMOylation, and ubiquitination in tau; TDP-43 synergy by crossing TDP-43 4xPTM with tau-Tg. Interestingly when crossing TDP-43 4xPTM with tau-Tg (low) we see a significant motility deficit between

TDP-43 4xPTM; tau-Tg (low) and tau-Tg (low) (Fig. 31). The radial locomotion of TDP-43 4xPTM; tau-Tg (low) visually looked less sick than TDP-43-Tg; tau-Tg (low) but there was no significance (Fig. 31A,B).

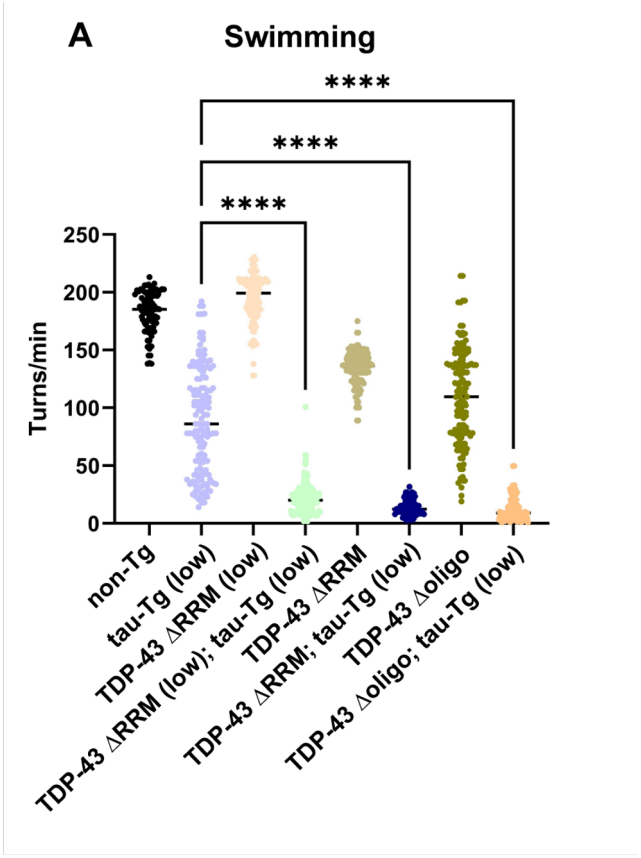

Fig. 30. Blocking TDP-43 RNA binding and oligomerization does not stop synergy with tau, when using a lower expressing tau-Tg strain. (A) Swimming (rates of thrashing in liquid for a minute). TDP-43 ΔRRM (low); tau-Tg (low), TDP-43 ΔRRM; tau-Tg (low), and TDP-43 Δoligo; tau-Tg (low) has worse motility than tau-Tg (low) alone. One-way ANOVA with Tukey's multiple comparison test. ****p<0.0001. Data are mean ± s.e.m.

From this data we still think acetylation, SUMOylation, and ubiquitination could play a role in TDP-43; tau synergy but it does not seem to be the main cause of it. We plan on crossing the TDP-43 4xPTM strain into a third tau strain to help us understand our slightly different findings between tau-Tg and tau-Tg (low). Additionally, we made single and double PTM mutants. These three strains had TDP-43 point mutations at K84R, K136/145R, and 192R. We crossed these three strains to tau-Tg (low) and plan on doing motility assays to determine which location is most important for synergy with tau.

In (Fig. 6) we showed mutating the NLS of TDP-43 with (K82A/R83A/K84A) causes TDP-43 to be localized in the cytoplasm and not the nucleus. In (Fig. 23) we showed

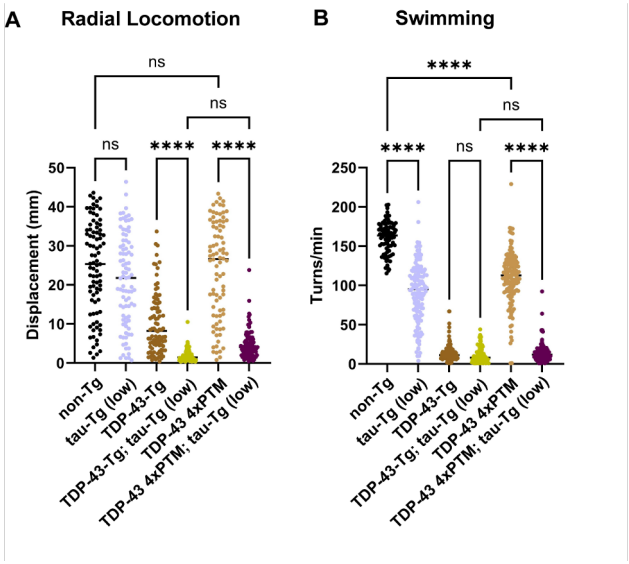

Fig. 31. TDP-43 4xPTM has reduced neurotoxic synergy with tau-Tg. (A,B) Motility impairment of TDP-43 4xPTM as measured by **(A)** radial locomotion (linear distance crawling in one hour on an agar plate) or **(B)** swimming (rates of thrashing in liquid for a minute). TDP-43 4xPTM worms had decreased crawling and swimming when crossed to tau-Tg. This deficit was not significantly less than tau-Tg alone. One-way ANOVA with Tukey's multiple comparison test. ***p<0.001,****p<0.0001, ns, not significant. Data are mean ± s.e.m.

cytoplasmic TDP-43 has less synergy with tau, especially with the weakest TDP-43 ΔNLS strain. When we crossed TDP-43 ΔNLS (med) with tau-Tg (low) we saw similar results to TDP-43 4xPTM; tau (low), where TDP-43 ΔNLS (med); tau-Tg (low) is sicker than tau-Tg (low). We are working on completing motility assays to confirm the plate phenotype. We are also going to add TDP-43-Tg and TDP-43-Tg; tau-Tg (low) to each behavior experiment as controls to better characterize the synergy.

Discussion

It is known that Alzheimer disease cases with TDP-43 have an increased burden of pre-tangles and phosphorylated tau (Tome et al., 2023), and *C. elegans* co-expressing human tau and human TDP-43, cause increased neuronal dysfunction compared to either protein alone (Latimer et al., 2022). The reason for the increased toxicity of tau in this co-pathology is unknown. In this chapter we investigated if TDP-43 location, oligomerization, RNA binding, or post translational modifications were important for its neurotoxic synergy with tau. We did this by making transgenic *C. elegans* that had various mutant forms of human TDP-43 expressed pan-neuronally. These TDP-43 mutants had the goal of altering TDP-43 functions, such as blocking specific PTM sites, or inhibiting TDP-43 from binding to RNA. We then crossed all of these mutant TDP-43 strains to two tau-Tg strains, with one tau-Tg strain, tau-Tg (low), having much lower tau expression than the other.

We were able to conclude that phosphorylation of S409/410, TDP-43 RNA binding, and TDP-43 oligomerization do not play an important role in tau;TDP-43 synergy. In tau-Tg and tau-Tg (low) lines it was clear that there was still very strong synergy when these TDP-43 functions or sites were blocked. Interestingly, when blocking potential acetylation, ubiquitination, and SUMOylation sites on TDP-43, we saw a reduction in synergy with tau compared to tau-Tg. Although when compared to tau-Tg (low) we did not see the same effect. This pattern was also seen when looking at cytoplasmic TDP-43;tau synergy. One possible explanation is that there was a floor effect when using tau-Tg, and tau-Tg (low) allows additional range to detect synergy with the TDP-43 4xPTM and TDP-43 NLS (med) lines. Another explanation is that the synergy is strain specific since the tau-Tg (low) seems to be more sensitive to synergy with TDP-43 than tau-Tg. Crossing a third tau-Tg strain with a few of these TDP-43 mutants could help solidify if synergy is altered or not.

Regardless of if there is a true reduction of synergy with tau in the TDP-43 4xPTM and TDP-43 NLS lines I do not think we uncovered the main cause of neurotoxic synergy between the two proteins. Both TDP-43 4xPTM and TDP-43 NLS only showed partial stoppage of synergy and there was no clear rescue of phenotype with behavioral assays. The TDP-43 4xPTM strain is also crude, where we are not exactly sure which point mutation is doing what. We do not want one point mutation to be covering up the effects of the other point mutations. This is why it is important to also test TDP-43 K84R; tau-Tg (low), K136R/K145R; tau-Tg (low), and 192R; tau-Tg (low) strains, which have been generated but we need to run motility assays to characterize the plate phenotype. During the course of this project, we have also found other possible targets on TDP-43 that could be exciting to investigate. One of them is TDP-43 K408, a SUMOylation site that has been shown to have an inverse relationship with phosphorylation S409/410 (Suk et al., 2025). Blocking phosphorylation of S409/410 might have worsened synergy with tau. It is possible that this might have been due to increased SUMOylation of K408. This makes us think that blocking SUMOylation of K408 might reduce TDP-43; tau neurotoxic synergy.

Another possible avenue to explore is TDP-43 and mitochondria, to see if TDP-43 is disturbing mitochondria, which is affecting tau. TDP-43 has been shown to co-localize with mitochondria in ALS spinal cord motor neurons and FTD cortical neurons. TDP-43 has six predicted mitochondrial localization sequences, named M1-M6, with deletion of M1 (35-41), M3 (146-150), or M5 (294-300) significantly reducing mitochondrial localization and rescuing phenotype (Wang et al., 2016). Our lab has shown in the past that TDP-43 causes

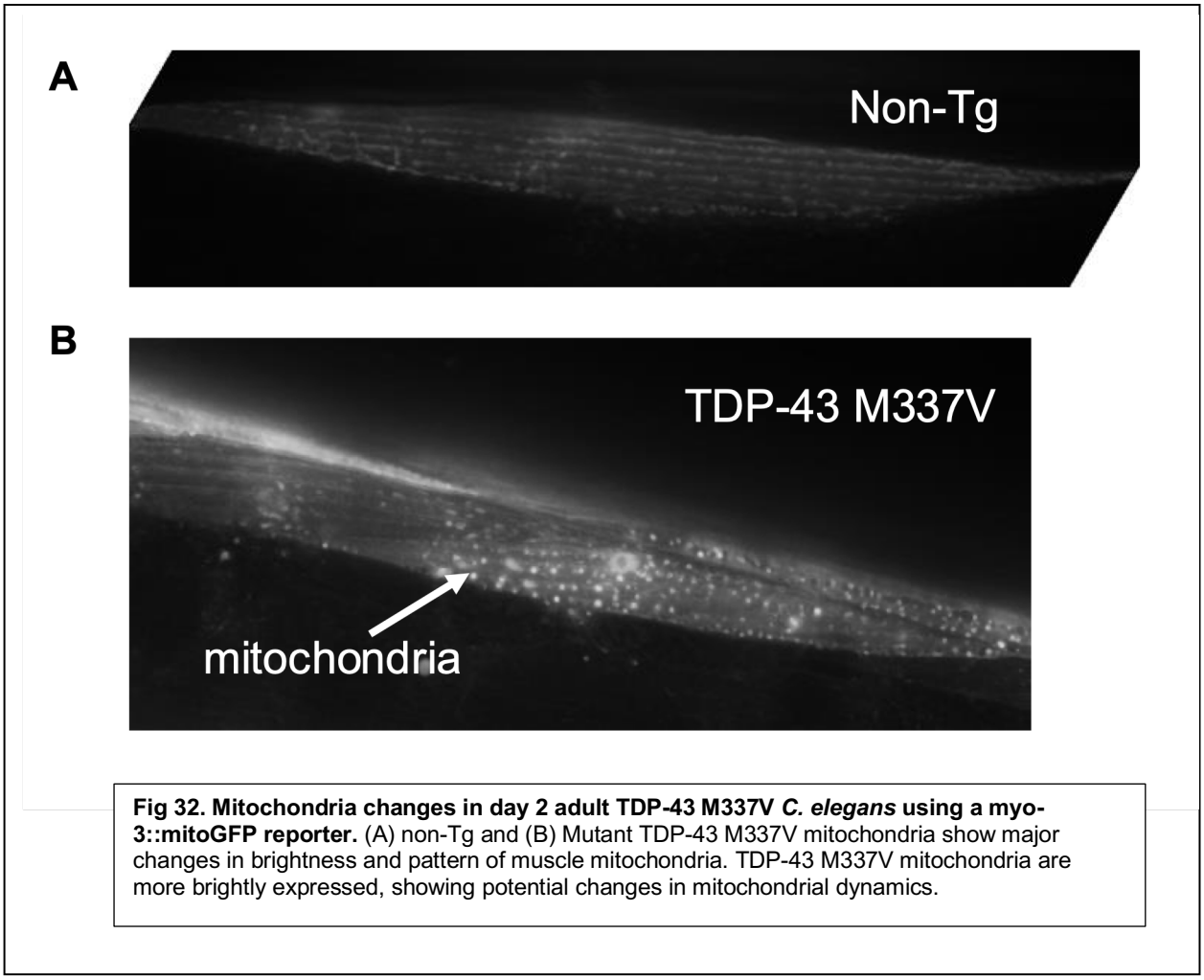

Fig 32. Mitochondria changes in day 2 adult TDP-43 M337V *C. elegans* using a myo-3::mitoGFP reporter. (A) non-Tg and (B) Mutant TDP-43 M337V mitochondria show major changes in brightness and pattern of muscle mitochondria. TDP-43 M337V mitochondria are more brightly expressed, showing potential changes in mitochondrial dynamics.

mitochondrial dysfunction in *C. elegans*, with TDP-43 M337V having much brighter mito-GFP, indicating potential mitochondrial hyperfusion (Fig. 32A,B). First, we will need to better characterize how TDP-43 alters mitochondria in *C. elegans*. Then we can ask the question if mitochondrial dysfunction, mitochondrial changes, of TDP-43 localization to mitochondria, alters TDP-43;tau synergy.

This work has begun understanding which aspects of TDP-43 function are important for tau synergy. Our work suggests blocking disease related post translational modifications, TDP-43 location, and downstream pathways from TDP-43 aggregation, could be important for altering TDP-43; tau synergy. This work aims to better understanding the mechanisms of synergy to lead to potential therapeutic targets to treat individuals with AD LATE and other TDP-43; tau co-pathologies.

Chapter 3: Sex specific behavior changes in an aged tau; TDP-43 mouse model

Introduction

In chapters 1 and 2 we used *C. elegans* to model human disease by expressing human tau and human TDP-43 in *C. elegans*. While *C. elegans* are a great model for investigating disease mechanisms quickly, it is also important to reproduce those results in model organisms that are closer to humans. *C. elegans* have a 40% homology to human genes, while mice have an 80% homology (Castillo and de la Guardia, 2017). While there have been many mouse models created that express human tau or human TDP-43, there have also been difficulty closely replicating human TDP-43 and tau disease pathology in mice (Armas et al., 2025, Jagaraj et al., 2025, Langness et al., 2025). Compared to *C. elegans,* mice have much more cellular complexity, with genome of 3,500 million bp, compared to 100 million bp, as well as a much more complicated nervous system, making results harder to interpret, and experiments to characterize them more time consuming and financially expensive (Castillo and de la Guardia, 2017, Zeisel et al., 2018). Improving TDP-43 and tau mouse models is crucial to improving our understanding of TDP-43 and tau and will also greatly impact the field.

As we have shown using *C. elegans* in chapters 1 and 2, human TDP-43 can be very toxic when expressed in model organisms. This is also seen in mice, with the homozygous Kumar-Singh mouse model overexpresses wild-type TDP-43 in postnatal neurons causing severe motor impairment and death by one month of age (Wils et al., 2010). Old age is the main risk factor for most diseases that have TDP-43 pathology, such as LATE, FTD, or ALS (Uemura et al., 2022). It is important to have mouse models that can age and not die young to adequately recapitulate what we are seeing human TDP-43 disease.

In chapter 2 we investigated the neurotoxic synergy of TDP-43 and tau in *C. elegans*. In chapter 3 we characterize a new TDP-43-Tg; tau-Tg mouse model by crossing a hemizygous TAR4 Kumar-Singh mice (TDP-43-Tg) and WT human tau expressing Tau4Rtg2652 mice (tau-Tg) (Fig. 33).

The Kumar-Singh lab created TDP-43 mice that had dose dependent TDP-43 neurodegeneration. They created a homozygous mouse (TAR4/4), that had significantly more TDP-43 mRNA in mouse brains than their hemizygous mouse (TAR4). (Wils et al., 2010). TAR4/4 mice had abnormal clasping by 14 days while TAR4 mice had abnormal clasping by 14 months. TAR4 mice also only survived on average to 24 days. These TDP-43 mice had accumulation of TDP-43 in the spinal cord and brain had nuclear and cytoplasmic TDP-43 aggregates, as well as phosphorylated TDP-43 (Wils et al., 2010). Due to the toxicity of

homozygous TAR4/4, we decided to use hemizygous TAR4 Kumar-Singh mice to study TDP-43 pathology along with aging.

The Kraemer lab has designed a tau mouse model, Tau4Rtg2652, that expresses high levels of human 4R1N tau in neurons. The tau drives pre-tangle pathology in young mice, resulting in behavior deficits associated with cognitive impairment. These Tau4Rtg2652 have anormal lifespan and have phosphorylated tau (Wheeler et al., 2015).

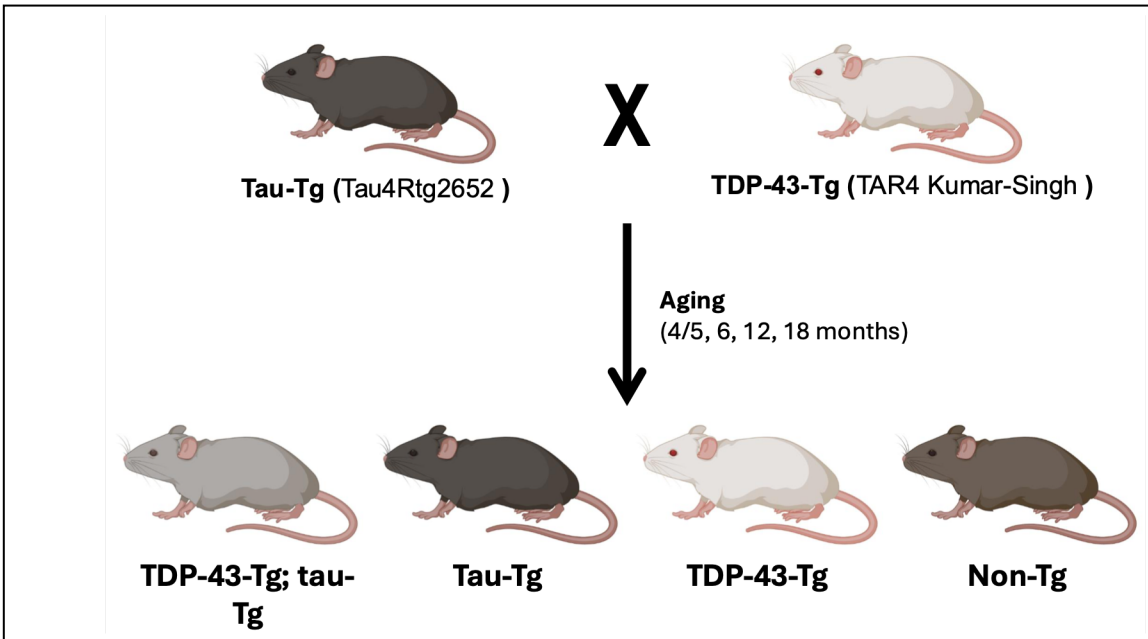

Fig. 33. Mouse breeding schematic. Tau4Rtg2652 mice were bred with TAR4 Kumar-Singh mice to get Tau4Rtg2652;TAR4 double transgenic mice. We had four experimental groups: Non-Tg, TDP-43, tau, and TDP-43 tau.

Both the TAR4 Kumar-Singh mice and the Tau4Rtg2652 mice have a normal lifespan. We thought using an early-stage disease tau model and a lower expression TDP-43 model would allow for the double transgenic mice to be viable and to allow us to study TDP-43 and tau synergy in an aging mouse model (Fig. 33) (Wheeler et al., 2015, Wils et al., 2010). Other researchers in our lab ran behavior tests and collected tissue from mice at 4-6 and 12 months. Behavior and from as old as 12 months did not show any trends showing synergy with tau and TDP-43. I took over the TDP-43-Tg; tau-Tg mice for the 18 month cohort, with the hope to see behavior and pathological changes with aging (Wheeler et al., 2015, Wils et al., 2010).

Materials and Methods

Weight and clasping

Every 3 weeks, starting around 12 months mice were subject to weighing, clasping. Hind limb clasping score were recorded when the mice were weighed. A score of 0 indicated no clasping, with hind limbs spread out. A score of 1 indicated partial clasping, usually of one hind limb clasping while the other is spread out. A score of 2 indicated full clasping with both hind limbs tucked into their body when picked up (McMillan et al., 2020).

Open Field

Open field testing was conducted in an opaque round arena 30 inches in diameter. Animals were habituated in the testing room for 45 min before testing. During the open field experiment animals were free to roam the arena for 10 min. Everything was cleaned with 70% ethanol before the start of testing and between each animal. Animals were tracked the whole time using ANY-maze tracking system (Stoelting Co) (McMillan et al., 2020).

Y-maze

Animals were habituated in the testing room for 45 min before testing. Mice were put into one of the 3 arms of the y-maze apparatus. They were free to roam for 8 minutes while being tracked by ANY-maze tracking system (Stoelting Co). Everything was cleaned with 70% ethanol before the start of testing and between each animal. When the mouse entered all three arms consecutively, it counted as one alteration. The number of alterations (A) was marked and was used to calculate the alteration rate along with the total number of arm entries. ANY-maze calculated the percent spontaneous alteration by using the formula percent spontaneous alteration (%) = [A/(E-2)] x100 (Long et al., 2017).

Rotarod

Animals were habituated in the testing room for 45 min before testing. There were two days of testing, one for learning/training, and one for the experiment. The training day consisted of 3 150 second trials per mouse, where the rotarod goes from 5 RPM to 20 RPM over 120 seconds, increasing by 5 RPM every 30 seconds. During the experimental day each mouse goes through 4 150 second trials, with the max RPM for each trial being 8, 16, 24, and 32 RMP. Every 30 seconds the RMP would increase by 2, 4, 6, or 7 RPM. For training and the experiment, mice were on the rotarod until they fell off. Everything was cleaned with 70% ethanol before the start of testing and between each animal. The rotarod latency to fall was calculated as the time it took them to fall during each test.

Mouse brain collection

Animals were divided into two groups, fixed tissue and fresh tissue. Fixed tissue animals were anesthetized with pentobarbitol, transcardial perfusion was performed with saline then 4% paraformaldehyde. Fixed brains were removed from the skull and stored in 80% ethanol. Fresh tissue animals were euthanized by CO2 asphyxiation., and brains were either split down the midline, with one half being collected whole and the other dissected into regions. The dissected half was dissected into the cortex, hippocampus, striatum, and cerebellum/miscellaneous. Tissue was snap frozen in liquid nitrogen then stored at -80 °C.

Results

For the younger cohorts, we did not see any neurotoxic synergy between TDP-43 and tau. The 18-month cohort allows for aging to be a bigger variable, like humans, where older adults tend to get AD-LATE (Nelson et al., 2019). The 18-month cohort consisted of 61 mice: 15 TDP-43;tau, 16 tau, 16 TDP-43, and 14 non-Tg. Less invasive tests, such as weight and Hind

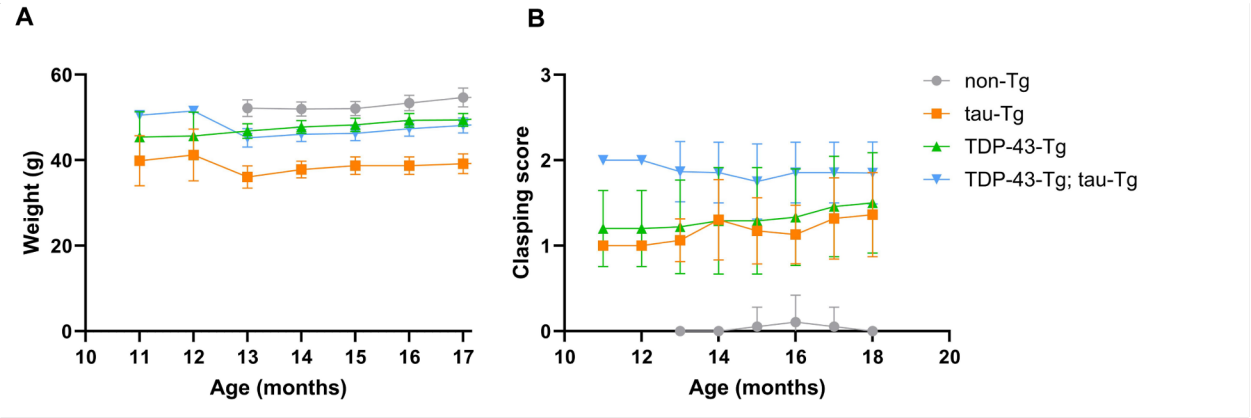

Fig. 34. Weight and clasping scores of 18-month mouse cohort. (A) weight of mice in grams. **(B)** Clasping score of 0, 1, or 2. A 2 indicates full clasping with both hind limbs.

leg clasping were recorded every three weeks, starting at 12 months and ending at around 18 months (Fig. 34A,B). Tau-Tg mice weighed the least, and non-Tg mice weighed the most (Fig. 34A). Hind limb clasping was predominantly only seen in Tg animals. Tau-Tg and TDP-43-Tg mice had similar clasping score, while TDP-43-Tg; Tau-Tg mice had significantly higher clasping score (Fig. 34B). Higher clasping scores, indicate a motor deficit, indicating neurotoxic synergy between TDP-43 and Tau-Tg.

To test spatial working memory and the propensity of mice to explore new environments had mice navigate a Y maze (Long et al., 2017). There were no significant differences between

the four groups (Fig. 35A). When we divided mice by sex, we still saw no changes in percent spontaneous alteration (Fig. 35B).

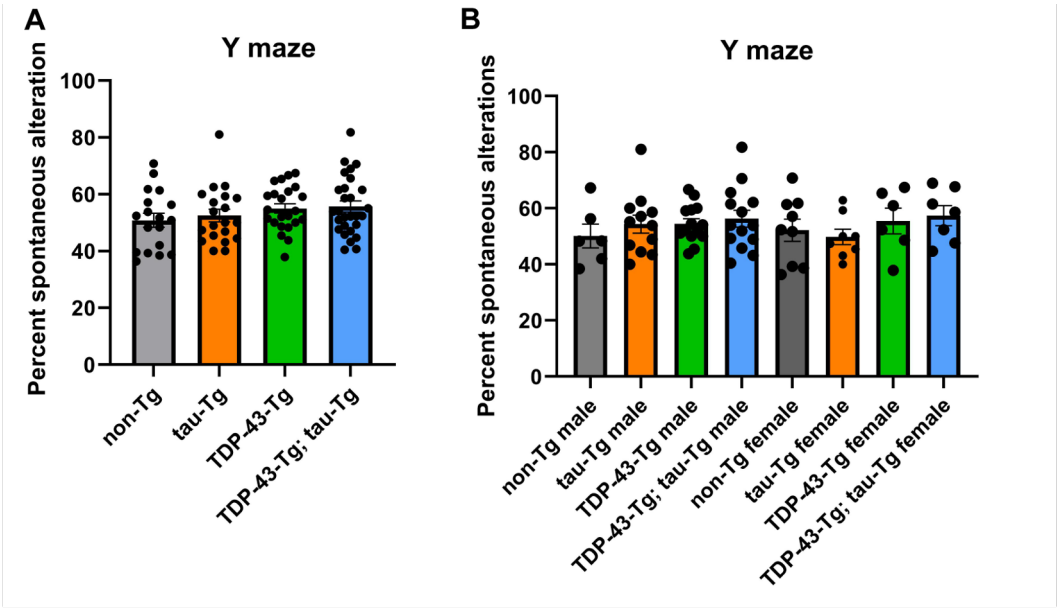

Fig. 35. Percent spontaneous alterations in a Y maze. (A) No difference between mouse groups. **(B)** There were no sex differences either.

To measure locomotor behavior and anxiety-like behavior, we had mice put in an Open field apparatus for 10 minutes (Ono and Aoki, 2026, Seibenhener and Wooten, 2015). Open field measures the time mice stay in the center of the periphery of the circular chamber. It also measures freezing, distance traveled, and speed of the mice. Overall, there were no trends that were uniquely significant for TDP-43-Tg; tau-Tg mice compared to TDP-43-Tg or Tau-Tg mice. In (Fig. 36A,B) we show there are sex differences in distance the mice traveled over the 10 minutes in the open field test. When not divided by sex, all 4 groups traveled a similar distance (Fig. 36A). When divided by sex, female mice had significant differences from each other, with TDP-43-Tg mice moving further than TDP-43-Tg; tau-Tg and WT mice. When looking at max speed (meters/sec), non-Tg mice moved faster than TDP-43-Tg and TDP-43-Tg; tau-Tg mice (Fig. 36C). This pattern of max speed stayed similar when looking at male mice, but the female mice TDP-43-Tg mice had the highest max speed (Fig. 36D). Open field did not show any neurotoxic synergy between TDP-43 and tau but did show some sex differences.

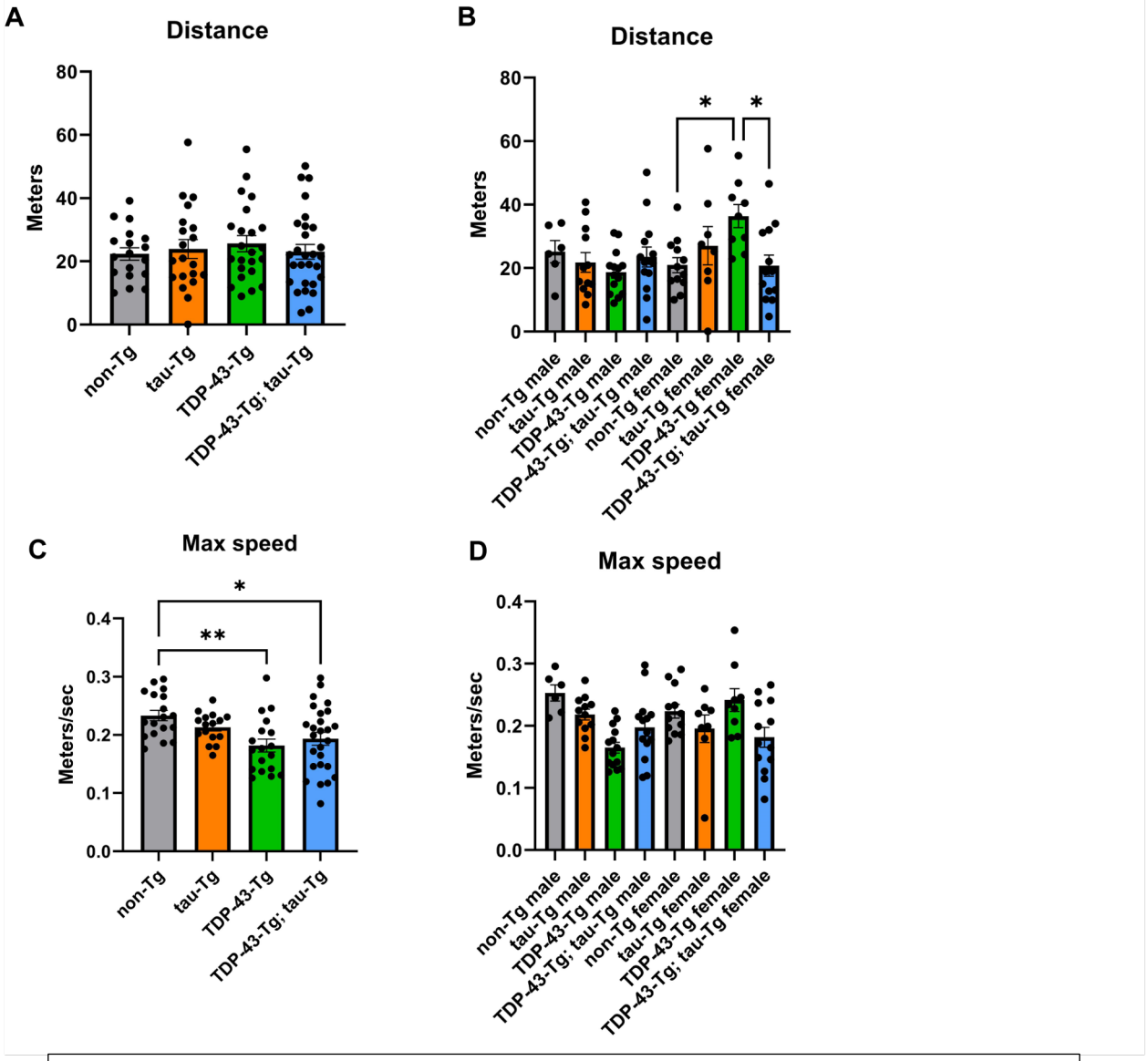

Fig. 36. Open field distance traveled and max speed. **(A)** All four groups moved a similar distance. **(B)** When divided by sex, female mice had some differences. With TDP-43-Tg mice traveling the furthest distance. **(C)** TDP-43-Tg and TDP-43-Tg; tau;Tg mice moved at a slower max speed than non-Tg mice. **(D)** This max speed difference was less clear when divided by sex. One-way ANOVA with Tukey's multiple comparison test. *p<0.05,**p<0.01. Data are mean ± s.e.m.

To measure motor performance and motor learning we tested mice on a Rotarod (Zhang et al., 2019). This test had a learning component, with training of the test on day one. On day two we measured how long a mouse could stay on a moving rod, as it accelerates. Similar to clasping, the Rotarod showed there is more motor dysfunction in TDP-43-Tg; tau-Tg mice compared to TDP-43-Tg or tau-Tg mice alone (Fig. 37A). This neurotoxic synergy was only present at the

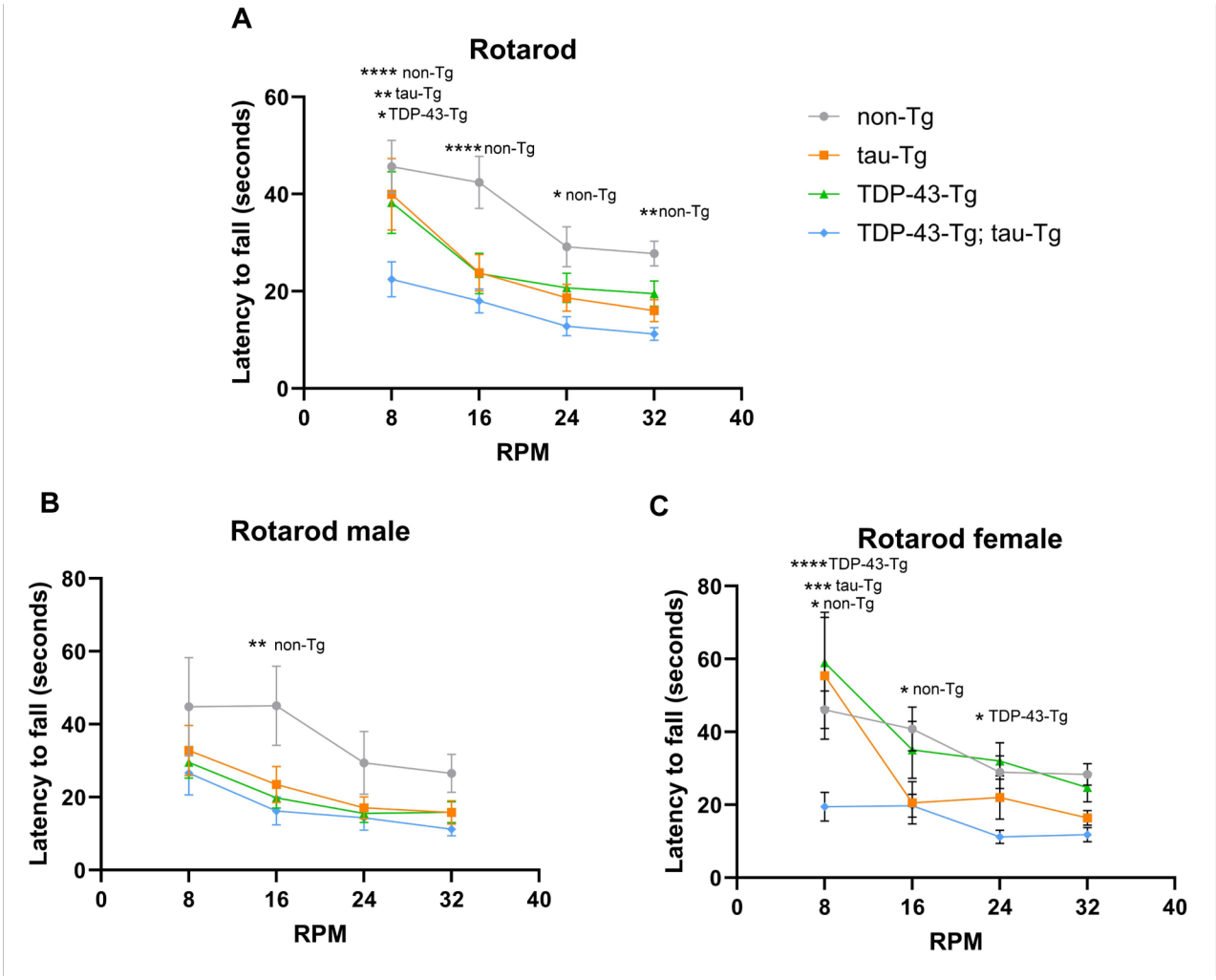

Fig 37. Female TDP-43-Tg; tau-Tg mice have impaired motor function on the Rotarod. (A) TDP-43-Tg; tau-Tg mice have a lower latency to fall than tau-Tg and TDP-43-Tg mice at 8 RPM. **(B)** When looking at just male mice, TDP-43-Tg mice have a very similar latency to fall pattern as tau-Tg and TDP-43-Tg mice. **(C)** Female TDP-43-Tg; tau-Tg mice have a much lower latency to fall than tau-Tg and TDP-43-Tg mice at 8RPM. When The rotarod is sped up, the gap shrinks but there is still a difference with TDP-43-Tg mice at 24 RPM. All significance shown is in comparison with TDP-43-Tg; tau-Tg mice. One-way ANOVA with Tukey's multiple comparison test. *p<0.05,**p<0.01, ***p<0.001,****p<0.0001. Data are mean ± s.e.m.

lowest speed of 8 RPM, indicating that TDP-43-Tg and tau-Tg mice started struggling to stay on the rod in a similar fashion as the RPM increased. Interestingly when dividing the groups by sex, there were stark sex differences (Fig. 37B,C). Male TDP-43-Tg; tau-Tg mice had a similar latency to fall as male TDP-43-Tg or tau-Tg mice (Fig. 37B). Female TDP-43-Tg; tau-Tg mice had a much lower latency to fall than female TDP-43-Tg or tau-Tg mice at 8RPM. Female TDP-43-Tg; tau-Tg also had a lower latency to fall at 24 RMP compared to TDP-43-Tg mice (Fig. 37C). This result on the Rotarod indicates that there is neurotoxic synergy between TDP-43 and tau but it is specific to certain behaviors and is influenced by sex differences.

Discussion

We chose to use the TAR4 Kumar-Singh (TDP-43-Tg) mice and the Tau4Rtg2652 (tau-Tg) mice to study neurotoxic synergy between TDP-43 and tau due to their mild phenotypes and normal lifespan (Wheeler et al., 2015, Wils et al., 2010). We did not see clear behavior or immunohistochemistry (IHC) changes that indicate neurotoxic synergy at 12 months. At 18 months we started to see some behavior changes, with worse clasping score (Fig 34) as well as more difficulty on the Rotarod (Fig 37) in TDP-43-Tg; tau-Tg mice compared to the TDP-43-Tg and tau-Tg mice alone. Both Rotarod and and clasping differences show there is some enhanced motor dysfunction in the TDP-43-Tg; tau-Tg mice. Additionally, we saw sex specific differences in Open field, with female mice being more affected (Fig. 36B) and Rotarod (Fig. 37BC).

Conclusions and Future Directions

Over the past 3 chapters we created and characterized a cytoplasmic TDP-43 *C. elegans* model, used point mutations to alter TDP-43 domains in *C. elegans* to study its neurotoxic co-pathology with tau, and found age related sex and behavioral differences in a new TDP-43; tau transgenic mouse strain. These 3 chapters better our understanding of cytoplasmic and nuclear TDP-43, as well as our understanding of what is important for TDP-43; tau neurotoxic synergy. Each chapter also improved our tools and knowledge to further study TDP-43 and tau in neurodegenerative diseases.

In chapter 1, we created TDP-43 ΔNLS stains that allow the study of cytoplasmic TDP-43 in *C. elegans*. Prior to these strains, TDP-43 gain-of-function models in *C. elegans* expressed TDP-43 and pTDP-43 in the nucleus and not the cytoplasm (Liachko et al., 2010).

The three TDP-43 ΔNLS strains we generated showed dose dependent behavior deficits (Fig. 8) and neurodegeneration (Fig. 11). In humans, TDP-43 pathology can be categorized into different types, with FTLD-TDP type A being nuclear and cytoplasmic, FTLD-TDP type B and C being cytoplasmic, and FTLD-TDP type D being nuclear (Neumann et al., 2021). Most TDP-43 pathology is cytoplasmic, making it important to have a cytoplasmic TDP-43 model in *C. elegans*. Understanding differences in cytoplasmic and nuclear TDP-43 pathology can help up have more disease specific treatments.

In chapter 1 we saw interesting proteostasis differences between *C. elegans* expressing cytoplasmic or nuclear TDP-43. Interestingly, the overexpression of the transcription factor, xbp-1s, rescued the behavioral phenotype of TDP-43 ΔNLS (med) (Fig. 16B) and TDP-43 ΔNLS (high) (Fig. 17B) while not rescuing TDP-43-Tg (Fig. 16A) or TDP-43-Tg (low) (Fig. 17A). These differences indicate a potential difference in the unfolded protein response (UPR^{ER}) for cytoplasmic TDP-43 vs nuclear TDP-43. Looking more into the mechanism of the UPR^{ER} in relation to cytoplasmic and nuclear TDP-43 could be essential to finding ways to clear cytoplasmic TDP-43. Future experiments, trying to block the UPR^{ER} to confirm its role in rescuing the motility of cytoplasmic TDP-43 will be important. We will also look at protein levels of TDP-43 and pTDP-43 in TDP-43-Tg, TDP-43 ΔNLS, TDP-43-Tg; xbp-1s, and TDP-43 ΔNLS; xbp-1s to determine if TDP-43 is being degraded by the upregulation of the UPR^{ER}.

In chapter 2 we used point mutations to alter TDP-43 domains, allowing us to see functional changes and to determine if those mutations stop the neurotoxic synergy with tau. While we saw some reduction of synergy when tau-Tg was crossed with TDP-43 4xPTM (Fig. 27) and TDP-43 ΔNLS (Fig. 23), there were no clear results that completely stopped the neurotoxic synergy. The TDP-43 4xPTM strain is a bit crude, with point mutations in the NLS, RRM1 and RRM2. To have a more nuanced approach, we created 3 more PTM strains: TDP-43 K84R, TDP-43 K136/145R, and TDP-43 K192R (table 4). We have crossed all three of these strains with tau-Tg (low) and will soon characterize their behavior.

There is a major disease SUMOylation site, TDP-43 K408, that we have yet to investigate. Interestingly, SUMOylation of TDP-43 K408 has an inverse relationship with phosphorylation of TDP-43 S409/410 (Suk et al., 2025). Blocking phosphorylation of TDP-43 S409/410 may be increasing SUMOylation of K408. Since blocking phosphorylation of TDP-43 S409/410 does not rescue TDP-43; tau synergy (Fig. 29), there might be a chance that blocking SUMOylation of K408 might alter the synergy. We already have TDP-43 K408R mutants created in our lab and will just need to cross them with tau-Tg (low) and run behavior assays.

The importance of mitochondrial changes in TDP-43 pathologies has been brought up in both chapter 1 and 2 (Fig. 32). In addition to further looking into the role of TDP-43 in mitochondrial dysfunction in *C. elegans*, we could also look at mitochondrial dysfunction in the TDP-tg; tau-Tg mice in chapter 3. TDP-43 can co-localize with mitochondria (Wang et al., 2016), and can cause mitochondrial dysfunction, increased reactive oxygen species (ROS), decreased mitochondrial membrane potential, and the triggering of the mitochondrial unfolded protein response (UPR^{mt}) (Torres et al., 2024). In chapter 1, we show ZIP-2 is upregulated in TDP-43 ΔNLS but downregulated in TDP-43-Tg (Fig. 13B,D). ZIP-2 has been shown to be related to age-related mitochondrial dysfunction in *C. elegans* (Hahm et al., 2020). The mitochondrial protease LonP1 can regulate TDP-43, with down-regulation of LonP1 resulting in increased mitochondrial TDP-43 levels (Wang et al., 2019) In LONP-1 deficient *C. elegans*, ZIP-2 is activated in a PMK-3-dependent manner, making it a potential response to mitochondrial stress in *C. elegans*. The large contrasting regulation of ZIP-2 in nuclear vs cytoplasmic TDP-43 strains, could be due to more mitochondrial dysfunction in TDP-43 ΔNLS. It will be important to characterize mitochondrial function in TDP-43 ΔNLS and compare it to TDP-43-Tg. In the chapter 2 discussion we showed TDP-43 M337V had increased mitochondrial dysfunction (Fig. 32). TDP-43 could be altering mitochondrial function in *C. elegans* and possibly co-localizing with mitochondria. This stress to mitochondria could be causing the neurotoxicity with tau. TDP-43 has been shown to co-localize with mitochondria in ALS and FTD patients and TDP-43 has six predicted mitochondrial localization sequences (Wang et al., 2016). Characterizing mitochondrial dysfunction in TDP-43 and tau *C. elegans* would improve our understanding of those proteins as well as their synergy. Generating strains that have mutations in the mitochondrial localization sequences of TDP-43, such as M1 (35-41), M3 (146-150), or M5 (294-300), would help us understand if TDP-43 is affecting mitochondria (Wang et al., 2016).

Fig. 38 helps summarize the findings and future directions of chapter 2. We will continue to alter TDP-43 domains and determine if those alterations reduce TDP-43; tau synergy. Through RNAseg, TDP-43 Δoligo, and TDP-43 ΔRRM, we have learned that RNA binding and RNA metabolism is less important in our TDP-43 gain of function *C. elegans* models. Looking at more downstream pathways, including mitochondrial changes, and proteostasis, could be key to understanding TDP-43; tau synergy and the differences between nuclear and cytoplasmic TDP-43. It will also be important to use TDP-43-Tg and TDP-43-Tg; tau-Tg (low) as extra controls in future experiments to better determine if what we are seeing is synergy.

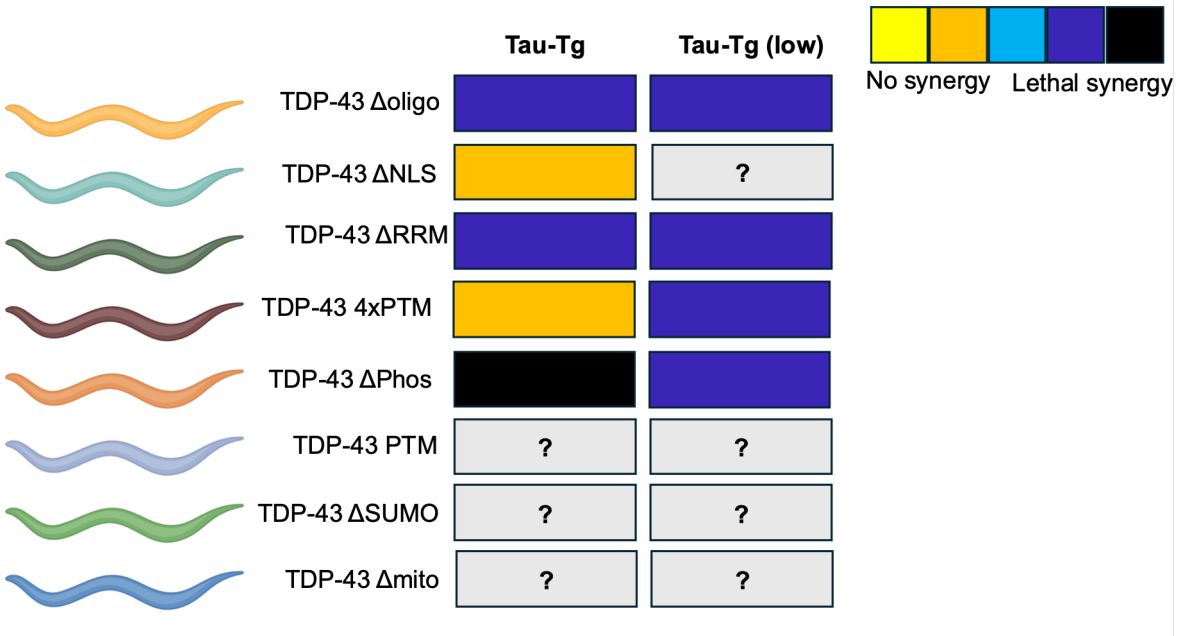

Fig. 38. Summary of TDP-43;tau crosses and future crosses. We saw slight changes in synergy when crossing cytoplasmic TDP-43 and the 4xPTM mutant with tau-Tg (low). We plan to look into single PTM sites 84, 136, 145, 192, and 408. We also plan to look at if mitochondria are playing a role in TDP-43; tau synergy.

In chapter 3 we characterized the behavior of an 18 month cohort of TDP-tg; tau-Tg mice. While we saw some neurotoxic synergy between TDP-43 and tau (Fig. 34B, Fig. 37) and some sex differences (Fig. 36B, Fig. 37B,C) but overall saw mild phenotype. We have started processing hippocampal tissue for IHC but have not seen an increase in pTDP-43 in the TDP-43-Tg; tau-Tg mice (data not shown). Neuronal loss in the CA1 of the hippocampus seems to be tau driven, with similar brain changes in male and female mice (data not shown).

While we have mostly looked at the hippocampus, there are other brain regions that could be more affected by the TDP-43; tau co-pathology. The behavior tests that showed significant neurotoxic synergy were all motor related. Testing the cerebellum, cortex, and other regions are logical next steps to see potential changes that are driving behavior. Additionally, the Amygdala and the Entorhinal cortex have large amounts of TDP-43 and tau pathology in human brains (Wisse et al., 2025). Looking for synergy in those brain areas will be a logical next step. While we saw some behavioral changes at 18 months, the overall phenotype of our TDP-43-Tg; tau-Tg mouse model was mild. Using a stronger TDP-43 mouse could increase toxicity enough to see clearer synergy, especially with the histology.

These past three chapters have improved the current models for studying TDP-43 in *C. elegans* with the hopes that the cytoplasmic TDP-43 models will lead to more translational

experiments by more closely resembling the most common TDP-43 pathology. While we have not fully figured out what is causing the neurotoxic synergy between TDP-43 and tau, we have narrowed down the potential mechanism and are continuing to generate and test TDP-43-Tg strains with point mutations that alter domain functions. Based on our previous domain alterations, we have determined that TDP-43 RNA functions are less important for synergy and we should focus on more downstream pathways. While we are continuing to process tissue for the TDP-43-Tg; tau-Tg study, we are excited to see some neurotoxic synergy with clasping (Fig. 34B) and rotarod (Fig. 37) and we found some exciting sex differences (Fig. 37A,B). We will be finishing up the sample processing, by running western blots for cortex, hippocampus, striatum, and cerebellum/miscellaneous tissues as well as continue to look at IHC at potentially damaged brain regions. So far, we have focused on the hippocampus, seeing tau driven neuronal loss in the CA1 region but we still need to look at the entorhinal cortex and the amygdala, both regions that show tau and TDP-43 pathology in human autopsies of AD LATE brains (Wisse et al., 2025). Uncovering the vulnerable areas for TDP-43; tau synergy in our mice will allow for intervention mouse studies and more translational experiments.

Overall, these three chapters show that TDP-43 gain-of-function is a major contributor to neurotoxicity and is much more important than TDP-43 loss of function in *C. elegans*. There needs to be better characterization of cytoplasmic vs nuclear TDP-43 aggregates, with comparisons to human tissue samples. The ER unfolded protein response and the mitochondrial unfolded protein response could be playing an important role in TDP-43 pathology, and both pathways in relation to TDP-43 need to be studied more. The role of TDP-43 localization with mitochondria also needs to be characterized better, and it could be playing an important role in cytoplasmic vs nuclear TDP-43 differences as well as TDP-43; tau synergy. Lastly, more mouse and human samples need to be divided by sex. Understanding why female TDP-43; tau mice performed worse on the rotarod is important to understanding the way TDP-43 affects females vs men. Our mouse findings reinforce the importance of always looking for sex differences in human studies.

ARAI, T., HASEGAWA, M., AKIYAMA, H., IKEDA, K., NONAKA, T., MORI, H., MANN, D., TSUCHIYA, K., YOSHIDA, M., HASHIZUME, Y. & ODA, T. 2006. TDP-43 is a component of ubiquitin-positive tau-negative inclusions in frontotemporal lobar degeneration and amyotrophic lateral sclerosis. *Biochem Biophys Res Commun,* 351**,** 602-11.

ARMAS, J. M. B., TAORO-GONZALEZ, L., FISHER, E. M. C. & ACEVEDO-AROZENA, A. 2025. Challenges of modelling TDP-43 pathology in mice. *Mamm Genome,* 36**,** 465-481.

ASH, P. E., ZHANG, Y. J., ROBERTS, C. M., SALDI, T., HUTTER, H., BURATTI, E., PETRUCELLI, L. & LINK, C. D. 2010. Neurotoxic effects of TDP-43 overexpression in C. elegans. *Hum Mol Genet,* 19**,** 3206-18.

AYALA, Y. M., DE CONTI, L., AVENDANO-VAZQUEZ, S. E., DHIR, A., ROMANO, M., D'AMBROGIO, A., TOLLERVEY, J., ULE, J., BARALLE, M., BURATTI, E. & BARALLE, F. E. 2011. TDP-43 regulates its mRNA levels through a negative feedback loop. *EMBO J,* 30**,** 277-88.

BADIA-I-MOMPEL, P., VÉLEZ SANTIAGO, J., BRAUNGER, J., GEISS, C., DIMITROV, D., MÜLLER-DOTT, S., TAUS, P., DUGOURD, A., HOLLAND, C. H., RAMIREZ FLORES, R. O. & SAEZ-RODRIGUEZ, J. 2022. decoupleR: ensemble of computational methods to infer biological activities from omics data. *Bioinform Adv,* 2**,** vbac016.

BALENDRA, R., SREEDHARAN, J., HALLEGGER, M., LUISIER, R., LASHUEL, H. A., GREGORY, J. M. & PATANI, R. 2025. Amyotrophic lateral sclerosis caused by TARDBP mutations: from genetics to TDP-43 proteinopathy. *Lancet Neurol,* 24**,** 456-470.

BENARD, C., TJOE, N., BOULIN, T., RECIO, J. & HOBERT, O. 2009. The small, secreted immunoglobulin protein ZIG-3 maintains axon position in Caenorhabditis elegans. *Genetics,* 183**,** 917-27.

BORRONI, B., BONVICINI, C., ALBERICI, A., BURATTI, E., AGOSTI, C., ARCHETTI, S., PAPETTI, A., STUANI, C., DI LUCA, M., GENNARELLI, M. & PADOVANI, A. 2009. Mutation within TARDBP leads to frontotemporal dementia without motor neuron disease. *Hum Mutat,* 30**,** E974-83.

BOYARKO, B. & HOOK, V. 2021. Human Tau Isoforms and Proteolysis for Production of Toxic Tau Fragments in Neurodegeneration. *Front Neurosci,* 15**,** 702788.

BRAAK, H., ALAFUZOFF, I., ARZBERGER, T., KRETZSCHMAR, H. & DEL TREDICI, K. 2006. Staging of Alzheimer disease-associated neurofibrillary pathology using paraffin sections and immunocytochemistry. *Acta Neuropathol,* 112**,** 389-404.

BRANDT, R., GERGOU, A., WACKER, I., FATH, T. & HUTTER, H. 2009. A Caenorhabditis elegans model of tau hyperphosphorylation: induction of developmental defects by transgenic overexpression of Alzheimer's disease-like modified tau. *Neurobiol Aging,* 30**,** 22-33.

BRENNER, S. 2003. Nature's gift to science (Nobel lecture). *Chembiochem,* 4**,** 683-7.

BUCIUC, M., WHITWELL, J. L., BOEVE, B. F., FERMAN, T. J., GRAFF-RADFORD, J., SAVICA, R., KANTARCI, K., FIELDS, J. A., KNOPMAN, D. S., PETERSEN, R. C., PARISI, J. E., MURRAY, M. E., DICKSON, D. W. & JOSEPHS, K. A. 2020. TDP-43 is associated with a reduced likelihood of rendering a clinical diagnosis of dementia with Lewy bodies in autopsy-confirmed cases of transitional/diffuse Lewy body disease. *J Neurol,* 267**,** 1444-1453.

BUTLER PAGNOTTI, R. M., PUDUMJEE, S. B., CROSS, C. L. & MILLER, J. B. 2023. Cognitive and Clinical Characteristics of Patients With Limbic-Predominant Age-Related TDP-43 Encephalopathy. *Neurology,* 100**,** e2027-e2035.

CALFON, M., ZENG, H., URANO, F., TILL, J. H., HUBBARD, S. R., HARDING, H. P., CLARK, S. G. & RON, D. 2002. IRE1 couples endoplasmic reticulum load to secretory capacity by processing the XBP-1 mRNA. *Nature,* 415**,** 92-6.

CARMEN-OROZCO, R. P., TSAO, W., YE, Y., SINHA, I. R., CHANG, K., TRINH, V. T., CHUNG, W., BOWDEN, K., TRONCOSO, J. C., BLACKSHAW, S., HAYES, L. R., SUN, S., WONG, P. C. & LING, J. P. 2024. Elevated nuclear TDP-43 induces constitutive exon skipping. *Mol Neurodegener,* 19**,** 45.

CASTILLO, A. & DE LA GUARDIA, Y. 2017. Spineless solutions: The potential of invertebrate animal models for advancing science in the developing world. *EMBO Rep,* 18**,** 1885-1888.

CHANG, C. K., WU, T. H., WU, C. Y., CHIANG, M. H., TOH, E. K., HSU, Y. C., LIN, K. F., LIAO, Y. H., HUANG, T. H. & HUANG, J. J. 2012. The N-terminus of TDP-43 promotes its oligomerization and enhances DNA binding affinity. *Biochem Biophys Res Commun,* 425**,** 219-24.

CHEN, S., ZHOU, Y., CHEN, Y. & GU, J. 2018. fastp: an ultra-fast all-in-one FASTQ preprocessor. *Bioinformatics,* 34**,** i884-i890.

CHIANG, P. M., LING, J., JEONG, Y. H., PRICE, D. L., AJA, S. M. & WONG, P. C. 2010. Deletion of TDP-43 down-regulates Tbc1d1, a gene linked to obesity, and alters body fat metabolism. *Proc Natl Acad Sci U S A,* 107**,** 16320-4.

CHIU, S. Y., BOWERS, D. & ARMSTRONG, M. J. 2022. Lewy Body Dementias: Controversies and Drug Development. *Neurotherapeutics,* 19**,** 55-67.

CINAR, H., KELES, S. & JIN, Y. 2005. Expression profiling of GABAergic motor neurons in Caenorhabditis elegans. *Curr Biol,* 15**,** 340-6.
COHEN, T. J., HWANG, A. W., RESTREPO, C. R., YUAN, C. X., TROJANOWSKI, J. Q. & LEE, V. M. 2015. An acetylation switch controls TDP-43 function and aggregation propensity. *Nat Commun,* 6**,** 5845.
COHEN, T. J., LEE, V. M. & TROJANOWSKI, J. Q. 2011. TDP-43 functions and pathogenic mechanisms implicated in TDP-43 proteinopathies. *Trends Mol Med,* 17**,** 659-67.
CONICELLA, A. E., ZERZE, G. H., MITTAL, J. & FAWZI, N. L. 2016. ALS Mutations Disrupt Phase Separation Mediated by alpha-Helical Structure in the TDP-43 Low-Complexity C-Terminal Domain. *Structure,* 24**,** 1537-49.
CORSI, A. K., WIGHTMAN, B. & CHALFIE, M. 2015. A Transparent Window into Biology: A Primer on Caenorhabditis elegans. *Genetics,* 200**,** 387-407.
CURREY, H. N., KRAEMER, B. C. & LIACHKO, N. F. 2023. sut-2 loss of function mutants protect against tau-driven shortened lifespan and hyperactive pharyngeal pumping in a C. elegans model of tau toxicity. *MicroPubl Biol,* 2023.
CURREY, H. N. & LIACHKO, N. F. 2021. Evaluation of Motor Impairment in C. elegans Models of Amyotrophic Lateral Sclerosis. *J Vis Exp*.
DAGAR, S., PATHAK, D., OZA, H. V. & MYLAVARAPU, S. V. S. 2021. Tunneling nanotubes and related structures: molecular mechanisms of formation and function. *Biochem J,* 478**,** 3977-3998.
DAVIS, S. A., GAN, K. A., DOWELL, J. A., CAIRNS, N. J. & GITCHO, M. A. 2017. TDP-43 expression influences amyloidbeta plaque deposition and tau aggregation. *Neurobiol Dis,* 103**,** 154-162.
DICKSON, D. W., KOURI, N., MURRAY, M. E. & JOSEPHS, K. A. 2011. Neuropathology of frontotemporal lobar degeneration-tau (FTLD-tau). *J Mol Neurosci,* 45**,** 384-9.
DOBIN, A., DAVIS, C. A., SCHLESINGER, F., DRENKOW, J., ZALESKI, C., JHA, S., BATUT, P., CHAISSON, M. & GINGERAS, T. R. 2013. STAR: ultrafast universal RNA-seq aligner. *Bioinformatics,* 29**,** 15-21.
DOLL, S. G., MESHKIN, H., BRYER, A. J., LI, F., KO, Y. H., LOKAREDDY, R. K., GILLILAN, R. E., GUPTA, K., PERILLA, J. R. & CINGOLANI, G. 2022. Recognition of the TDP-43 nuclear localization signal by importin alpha1/beta. *Cell Rep,* 39**,** 111007.
DUAN, L., ZAEPFEL, B. L., AKSENOVA, V., DASSO, M., ROTHSTEIN, J. D., KALAB, P. & HAYES, L. R. 2022. Nuclear RNA binding regulates TDP-43 nuclear localization and passive nuclear export. *Cell Rep,* 40**,** 111106.
DUAN, Y., DU, A., GU, J., DUAN, G., WANG, C., GUI, X., MA, Z., QIAN, B., DENG, X., ZHANG, K., SUN, L., TIAN, K., ZHANG, Y., JIANG, H., LIU, C. & FANG, Y. 2019. PARylation regulates stress granule dynamics, phase separation, and neurotoxicity of disease-related RNA-binding proteins. *Cell Res,* 29**,** 233-247.
DURAN-ANIOTZ, C., POBLETE, N., RIVERA-KRSTULOVIC, C., ARDILES, A. O., DIAZ-HUNG, M. L., TAMBURINI, G., SABUSAP, C. M. P., GERAKIS, Y., CABRAL-MIRANDA, F., DIAZ, J., FUENTEALBA, M., ARRIAGADA, D., MUNOZ, E., ESPINOZA, S., MARTINEZ, G., QUIROZ, G., SARDI, P., MEDINAS, D. B., CONTRERAS, D., PINA, R., LOURENCO, M. V., RIBEIRO, F. C., FERREIRA, S. T., ROZAS, C., MORALES, B., PLATE, L., GONZALEZ-BILLAULT, C., PALACIOS, A. G. & HETZ, C. 2023. The unfolded protein response transcription factor XBP1s ameliorates Alzheimer's disease by improving synaptic function and proteostasis. *Mol Ther,* 31**,** 2240-2256.
ECK, R. J., KRAEMER, B. C. & LIACHKO, N. F. 2021. Regulation of TDP-43 phosphorylation in aging and disease. *Geroscience,* 43**,** 1605-1614.
ECK, R. J., STAIR, J. G., KRAEMER, B. C. & LIACHKO, N. F. 2023. Simple models to understand complex disease: 10 years of progress from Caenorhabditis elegans models of amyotrophic lateral sclerosis and frontotemporal lobar degeneration. *Front Neurosci,* 17**,** 1300705.
ESTES, K. A., DUNBAR, T. L., POWELL, J. R., AUSUBEL, F. M. & TROEMEL, E. R. 2010. bZIP transcription factor zip-2 mediates an early response to Pseudomonas aeruginosa infection in Caenorhabditis elegans. *Proc Natl Acad Sci U S A,* 107**,** 2153-8.
FELDMAN, E. L., GOUTMAN, S. A., PETRI, S., MAZZINI, L., SAVELIEFF, M. G., SHAW, P. J. & SOBUE, G. 2022. Amyotrophic lateral sclerosis. *Lancet,* 400**,** 1363-1380.

FENG, Y., JOSHI, V., PANKIVSKYI, S., CLEMENT, M. J., RENGIFO-GONZALEZ, J. C., THUREAU, A., PASTRE, D. & BOUHSS, A. 2026. From TDP-43/RNA complex formation to disease-linked TDP-43 aggregation through a structural and cellular approach. *Nat Commun,* 17**,** 1631.

FERRI, A., NENCINI, M., BATTISTINI, S., GIANNINI, F., SICILIANO, G., CASALI, C., DAMIANO, M. G., CERONI, M., CHIO, A., ROTILIO, G. & CARRI, M. T. 2004. Activity of protein phosphatase calcineurin is decreased in sporadic and familial amyotrophic lateral sclerosispatients. *J Neurochem,* 90**,** 1237-42.

FRANCOIS-MOUTAL, L., PEREZ-MILLER, S., SCOTT, D. D., MIRANDA, V. G., MOLLASALEHI, N. & KHANNA, M. 2019. Structural Insights Into TDP-43 and Effects of Post-translational Modifications. *Front Mol Neurosci,* 12**,** 301.

FRENCH, R. L., GRESE, Z. R., ALIGIREDDY, H., DHAVALE, D. D., REEB, A. N., KEDIA, N., KOTZBAUER, P. T., BIESCHKE, J. & AYALA, Y. M. 2019. Detection of TAR DNA-binding protein 43 (TDP-43) oligomers as initial intermediate species during aggregate formation. *J Biol Chem,* 294**,** 6696-6709.

GAO, J., WANG, L., YAN, T., PERRY, G. & WANG, X. 2019. TDP-43 proteinopathy and mitochondrial abnormalities in neurodegeneration. *Mol Cell Neurosci,* 100**,** 103396.

GARCIA MORATO, J., HANS, F., VON ZWEYDORF, F., FEEDERLE, R., ELSASSER, S. J., SKODRAS, A. A., GLOECKNER, C. J., BURATTI, E., NEUMANN, M. & KAHLE, P. J. 2022. Sirtuin-1 sensitive lysine-136 acetylation drives phase separation and pathological aggregation of TDP-43. *Nat Commun,* 13**,** 1223.

GROSSMAN, M., SEELEY, W. W., BOXER, A. L., HILLIS, A. E., KNOPMAN, D. S., LJUBENOV, P. A., MILLER, B., PIGUET, O., RADEMAKERS, R., WHITWELL, J. L., ZETTERBERG, H. & VAN SWIETEN, J. C. 2023. Frontotemporal lobar degeneration. *Nat Rev Dis Primers,* 9**,** 40.

GUPTE, R., LIU, Z. & KRAUS, W. L. 2017. PARPs and ADP-ribosylation: recent advances linking molecular functions to biological outcomes. *Genes Dev,* 31**,** 101-126.

HAHM, J. H., JEONG, C., LEE, W., KOO, H. J., KIM, S., HWANG, D. & NAM, H. G. 2020. A cellular surveillance and defense system that delays aging phenotypes in C. elegans. *Aging (Albany NY),* 12**,** 8202-8220.

HAMPEL, H., HU, Y., HARDY, J., BLENNOW, K., CHEN, C., PERRY, G., KIM, S. H., VILLEMAGNE, V. L., AISEN, P., VENDRUSCOLO, M., IWATSUBO, T., MASTERS, C. L., CHO, M., LANNFELT, L., CUMMINGS, J. L. & VERGALLO, A. 2023. The amyloid-beta pathway in Alzheimer's disease: a plain language summary. *Neurodegener Dis Manag*.

HAN, M., SAXTON, A., CURREY, H., WALDHERR, S. M., LIACHKO, N. F. & KRAEMER, B. C. 2024. Transgenic Dendra2::tau expression allows in vivo monitoring of tau proteostasis in Caenorhabditis elegans. *Dis Model Mech,* 17.

HANS, F., ECKERT, M., VON ZWEYDORF, F., GLOECKNER, C. J. & KAHLE, P. J. 2018. Identification and characterization of ubiquitinylation sites in TAR DNA-binding protein of 43 kDa (TDP-43). *J Biol Chem,* 293**,** 16083-16099.

HARRISON, P. W., AMODE, M. R., AUSTINE-ORIMOLOYE, O., AZOV, A. G., BARBA, M., BARNES, I., BECKER, A., BENNETT, R., BERRY, A., BHAI, J., BHURJI, S. K., BODDU, S., BRANCO LINS, P. R., BROOKS, L., RAMARAJU, S. B., CAMPBELL, L. I., MARTINEZ, M. C., CHARKHCHI, M., CHOUGULE, K., ... & YATES, A. D. 2024. Ensembl 2024. *Nucleic Acids Res,* 52**,** D891-D899.

HE, J., ZHOU, Y. & SUN, L. 2024. Emerging mechanisms of the unfolded protein response in therapeutic resistance: from chemotherapy to Immunotherapy. *Cell Commun Signal,* 22**,** 89.

HIGASHI, S., ISEKI, E., YAMAMOTO, R., MINEGISHI, M., HINO, H., FUJISAWA, K., TOGO, T., KATSUSE, O., UCHIKADO, H., FURUKAWA, Y., KOSAKA, K. & ARAI, H. 2007. Concurrence of TDP-43, tau and alpha-synuclein pathology in brains of Alzheimer's disease and dementia with Lewy bodies. *Brain Res,* 1184**,** 284-94.

HOU, Y., DAN, X., BABBAR, M., WEI, Y., HASSELBALCH, S. G., CROTEAU, D. L. & BOHR, V. A. 2019. Ageing as a risk factor for neurodegenerative disease. *Nat Rev Neurol,* 15**,** 565-581.

HUANG, C., YAN, S. & ZHANG, Z. 2020. Maintaining the balance of TDP-43, mitochondria, and autophagy: a promising therapeutic strategy for neurodegenerative diseases. *Transl Neurodegener,* 9**,** 40.

JAGARAJ, C. J., MEHTA, P., HUNTER, J. & ATKIN, J. D. 2025. A Slower-Progressing TDP-43 rNLS8 Mouse Model for ALS: Implications for Preclinical and Mechanistic Studies. *Neuromolecular Med,* 27**,** 59.

JIANG, H. S., GHOSE, P., HAN, H. F., WU, Y. Z., TSAI, Y. Y., LIN, H. C., TSENG, W. C., WU, J. C., SHAHAM, S. & WU, Y. C. 2021. BLMP-1 promotes developmental cell death in C. elegans by timely repression of ced-9 transcription. *Development,* 148.

JIANG, L. L., XUE, W., HONG, J. Y., ZHANG, J. T., LI, M. J., YU, S. N., HE, J. H. & HU, H. Y. 2017. The N-terminal dimerization is required for TDP-43 splicing activity. *Sci Rep,* 7**,** 6196.

JIANG, L. L., ZHANG, X. L. & HU, H. Y. 2024. Co-Aggregation of TDP-43 with Other Pathogenic Proteins and Their Co-Pathologies in Neurodegenerative Diseases. *Int J Mol Sci,* 25.

JO, M., LEE, S., JEON, Y. M., KIM, S., KWON, Y. & KIM, H. J. 2020. The role of TDP-43 propagation in neurodegenerative diseases: integrating insights from clinical and experimental studies. *Exp Mol Med,* 52**,** 1652-1662.

JOSEPHS, K. A., WHITWELL, J. L., TOSAKULWONG, N., WEIGAND, S. D., MURRAY, M. E., LIESINGER, A. M., PETRUCELLI, L., SENJEM, M. L., IVNIK, R. J., PARISI, J. E., PETERSEN, R. C. & DICKSON, D. W. 2015. TAR DNA-binding protein 43 and pathological subtype of Alzheimer's disease impact clinical features. *Ann Neurol,* 78**,** 697-709.

JOSEPHS, K. A., WHITWELL, J. L., WEIGAND, S. D., MURRAY, M. E., TOSAKULWONG, N., LIESINGER, A. M., PETRUCELLI, L., SENJEM, M. L., KNOPMAN, D. S., BOEVE, B. F., IVNIK, R. J., SMITH, G. E., JACK, C. R., JR., PARISI, J. E., PETERSEN, R. C. & DICKSON, D. W. 2014. TDP-43 is a key player in the clinical features associated with Alzheimer's disease. *Acta Neuropathol,* 127**,** 811-24.

KATSUMATA, Y., WU, X., AUNG, K. Z., GAUTHREAUX, K., MOCK, C., FORREST, S. L., KOVACS, G. G. & NELSON, P. T. 2024. Pathologic correlates of aging-related tau astrogliopathy: ARTAG is associated with LATE-NC and cerebrovascular pathologies, but not with ADNC. *Neurobiol Dis,* 191**,** 106412.

KATTUAH, W., ROGELJ, B., KING, A., SHAW, C. E., HORTOBAGYI, T. & TROAKES, C. 2019. Heterogeneous Nuclear Ribonucleoprotein E2 (hnRNP E2) Is a Component of TDP-43 Aggregates Specifically in the A and C Pathological Subtypes of Frontotemporal Lobar Degeneration. *Front Neurosci,* 13**,** 551.

KAVANAGH, T., HALDER, A. & DRUMMOND, E. 2022. Tau interactome and RNA binding proteins in neurodegenerative diseases. *Mol Neurodegener,* 17**,** 66.

KEATING, S. S., BADEMOSI, A. T., SAN GIL, R. & WALKER, A. K. 2023. Aggregation-prone TDP-43 sequesters and drives pathological transitions of free nuclear TDP-43. *Cell Mol Life Sci,* 80**,** 95.

KEENAN, E. K., ZACHMAN, D. K. & HIRSCHEY, M. D. 2021. Discovering the landscape of protein modifications. *Mol Cell,* 81**,** 1868-1878.

KHOSRAVI, B., LACLAIR, K. D., RIEMENSCHNEIDER, H., ZHOU, Q., FROTTIN, F., MARELJIC, N., CZUPPA, M., FARNY, D., HARTMANN, H., MICHAELSEN, M., ARZBERGER, T., HARTL, F. U., HIPP, M. S. & EDBAUER, D. 2020. Cell-to-cell transmission of C9orf72 poly-(Gly-Ala) triggers key features of ALS/FTD. *EMBO J,* 39**,** e102811.

KLIM, J. R., WILLIAMS, L. A., LIMONE, F., GUERRA SAN JUAN, I., DAVIS-DUSENBERY, B. N., MORDES, D. A., BURBERRY, A., STEINBAUGH, M. J., GAMAGE, K. K., KIRCHNER, R., MOCCIA, R., CASSEL, S. H., CHEN, K., WAINGER, B. J., WOOLF, C. J. & EGGAN, K. 2019. ALS-implicated protein TDP-43 sustains levels of STMN2, a mediator of motor neuron growth and repair. *Nat Neurosci,* 22**,** 167-179.

KNIAZEVA, M. & RUVKUN, G. 2025. Translation elongation defects activate the Caenorhabditis elegans ZIP-2 bZIP transcription factor-mediated toxin defense. *Proc Natl Acad Sci U S A,* 122**,** e2423578122.

KO, Y. H., LOKAREDDY, R. K., DOLL, S. G., YEGGONI, D. P., GIRDHAR, A., MAWN, I., KLIM, J. R., RIZVI, N. F., MEYERS, R., GILLILAN, R. E., GUO, L. & CINGOLANI, G. 2024. Single Acetylation-mimetic Mutation in TDP-43 Nuclear Localization Signal Disrupts Importin alpha1/beta Signaling. *J Mol Biol,* 436**,** 168751.

KOGA, S., ZHOU, X., MURAKAMI, A., FERNANDEZ DE CASTRO, C., BAKER, M. C., RADEMAKERS, R. & DICKSON, D. W. 2022. Concurrent tau pathologies in frontotemporal lobar degeneration with TDP-43 pathology. *Neuropathol Appl Neurobiol,* 48**,** e12778.

KOIKE, Y. 2024. Abnormal Splicing Events due to Loss of Nuclear Function of TDP-43: Pathophysiology and Perspectives. *JMA J,* 7**,** 313-318.

KOOPMAN, M., GUNGORDU, L., JANSSEN, L., SEINSTRA, R. I., RICHMOND, J. E., OKERLUND, N., WARDENAAR, R., ISLAM, P., HOGEWERF, W., BROWN, A. E. X., JORGENSEN, E. M. &

NOLLEN, E. A. A. 2024. Rebalancing the motor circuit restores movement in a Caenorhabditis elegans model for TDP-43 toxicity. *Cell Rep,* 43**,** 114204.
KOVACS, G. G., FERRER, I., GRINBERG, L. T., ALAFUZOFF, I., ATTEMS, J., BUDKA, H., CAIRNS, N. J., CRARY, J. F., DUYCKAERTS, C., GHETTI, B., HALLIDAY, G. M., IRONSIDE, J. W., LOVE, S., MACKENZIE, I. R., MUNOZ, D. G., MURRAY, M. E., NELSON, P. T., TAKAHASHI, H., TROJANOWSKI, J. Q., ANSORGE, O., ARZBERGER, T., BABORIE, A., BEACH, T. G., BIENIEK, K. F., BIGIO, E. H., BODI, I., DUGGER, B. N., FEANY, M., GELPI, E., GENTLEMAN, S. M., GIACCONE, G., HATANPAA, K. J., HEALE, R., HOF, P. R., HOFER, M., HORTOBAGYI, T., JELLINGER, K., JICHA, G. A., INCE, P., KOFLER, J., KOVARI, E., KRIL, J. J., MANN, D. M., MATEJ, R., MCKEE, A. C., MCLEAN, C., MILENKOVIC, I., MONTINE, T. J., MURAYAMA, S., LEE, E. B., RAHIMI, J., RODRIGUEZ, R. D., ROZEMULLER, A., SCHNEIDER, J. A., SCHULTZ, C., SEELEY, W., SEILHEAN, D., SMITH, C., TAGLIAVINI, F., TAKAO, M., THAL, D. R., TOLEDO, J. B., TOLNAY, M., TRONCOSO, J. C., VINTERS, H. V., WEIS, S., WHARTON, S. B., WHITE, C. L., 3RD, WISNIEWSKI, T., WOULFE, J. M., YAMADA, M. & DICKSON, D. W. 2016. Aging-related tau astrogliopathy (ARTAG): harmonized evaluation strategy. *Acta Neuropathol,* 131**,** 87-102.
KOW, R. L., BLACK, A. H., SAXTON, A. D., LIACHKO, N. F. & KRAEMER, B. C. 2022. Loss of aly/ALYREF suppresses toxicity in both tau and TDP-43 models of neurodegeneration. *Geroscience,* 44**,** 747-761.
KRAEMER, B. C., BURGESS, J. K., CHEN, J. H., THOMAS, J. H. & SCHELLENBERG, G. D. 2006. Molecular pathways that influence human tau-induced pathology in Caenorhabditis elegans. *Hum Mol Genet,* 15**,** 1483-96.
KRAEMER, B. C. & SCHELLENBERG, G. D. 2007. SUT-1 enables tau-induced neurotoxicity in C. elegans. *Hum Mol Genet,* 16**,** 1959-71.
KRAEMER, B. C., SCHUCK, T., WHEELER, J. M., ROBINSON, L. C., TROJANOWSKI, J. Q., LEE, V. M. & SCHELLENBERG, G. D. 2010. Loss of murine TDP-43 disrupts motor function and plays an essential role in embryogenesis. *Acta Neuropathol,* 119**,** 409-19.
KRAEMER, B. C., ZHANG, B., LEVERENZ, J. B., THOMAS, J. H., TROJANOWSKI, J. Q. & SCHELLENBERG, G. D. 2003. Neurodegeneration and defective neurotransmission in a Caenorhabditis elegans model of tauopathy. *Proc Natl Acad Sci U S A,* 100**,** 9980-5.
KRAMER, M. L. & SCHULZ-SCHAEFFER, W. J. 2007. Presynaptic alpha-synuclein aggregates, not Lewy bodies, cause neurodegeneration in dementia with Lewy bodies. *J Neurosci,* 27**,** 1405-10.
LANGNESS, V. F., SIMMONS, D. A., MCHUGH, T. L. M., BUTLER, R. R., 3RD, ZHOU, J., LIU, H., YANG, T., ELLERBY, L. M. & LONGO, F. M. 2025. Twenty years of therapeutic development in tauopathy mouse models: a scoping review. *Alzheimers Dement,* 21**,** e70578.
LATIMER, C. S., STAIR, J. G., HINCKS, J. C., CURREY, H. N., BIRD, T. D., KEENE, C. D., KRAEMER, B. C. & LIACHKO, N. F. 2022. TDP-43 promotes tau accumulation and selective neurotoxicity in bigenic Caenorhabditis elegans. *Dis Model Mech,* 15.
LESTER, E., OOI, F. K., BAKKAR, N., AYERS, J., WOERMAN, A. L., WHEELER, J., BOWSER, R., CARLSON, G. A., PRUSINER, S. B. & PARKER, R. 2021. Tau aggregates are RNA-protein assemblies that mislocalize multiple nuclear speckle components. *Neuron,* 109**,** 1675-1691 e9.
LEUNG, A. K., VYAS, S., ROOD, J. E., BHUTKAR, A., SHARP, P. A. & CHANG, P. 2011. Poly(ADP-ribose) regulates stress responses and microRNA activity in the cytoplasm. *Mol Cell,* 42**,** 489-99.
LIACHKO, N. F., GUTHRIE, C. R. & KRAEMER, B. C. 2010. Phosphorylation promotes neurotoxicity in a Caenorhabditis elegans model of TDP-43 proteinopathy. *J Neurosci,* 30**,** 16208-19.
LIACHKO, N. F., SAXTON, A. D., MCMILLAN, P. J., STROVAS, T. J., CURREY, H. N., TAYLOR, L. M., WHEELER, J. M., OBLAK, A. L., GHETTI, B., MONTINE, T. J., KEENE, C. D., RASKIND, M. A., BIRD, T. D. & KRAEMER, B. C. 2016a. The phosphatase calcineurin regulates pathological TDP-43 phosphorylation. *Acta Neuropathologica,* 132**,** 545-561.
LIACHKO, N. F., SAXTON, A. D., MCMILLAN, P. J., STROVAS, T. J., CURREY, H. N., TAYLOR, L. M., WHEELER, J. M., OBLAK, A. L., GHETTI, B., MONTINE, T. J., KEENE, C. D., RASKIND, M. A., BIRD, T. D. & KRAEMER, B. C. 2016b. The phosphatase calcineurin regulates pathological TDP-43 phosphorylation. *Acta Neuropathol,* 132**,** 545-61.
LIAO, Y., SMYTH, G. K. & SHI, W. 2014. featureCounts: an efficient general purpose program for assigning sequence reads to genomic features. *Bioinformatics,* 30**,** 923-30.

LIAO, Y. Z., MA, J. & DOU, J. Z. 2022. The Role of TDP-43 in Neurodegenerative Disease. *Mol Neurobiol,* 59**,** 4223-4241.
LING, J. P., PLETNIKOVA, O., TRONCOSO, J. C. & WONG, P. C. 2015. TDP-43 repression of nonconserved cryptic exons is compromised in ALS-FTD. *Science,* 349**,** 650-5.
LOEWEN, C. A. & FEANY, M. B. 2010. The unfolded protein response protects from tau neurotoxicity in vivo. *PLoS One,* 5.
LONG, A., PARK, J. H., KLIMOVA, N., FOWLER, C., LOANE, D. J. & KRISTIAN, T. 2017. CD38 Knockout Mice Show Significant Protection Against Ischemic Brain Damage Despite High Level Poly-ADP-Ribosylation. *Neurochem Res,* 42**,** 283-293.
LONG, J. M. & HOLTZMAN, D. M. 2019. Alzheimer Disease: An Update on Pathobiology and Treatment Strategies. *Cell,* 179**,** 312-339.
LOVE, M. I., HUBER, W. & ANDERS, S. 2014. Moderated estimation of fold change and dispersion for RNA-seq data with DESeq2. *Genome Biol,* 15**,** 550.
LYE, Y. S. & CHEN, Y. R. 2022. TAR DNA-binding protein 43 oligomers in physiology and pathology. *IUBMB Life,* 74**,** 794-811.
LYKKE-ANDERSEN, S., ROUVIERE, J. O. & JENSEN, T. H. 2021. ARS2/SRRT: at the nexus of RNA polymerase II transcription, transcript maturation and quality control. *Biochem Soc Trans,* 49**,** 1325-1336.
MA, J., LIU, L., SONG, L., LIU, J., YANG, L., CHEN, Q., WU, J. Y. & ZHU, L. 2023. Integration of FUNDC1-associated mitochondrial protein import and mitochondrial quality control contributes to TDP-43 degradation. *Cell Death Dis,* 14**,** 735.
MACKENZIE, I. R. & RADEMAKERS, R. 2008. The role of transactive response DNA-binding protein-43 in amyotrophic lateral sclerosis and frontotemporal dementia. *Curr Opin Neurol,* 21**,** 693-700.
MAJUMDER, P., CHEN, Y. T., BOSE, J. K., WU, C. C., CHENG, W. C., CHENG, S. J., FANG, Y. H., CHEN, Y. L., TSAI, K. J., LIEN, C. C. & SHEN, C. K. 2012. TDP-43 regulates the mammalian spinogenesis through translational repression of Rac1. *Acta Neuropathol,* 124**,** 231-45.
MARASCHI, A., GUMINA, V., DRAGOTTO, J., COLOMBRITA, C., MOMPEAN, M., BURATTI, E., SILANI, V., FELIGIONI, M. & RATTI, A. 2021. SUMOylation Regulates TDP-43 Splicing Activity and Nucleocytoplasmic Distribution. *Mol Neurobiol,* 58**,** 5682-5702.
MAUREL, C., CHAMI, A. A., THEPAULT, R. A., MAROUILLAT, S., BLASCO, H., CORCIA, P., ANDRES, C. R. & VOURC'H, P. 2020. A role for SUMOylation in the Formation and Cellular Localization of TDP-43 Aggregates in Amyotrophic Lateral Sclerosis. *Mol Neurobiol,* 57**,** 1361-1373.
MCGURK, L., GOMES, E., GUO, L., MOJSILOVIC-PETROVIC, J., TRAN, V., KALB, R. G., SHORTER, J. & BONINI, N. M. 2018a. Poly(ADP-Ribose) Prevents Pathological Phase Separation of TDP-43 by Promoting Liquid Demixing and Stress Granule Localization. *Mol Cell,* 71**,** 703-717 e9.
MCGURK, L., GOMES, E., GUO, L., SHORTER, J. & BONINI, N. M. 2018b. Poly(ADP-ribose) Engages the TDP-43 Nuclear-Localization Sequence to Regulate Granulo-Filamentous Aggregation. *Biochemistry,* 57**,** 6923-6926.
MCMILLAN, P., WHEELER, J., GATLIN, R. E., TAYLOR, L., STROVAS, T., BAUM, M., BIRD, T. D., LATIMER, C., KEENE, C. D., KRAEMER, B. C. & LIACHKO, N. F. 2020. Adult onset pan-neuronal human tau tubulin kinase 1 expression causes severe cerebellar neurodegeneration in mice. *Acta Neuropathol Commun,* 8**,** 200.
MELAMED, Z., LOPEZ-ERAUSKIN, J., BAUGHN, M. W., ZHANG, O., DRENNER, K., SUN, Y., FREYERMUTH, F., MCMAHON, M. A., BECCARI, M. S., ARTATES, J. W., OHKUBO, T., RODRIGUEZ, M., LIN, N., WU, D., BENNETT, C. F., RIGO, F., DA CRUZ, S., RAVITS, J., LAGIER-TOURENNE, C. & CLEVELAND, D. W. 2019. Premature polyadenylation-mediated loss of stathmin-2 is a hallmark of TDP-43-dependent neurodegeneration. *Nat Neurosci,* 22**,** 180-190.
NAKASHIMA-YASUDA, H., URYU, K., ROBINSON, J., XIE, S. X., HURTIG, H., DUDA, J. E., ARNOLD, S. E., SIDEROWF, A., GROSSMAN, M., LEVERENZ, J. B., WOLTJER, R., LOPEZ, O. L., HAMILTON, R., TSUANG, D. W., GALASKO, D., MASLIAH, E., KAYE, J., CLARK, C. M., MONTINE, T. J., LEE, V. M. & TROJANOWSKI, J. Q. 2007. Co-morbidity of TDP-43 proteinopathy in Lewy body related diseases. *Acta Neuropathol,* 114**,** 221-9.
NAWROCKA, W. I., CHENG, S., HAO, B., ROSEN, M. C., CORTES, E., BALTRUSAITIS, E. E., AZIZ, Z., KOVACS, I. A. & OZKAN, E. 2024. Nematode Extracellular Protein Interactome Expands Connections between Signaling Pathways. *bioRxiv*.

NECARSULMER, J. C., SIMON, J. M., EVANGELISTA, B. A., CHEN, Y., TIAN, X., NAFEES, S., MARQUEZ, A. B., JIANG, H., WANG, P., AJIT, D., NIKOLOVA, V. D., HARPER, K. M., EZZELL, J. A., LIN, F. C., BELTRAN, A. S., MOY, S. S. & COHEN, T. J. 2023. RNA-binding deficient TDP-43 drives cognitive decline in a mouse model of TDP-43 proteinopathy. *Elife,* 12.

NELSON, P. T., DICKSON, D. W., TROJANOWSKI, J. Q., JACK, C. R., BOYLE, P. A., ARFANAKIS, K., RADEMAKERS, R., ALAFUZOFF, I., ATTEMS, J., BRAYNE, C., COYLE-GILCHRIST, I. T. S., CHUI, H. C., FARDO, D. W., FLANAGAN, M. E., HALLIDAY, G., HOKKANEN, S. R. K., HUNTER, S., JICHA, G. A., KATSUMATA, Y., KAWAS, C. H., KEENE, C. D., KOVACS, G. G., KUKULL, W. A., LEVEY, A. I., MAKKINEJAD, N., MONTINE, T. J., MURAYAMA, S., MURRAY, M. E., NAG, S., RISSMAN, R. A., SEELEY, W. W., SPERLING, R. A., WHITE, C. L., 3RD, YU, L. & SCHNEIDER, J. A. 2019. Limbic-predominant age-related TDP-43 encephalopathy (LATE): consensus working group report. *Brain,* 142**,** 1503-1527.

NEUMANN, M., KWONG, L. K., LEE, E. B., KREMMER, E., FLATLEY, A., XU, Y., FORMAN, M. S., TROOST, D., KRETZSCHMAR, H. A., TROJANOWSKI, J. Q. & LEE, V. M. 2009. Phosphorylation of S409/410 of TDP-43 is a consistent feature in all sporadic and familial forms of TDP-43 proteinopathies. *Acta Neuropathol,* 117**,** 137-49.

NEUMANN, M., LEE, E. B. & MACKENZIE, I. R. 2021. Frontotemporal Lobar Degeneration TDP-43-Immunoreactive Pathological Subtypes: Clinical and Mechanistic Significance. *Adv Exp Med Biol,* 1281**,** 201-217.

NEUMANN, M., SAMPATHU, D. M., KWONG, L. K., TRUAX, A. C., MICSENYI, M. C., CHOU, T. T., BRUCE, J., SCHUCK, T., GROSSMAN, M., CLARK, C. M., MCCLUSKEY, L. F., MILLER, B. L., MASLIAH, E., MACKENZIE, I. R., FELDMAN, H., FEIDEN, W., KRETZSCHMAR, H. A., TROJANOWSKI, J. Q. & LEE, V. M. 2006. Ubiquitinated TDP-43 in frontotemporal lobar degeneration and amyotrophic lateral sclerosis. *Science,* 314**,** 130-3.

NIGON, V. M. & FELIX, M. A. 2017. History of research on C. elegans and other free-living nematodes as model organisms. *WormBook,* 2017**,** 1-84.

NONAKA, T., MASUDA-SUZUKAKE, M., ARAI, T., HASEGAWA, Y., AKATSU, H., OBI, T., YOSHIDA, M., MURAYAMA, S., MANN, D. M., AKIYAMA, H. & HASEGAWA, M. 2013. Prion-like properties of pathological TDP-43 aggregates from diseased brains. *Cell Rep,* 4**,** 124-34.

NOURAEI, N., MASON, D. M., MINER, K. M., CARCELLA, M. A., BHATIA, T. N., DUMM, B. K., SONI, D., JOHNSON, D. A., LUK, K. C. & LEAK, R. K. 2018. Critical appraisal of pathology transmission in the alpha-synuclein fibril model of Lewy body disorders. *Exp Neurol,* 299**,** 172-196.

OKA, M. & YONEDA, Y. 2018. Importin alpha: functions as a nuclear transport factor and beyond. *Proc Jpn Acad Ser B Phys Biol Sci,* 94**,** 259-274.

ONO, H. & AOKI, Y. 2026. Neurological Behavioral Assessment of Exon-Skipping Therapy for Neuromuscular Disorders Using Displaced Object Recognition Test, Open Field Test, and Three-Chamber Social Approach Test. *Methods Mol Biol,* 2963**,** 195-203.

PARK, K. H., YU, E., CHOI, S., KIM, S., PARK, C., LEE, J. E. & KIM, K. W. 2025. Optogenetic induction of TDP-43 aggregation impairs neuronal integrity and behavior in Caenorhabditis elegans. *Transl Neurodegener,* 14**,** 20.

PEREZ, M. F. 2024. CelEst: a unified gene regulatory network for estimating transcription factor activities in C. elegans. *Genetics*.

PEREZ-BERLANGA, M., WIERSMA, V. I., ZBINDEN, A., DE VOS, L., WAGNER, U., FOGLIENI, C., MALLONA, I., BETZ, K. M., CLERY, A., WEBER, J., GUO, Z., RIGORT, R., DE ROSSI, P., MANGLUNIA, R., TANTARDINI, E., SAHADEVAN, S., STACH, O., HRUSKA-PLOCHAN, M., ALLAIN, F. H., PAGANETTI, P. & POLYMENIDOU, M. 2023. Loss of TDP-43 oligomerization or RNA binding elicits distinct aggregation patterns. *EMBO J,* 42**,** e111719.

PIERCE-SHIMOMURA, J. T., CHEN, B. L., MUN, J. J., HO, R., SARKIS, R. & MCINTIRE, S. L. 2008. Genetic analysis of crawling and swimming locomotory patterns in C. elegans. *Proc Natl Acad Sci U S A,* 105**,** 20982-7.

PIR, G. J., BUDDENKOTTE, J., ALAM, M. A., OWN, A., ECK, R. J., KRAEMER, B. C., MANDELKOW, E. & STEINHOFF, M. 2025. TDP-43 proteinopathies and neurodegeneration: insights from Caenorhabditis elegans models. *FEBS J*.

PIR, G. J., BUDDENKOTTE, J., ALAM, M. A., OWN, A., ECK, R. J., KRAEMER, B. C., MANDELKOW, E. & STEINHOFF, M. 2026. TDP-43 proteinopathies and neurodegeneration: insights from Caenorhabditis elegans models. *FEBS J,* 293**,** 348-384.

PRASAD, A., BHARATHI, V., SIVALINGAM, V., GIRDHAR, A. & PATEL, B. K. 2019. Molecular Mechanisms of TDP-43 Misfolding and Pathology in Amyotrophic Lateral Sclerosis. *Front Mol Neurosci,* 12**,** 25.

RAMAZI, S. & ZAHIRI, J. 2021. Posttranslational modifications in proteins: resources, tools and prediction methods. *Database (Oxford),* 2021.

RUMMENS, J. & DA CRUZ, S. 2025. RNA-binding proteins in ALS and FTD: from pathogenic mechanisms to therapeutic insights. *Mol Neurodegener,* 20**,** 64.

SALDI, T. K., ASH, P. E., WILSON, G., GONZALES, P., GARRIDO-LECCA, A., ROBERTS, C. M., DOSTAL, V., GENDRON, T. F., STEIN, L. D., BLUMENTHAL, T., PETRUCELLI, L. & LINK, C. D. 2014. TDP-1, the Caenorhabditis elegans ortholog of TDP-43, limits the accumulation of double-stranded RNA. *EMBO J,* 33**,** 2947-66.

SCHELTENS, P., DE STROOPER, B., KIVIPELTO, M., HOLSTEGE, H., CHETELAT, G., TEUNISSEN, C. E., CUMMINGS, J. & VAN DER FLIER, W. M. 2021. Alzheimer's disease. *Lancet,* 397**,** 1577-1590.

SCHOLZ, S. W., OKUBADEJO, N. U., PRAKASH, P., LIDDELOW, S. A., RYTEN, M. & HALLIDAY, G. M. 2025. Advances in the genetics and pathology of Lewy body dementia. *Lancet Neurol,* 24**,** 1026-1037.

SCHUSKE, K., BEG, A. A. & JORGENSEN, E. M. 2004. The GABA nervous system in C. elegans. *Trends Neurosci,* 27**,** 407-14.

SEIBENHENER, M. L. & WOOTEN, M. C. 2015. Use of the Open Field Maze to measure locomotor and anxiety-like behavior in mice. *J Vis Exp***,** e52434.

SEPHTON, C. F., CENIK, B., CENIK, B. K., HERZ, J. & YU, G. 2012. TDP-43 in central nervous system development and function: clues to TDP-43-associated neurodegeneration. *Biol Chem,* 393**,** 589-94.

SEPHTON, C. F., GOOD, S. K., ATKIN, S., DEWEY, C. M., MAYER, P., 3RD, HERZ, J. & YU, G. 2010. TDP-43 is a developmentally regulated protein essential for early embryonic development. *J Biol Chem,* 285**,** 6826-34.

SPENCE, H., WALDRON, F. M., SALEEB, R. S., BROWN, A. L., RIFAI, O. M., GILODI, M., READ, F., ROBERTS, K., MILNE, G., WILKINSON, D., O'SHAUGHNESSY, J., PASTORE, A., FRATTA, P., SHNEIDER, N., TARTAGLIA, G. G., ZACCO, E., HORROCKS, M. H. & GREGORY, J. M. 2024. RNA aptamer reveals nuclear TDP-43 pathology is an early aggregation event that coincides with STMN-2 cryptic splicing and precedes clinical manifestation in ALS. *Acta Neuropathol,* 147**,** 50.

SPILLER, K. J., CHEUNG, C. J., RESTREPO, C. R., KWONG, L. K., STIEBER, A. M., TROJANOWSKI, J. Q. & LEE, V. M. 2016. Selective Motor Neuron Resistance and Recovery in a New Inducible Mouse Model of TDP-43 Proteinopathy. *J Neurosci,* 36**,** 7707-17.

SREEDHARAN, J., BLAIR, I. P., TRIPATHI, V. B., HU, X., VANCE, C., ROGELJ, B., ACKERLEY, S., DURNALL, J. C., WILLIAMS, K. L., BURATTI, E., BARALLE, F., DE BELLEROCHE, J., MITCHELL, J. D., LEIGH, P. N., AL-CHALABI, A., MILLER, C. C., NICHOLSON, G. & SHAW, C. E. 2008. TDP-43 mutations in familial and sporadic amyotrophic lateral sclerosis. *Science,* 319**,** 1668-72.

SUK, T. R., PART, C. E., ZHANG, J. L., NGUYEN, T. T., HEER, M. M., CABALLERO-GOMEZ, A., GRYBAS, V. S., MCKEEVER, P. M., NGUYEN, B., ALI, T., CALLAGHAN, S. M., WOULFE, J. M., ROBERTSON, J. & ROUSSEAUX, M. W. C. 2025. A stress-dependent TDP-43 SUMOylation program preserves neuronal function. *Mol Neurodegener,* 20**,** 38.

TAOUKTSI, E., KYRIAKOU, E., SMYRNIOTIS, S., BORBOLIS, F., BONDI, L., AVGERIS, S., TRIGAZIS, E., RIGAS, S., VOUTSINAS, G. E. & SYNTICHAKI, P. 2022. Organismal and Cellular Stress Responses upon Disruption of Mitochondrial Lonp1 Protease. *Cells,* 11.

TAOUKTSI, E., KYRIAKOU, E., VOULGARAKI, E., VERGANELAKIS, D., KROKOU, S., RIGAS, S., VOUTSINAS, G. E. & SYNTICHAKI, P. 2023. Mitochondrial p38 Mitogen-Activated Protein Kinase: Insights into Its Regulation of and Role in LONP1-Deficient Nematodes. *Int J Mol Sci,* 24.

TAYLOR, M., MARX, O. & NORRIS, A. 2023. TDP-1 and FUST-1 co-inhibit exon inclusion and control fertility together with transcriptional regulation. *Nucleic Acids Res*.

TAYLOR, R. C. & DILLIN, A. 2013. XBP-1 is a cell-nonautonomous regulator of stress resistance and longevity. *Cell,* 153**,** 1435-47.

TEAM, R. C. 2021. R: A language and environment for statistical computing. R Foundation for Statistical Computing, Vienna, Austria. https://www.R-project.org/.

TOME, S. O., GOMES, L. A., LI, X., VANDENBERGHE, R., TOUSSEYN, T. & THAL, D. R. 2021. TDP-43 interacts with pathological tau protein in Alzheimer's disease. *Acta Neuropathol,* 141**,** 795-799.
TOME, S. O., TSAKA, G., RONISZ, A., OSPITALIERI, S., GAWOR, K., GOMES, L. A., OTTO, M., VON ARNIM, C. A. F., VAN DAMME, P., VAN DEN BOSCH, L., GHEBREMEDHIN, E., LAUREYSSEN, C., SLEEGERS, K., VANDENBERGHE, R., ROUSSEAU, F., SCHYMKOWITZ, J. & THAL, D. R. 2023. TDP-43 pathology is associated with increased tau burdens and seeding. *Mol Neurodegener,* 18**,** 71.
TORRES, A. K., FLEISCHHART, V. & INESTROSA, N. C. 2024. Mitochondrial unfolded protein response (UPR(mt)): what we know thus far. *Front Cell Dev Biol,* 12**,** 1405393.
TORRES, A. K., MIRA, R. G., PINTO, C. & INESTROSA, N. C. 2025. Studying the mechanisms of neurodegeneration: C. elegans advantages and opportunities. *Front Cell Neurosci,* 19**,** 1559151.
UEMURA, M. T., ROBINSON, J. L., COUSINS, K. A. Q., TROPEA, T. F., KARGILIS, D. C., MCBRIDE, J. D., SUH, E., XIE, S. X., XU, Y., PORTA, S., UEMURA, N., VAN DEERLIN, V. M., WOLK, D. A., IRWIN, D. J., BRUNDEN, K. R., LEE, V. M., LEE, E. B. & TROJANOWSKI, J. Q. 2022. Distinct characteristics of limbic-predominant age-related TDP-43 encephalopathy in Lewy body disease. *Acta Neuropathol,* 143**,** 15-31.
VERDE, E. M., ANTONIANI, F., MEDIANI, L., SECCO, V., CROTTI, S., FERRARA, M. C., VINET, J., SERGEEVA, A., YAN, X., HOEGE, C., STUANI, C., PARON, F., KAO, T. T., SHRIVASTAVA, R., POLANOWSKA, J., BAILLY, A., ROSA, A., ARONICA, E., GOSWAMI, A., SHNEIDER, N., HYMAN, A. A., BURATTI, E., XIRODIMAS, D., FRANZMANN, T. M., ALBERTI, S. & CARRA, S. 2025. SUMO2/3 conjugation of TDP-43 protects against aggregation. *Sci Adv,* 11**,** eadq2475.
WAGEY, R., KRIEGER, C. & SHAW, C. A. 1997. Abnormal dephosphorylation effect on NMDA receptor regulation in ALS spinal cord. *Neurobiol Dis,* 4**,** 350-5.
WALDHERR, S. M., ECK, R. J., HINCKS, J. C., CURREY, H. N., GOLDBERG, M., MCMILLAN, P. J., SAXTON, A. D., HULSEY-VINCENT, H. J., LATIMER, C. S., KRAEMER, B. C. & LIACHKO, N. F. 2026. Calcineurin depletion coincides with phosphorylated TDP-43 deposition in a mouse model of ALS/FTLD-TDP. *Acta Neuropathol Commun*.
WALDHERR, S. M., HAN, M., SAXTON, A. D., VADSET, T. A., MCMILLAN, P. J., WHEELER, J. M., LIACHKO, N. F. & KRAEMER, B. C. 2024. Endoplasmic reticulum unfolded protein response transcriptional targets of XBP-1s mediate rescue from tauopathy. *Commun Biol,* 7**,** 903.
WALDHERR, S. M., STROVAS, T. J., VADSET, T. A., LIACHKO, N. F. & KRAEMER, B. C. 2019. Constitutive XBP-1s-mediated activation of the endoplasmic reticulum unfolded protein response protects against pathological tau. *Nat Commun,* 10**,** 4443.
WALKER, A. K., SPILLER, K. J., GE, G., ZHENG, A., XU, Y., ZHOU, M., TRIPATHY, K., KWONG, L. K., TROJANOWSKI, J. Q. & LEE, V. M. 2015. Functional recovery in new mouse models of ALS/FTLD after clearance of pathological cytoplasmic TDP-43. *Acta Neuropathol,* 130**,** 643-60.
WANG, A., CONICELLA, A. E., SCHMIDT, H. B., MARTIN, E. W., RHOADS, S. N., REEB, A. N., NOURSE, A., RAMIREZ MONTERO, D., RYAN, V. H., ROHATGI, R., SHEWMAKER, F., NAIK, M. T., MITTAG, T., AYALA, Y. M. & FAWZI, N. L. 2018. A single N-terminal phosphomimic disrupts TDP-43 polymerization, phase separation, and RNA splicing. *EMBO J,* 37.
WANG, P., DENG, J., DONG, J., LIU, J., BIGIO, E. H., MESULAM, M., WANG, T., SUN, L., WANG, L., LEE, A. Y., MCGEE, W. A., CHEN, X., FUSHIMI, K., ZHU, L. & WU, J. Y. 2019. TDP-43 induces mitochondrial damage and activates the mitochondrial unfolded protein response. *PLoS Genet,* 15**,** e1007947.
WANG, W., WANG, L., LU, J., SIEDLAK, S. L., FUJIOKA, H., LIANG, J., JIANG, S., MA, X., JIANG, Z., DA ROCHA, E. L., SHENG, M., CHOI, H., LEROU, P. H., LI, H. & WANG, X. 2016. The inhibition of TDP-43 mitochondrial localization blocks its neuronal toxicity. *Nat Med,* 22**,** 869-78.
WEGMANN, S., BIERNAT, J. & MANDELKOW, E. 2021. A current view on Tau protein phosphorylation in Alzheimer's disease. *Curr Opin Neurobiol,* 69**,** 131-138.
WEINGARTEN, M. D., LOCKWOOD, A. H., HWO, S. Y. & KIRSCHNER, M. W. 1975. A protein factor essential for microtubule assembly. *Proc Natl Acad Sci U S A,* 72**,** 1858-62.
WHEELER, J. M., MCMILLAN, P. J., HAWK, M., IBA, M., ROBINSON, L., XU, G. J., DOMBROSKI, B. A., JEONG, D., DICHTER, M. A., JUUL, H., LOOMIS, E., RASKIND, M., LEVERENZ, J. B., TROJANOWSKI, J. Q., LEE, V. M., SCHELLENBERG, G. D. & KRAEMER, B. C. 2015. High copy wildtype human 1N4R tau expression promotes early pathological tauopathy accompanied

by cognitive deficits without progressive neurofibrillary degeneration. *Acta Neuropathol Commun,* 3**,** 33.
WHITE, J. G., SOUTHGATE, E., THOMSON, J. N. & BRENNER, S. 1986. The structure of the nervous system of the nematode Caenorhabditis elegans. *Philos Trans R Soc Lond B Biol Sci,* 314**,** 1-340.
WICKHAM, H. 2016. Ggplot2 : elegant graphics for data analysis. *Use R!* Second edition. ed. Switzerland: Springer,.
WILS, H., KLEINBERGER, G., JANSSENS, J., PERESON, S., JORIS, G., CUIJT, I., SMITS, V., CEUTERICK-DE GROOTE, C., VAN BROECKHOVEN, C. & KUMAR-SINGH, S. 2010. TDP-43 transgenic mice develop spastic paralysis and neuronal inclusions characteristic of ALS and frontotemporal lobar degeneration. *Proc Natl Acad Sci U S A,* 107**,** 3858-63.
WILSON, R. S., YU, L., TROJANOWSKI, J. Q., CHEN, E. Y., BOYLE, P. A., BENNETT, D. A. & SCHNEIDER, J. A. 2013. TDP-43 pathology, cognitive decline, and dementia in old age. *JAMA Neurol,* 70**,** 1418-24.
WINTON, M. J., IGAZ, L. M., WONG, M. M., KWONG, L. K., TROJANOWSKI, J. Q. & LEE, V. M. 2008. Disturbance of nuclear and cytoplasmic TAR DNA-binding protein (TDP-43) induces disease-like redistribution, sequestration, and aggregate formation. *J Biol Chem,* 283**,** 13302-9.
WISSE, L. E. M., WUESTEFELD, A., MURRAY, M. E., JAGUST, W. & LA JOIE, R. 2025. Role of tau versus TDP-43 pathology on medial temporal lobe atrophy in aging and Alzheimer's disease. *Alzheimers Dement,* 21**,** e14582.
WOLOZIN, B., GABEL, C., FERREE, A., GUILLILY, M. & EBATA, A. 2011. Watching worms whither: modeling neurodegeneration in C. elegans. *Prog Mol Biol Transl Sci,* 100**,** 499-514.
WU, L. S., CHENG, W. C., HOU, S. C., YAN, Y. T., JIANG, S. T. & SHEN, C. K. 2010. TDP-43, a neuro-pathosignature factor, is essential for early mouse embryogenesis. *Genesis,* 48**,** 56-62.
XU, Y. F., GENDRON, T. F., ZHANG, Y. J., LIN, W. L., D'ALTON, S., SHENG, H., CASEY, M. C., TONG, J., KNIGHT, J., YU, X., RADEMAKERS, R., BOYLAN, K., HUTTON, M., MCGOWAN, E., DICKSON, D. W., LEWIS, J. & PETRUCELLI, L. 2010. Wild-type human TDP-43 expression causes TDP-43 phosphorylation, mitochondrial aggregation, motor deficits, and early mortality in transgenic mice. *J Neurosci,* 30**,** 10851-9.
ZEISEL, A., HOCHGERNER, H., LONNERBERG, P., JOHNSSON, A., MEMIC, F., VAN DER ZWAN, J., HARING, M., BRAUN, E., BORM, L. E., LA MANNO, G., CODELUPPI, S., FURLAN, A., LEE, K., SKENE, N., HARRIS, K. D., HJERLING-LEFFLER, J., ARENAS, E., ERNFORS, P., MARKLUND, U. & LINNARSSON, S. 2018. Molecular Architecture of the Mouse Nervous System. *Cell,* 174**,** 999-1014 e22.
ZHANG, T., HWANG, H. Y., HAO, H., TALBOT, C., JR. & WANG, J. 2012. Caenorhabditis elegans RNA-processing protein TDP-1 regulates protein homeostasis and life span. *J Biol Chem,* 287**,** 8371-82.
ZHANG, Z., LI, R., ZHANG, X., WEI, Y., MA, H., ZHU, L. & YIN, R. 2019. Voluntary exercise promotes neurotrophic factor and suppresses apoptosis in hippocampal ischemia. *J Integr Neurosci,* 18**,** 65-70.
ZHEN, M. & SAMUEL, A. D. 2015. C. elegans locomotion: small circuits, complex functions. *Curr Opin Neurobiol,* 33**,** 117-26.